tRNA Processing and Quality Control in Bacteria

by

Ravi Kumar Alluri

A Dissertation Submitted to the Faculty of

The Charles E. Schmidt College of Science

in Partial Fulfillment of the Requirements for the Degree of

Doctor of Philosophy

Florida Atlantic University

Boca Raton, FL

May 2013

tRNA Processing and Quality Control in Bacteria

by

Ravi Kumar Alluri

This dissertation was prepared under the direction of the candidate's dissertation advisor, Dr. Zhongwei Li, Department of Biomedical Science, and has been approved by the members of his supervisory committee. It was submitted to the faculty of the Charles E. Schmidt College of Science and was accepted in partial fulfillment of the requirements for the Degree of Philosophy.

SUPERVISORY COMMITTEE:

Zhongwei Li, Ph.D.
Dissertation Advisor

Howard M. Prentice, Ph.D.

Kasirajan Ayyanathan, Ph.D.

Massimo Caputi, Ph.D.

Rodney K. Murphey, Ph.D.
Chair, Department of Biological Sciences

Gary W. Perry, Ph.D.
Dean, The Charles E. Schmidt College of Science

Barry T. Rosson, Ph.D.
Dean, Graduate College

March 21, 2013
Date

Acknowledgements

The author wishes to express his sincere appreciation to his advisor, Dr. Zhongwei Li, for his guidance during his research and study at Florida Atlantic University. The author is grateful to his other committee members, Dr. Howard M. Prentice, Dr. Christopher M. Burns, Dr. Kasirajan Ayyanathan, Dr. Arun Malhotra, and Dr. Massimo Caputi for their time and assistance throughout the graduate study. The author thanks all his family members, Sujatha, Leela, Mano, Cherry, Prathima, Sandhya and Kishore for their constant support and encouragement. The author also would like to thank his always special friends Hari, Rajendra, Royal and Shiva for their prayers and encouragement over the years.

The author wishes to express his gratitude towards the families of Abel & Anthonamma, Srinu & Nirmala, Sunder & Ratnamma, Vijaya paul & Amulu, Prasad & Lucy, Martin & Therosulu, Royal & Angel, Garreth & Carole, Yesuratnam & Kalyani, Kishore & Gayatri, Eric & Diane. The author also wishes to thank his friends and colleagues Cnu, Sappidi, Girish, Gauri, Chandana, Janet, Min, Xin, Hyin, Gongliang, Samrat dutta and Sulochan. The author specially thanks Dr. Vijaya, Dr. Piere, Dr. Santosh and Dr. Girish, Dr. Sekhar Reddy, for their kind support in his toughest situations.

Finally all Glory and Honor to my Lord God, **JESUS CHRIST** alone. In **HIM** alone I have victory, peace and everlasting life.

Abstract

Author: Ravi Kumar Alluri

Title: tRNA Processing and Quality Control in Bacteria

Institution: Florida Atlantic University

Dissertation Advisor: Dr. Zhongwei Li

Degree: Doctor of Philosophy

Year: 2013

In this work, we report that the only exoribonuclease in *M. genitalium*, RNase R, is able to generate mature 3'-ends. The aminoacyl-acceptor stem, CCA terminus and discriminator residue plays an important role in stopping RNase R digestion at the mature 3'-end. Disruption of the stem causes partial or complete degradation of the pre-tRNA, whereas extension of the stem results in the formation of a mature 3'-end. CC residues in CCA terminus and A or G residues at discriminator position are the most preferred residues for precise stopping of RNase R at mature 3' end. The significance of this works shows that *M. genitalium* RNase R generates mature tRNA in a single step by recognizing features in the terminal domains of tRNA, a process requiring multiple RNases in most bacteria.

Ours studies with *in vivo* and *in vitro* oxidation of *Escherichia coli* tRNA revealed that 8-hydroxyguanosine (8-oxo-G) levels of tRNA increased upon treatment with hydrogen peroxide (H_2O_2) in a dose dependent manner. Interestingly, native tRNA was oxidized to higher level than its corresponding heat-denatured tRNA. This demonstrates that higher order structures in tRNA promote tRNA oxidative damage.

E. coli tRNA pseudouridine synthase TruD catalyzes pseudouridylation of U13 of $tRNA^{Glu}$. TruD protein binds to oxidized RNA with high affinity and protects cells under oxidative stress. Extensive RNA binding experiments revealed that only wild type TruD can differentiate normal and oxidized RNA. Surprisingly active site mutant proteins D80N and D80T did not show such differential specificity demonstrating the importance of charged aspartic acid in the active site. Studies to show the biochemical evidence behind protective role of TruD under oxidative stress revealed no concrete evidence. Our attempts have shown that under oxidative stress conditions, in cells lacking TruD aminoacylation of $tRNA^{Glu}$ was unaffected and $tRNA^{Glu}$ was stable. TruD was also not involved in the specific removal of 8-oxo-G containing RNA and oxidized base repair. The significance of this work shows the ability of TruD binding to oxidized RNA with high affinity and protects cells under oxidative stress. This demonstrates the existence of unknown biochemical mechanism behind the protective role of TruD which is yet to be elucidated.

Dedication

The dissertation is dedicated to my beloved parents Sri. Alluri Arogyaswamy, Smt. Alluri. Stannislasamma, for their continuous prayers, support, and encouragement. I succeeded in this Ph.D program only because of the enormous grace, blessings and power of my savior and counselor **LORD JESUS CHRIST**. Without **JESUS** I am nothing.

tRNA Processing and Quality Control in Bacteria

List of Tables

List of Figures

1. Introduction: Gene Organization, Processing and Quality Control of Bacterial tRNA

Transfer RNAs (tRNAs) are important and obligatory in decoding the information embedded in mRNA during protein synthesis. They are highly conserved in structure, and account for up to 20% of total RNA mass in bacteria. Functional tRNAs are produced by processing of the primary tRNA transcripts. Many factors may affect the production and maintenance of functional tRNA in a cell. It has been recognized that aberrant tRNAs may cause numerous problems to cells and organisms and they must be eliminated by RNA quality control mechanisms.

tRNAs are encoded by genes that are organized into either polycistronic or monocistronic transcriptional units. In bacteria, a polycistronic tRNA transcript may contain only tRNAs, or sometime contain other RNA species such as rRNA or mRNA. The abundance of a tRNA is determined not only by the number of genes encoding the tRNA, but also by the strength of the promoter for producing the transcript. It has been well recognized that the levels of specific tRNAs significantly contribute to the varied levels of codon usage among different organisms. Thus, tRNA species recognizing rare codons are usually present in fewer copies (Ikemura, 1981). Recent achievements in tRNA genomics made significant developments towards identification, classification,

secondary structure prediction and generation of tRNA databases using bioinformatics approach. (Lowe and Eddy, 1997; Laslett *et al*., 2004; Tåquist *et al*., 2007)

Bacterial tRNAs are invariably transcribed into precursors with extra sequences at the 5' and 3' end. These extra sequences are removed by processing by ribonucleases (RNases) and other enzymes in order to generate functional tRNA. The factory of RNases involved in tRNA processing varies among different bacteria, including exoribonucleases that digest RNA from one end and endoribonucleases that cleave RNA in the middle of the molecule. Among the endoribonucleases, RNase P is involved in maturation of 5' end and both the enzyme and its function are conserved in bacteria and other living organisms. Removal of the 3' extra sequence from tRNA precursors is more complicated in bacteria, involving multiple endoribonucleases (Li *et al*., 1999, Li and Deutscher, 2002; Pellegrini *et al*., 2003), and the exoribonucleases (Z. Li and Murray P. Deutscher 1995, 1996; Mohanty anf Kushner, 2010, and Pellegrini *et al*., 2003; Condon, 2003) As discussed below, it is interesting to note that the sequence of a tRNA transcript has a profound effect on tRNA processing reactions.

Structural and sequence variations in tRNA transcript can lead to abnormal processing and generate aberrant tRNAs which will undergo degradation by exoribonucleases via polyadenylation by polyadenylate polymerase (PAP) (Li *et al*., 2002). Accumulation of defective, nonfunctional tRNAs can cause deleterious effects on cell growth and thus degradation or repair of defective tRNAs is an inevitable and more complex process.

Biochemical studies have been used to understand the tRNA processing and degradation mechanisms, with less emphasis on bioinformatics approach. Bioinformatics

can play an important role in studying the structural and sequence variations in tRNA species which are the prime determinants for processing and degradation machinery. In the past genomic era identification of tRNA genes was a difficult task and involved manual analysis but in the recent years with the availability of genome sequence and several bioinformatics programs, identification, classification and secondary structure determination of tRNAs made it easy to study and analyze structural and sequential variations in tRNA transcripts. Structural and sequence analysis of tRNA transcripts with the availability of factory of tRNA processing ribonucleases will help us to understand the type of processing/degradation pathway that each tRNA species in different organisms can possibly undergo.

1.1 Identification and organization of tRNA genes

Towards the identification and extraction of tRNA genes from genome sequences, several bioinformatics program have been developed of which tRNAscan-SE is the primary program developed to identify tRNA genes, which is widely used by many researchers (Lowe and Eddy, 1997). Later several programs were developed with advanced applications which includes ARAGORN, a program used to identify tRNA, tmRNA genes and pseudo tRNAs from genomic sequences (Laslett *et al*., 2004). Very recently, tRNA function classifier (TFAM) program has been developed to classify tRNA gene families (Tåquist *et al*., 2007). The widely accepted RNA secondary structure program MFOLD which is recently replaced by UNAF fold has been developed to solve the problems of tRNA secondary structure prediction (Mathews *et al*., 1999, 2007). GtRDB, a genomic tRNA database developed using tRNAscan-SE program which includes all eukaryotes and prokaryotic tRNA genes with an easy access to tRNA genes,

gene alignments and secondary structures (Lowe and Eddy, 1997). A list of the important bioinformatics programs available for studying the tRNA genomics are shown in Table 1.

Table 1. List of bioinformatics programs and databases available for tRNA genomics study

Program Name	Purpose	Website
tRNAscan-SE	tRNA gene identification	http://lowelab.ucsc.edu/tRNAscan-SE/
ARAGORN	tRNA gene identification	http://130.235.46.10/ARAGORN/
TFAM	Classification of tRNA gene families	http://tfam.lcb.uu.se
MFOLD/UNA Ffold	RNA Secondary structure prediction	http://frontend.bioinfo.rpi.edu/zukerm/export/mfold-3.html
Vienna RNA package	RNA secondary structure prediction	http://www.tbi.univie.ac.at/RNA/
GtRDB STAR	Genomic tRNA database Structure analysis of RNA	http://lowelab.ucsc.edu/GtRNAdb/ http://wwwbio.leidenuniv.nl/~Batenburg/STAR.html

Bacterial tRNA genes are present in single to multiple copies and are sometimes associated with rRNA gens (rRNA operons); with protein coding genes (mixed operons). Many of the tRNA genes are organized into transcripts containing a tandem array of tRNAs (tRNA operons). In most of the prokaryotes rRNA operons are organized in different structural patterns. In *E. coli* the seven rRNA operons are arranged in three different patterns which include the following in the 5' to 3' direction: 16S-Ile-Ala-23S-5S (*rrnA* and *rrnH*); 16S -Ile-Ala-23S-5S-Thr-5S (*rrnD*); 16S-Glu-23S-5S (*rrnB, rrnC, rrnE,* and *rrnG*); (Liao, 2000; Condon *et al*., 1995). They are widely spread among

different organisms; however some prokaryotes don't have such operons in them. In comparison to *E. coli*, *B. subtilis* has 10 rRNA operons which are highly clustered near the origin of replication (Lafauci *et al*., 1986; Samarrai *et al*., 2011) and are present in two different structural patterns which includes 16S- 23S-5S-tRNAs (*rrnB, rrnD, rrnE, rrnH, rrnI, rrnJ, rrnG* and *rrnW) and* 16S-Ile-Ala-23S-5S(*rrnA* and *rrnO*) (Liao, 2000; Dittmar *et al*., 2004). In *B. subtilis* 57 tRNA genes are associated with rRNA operons of which 53 tRNA genes are located immediate downstream of 5S rRNA gene (Dittmar *et al*., 2004). Whereas *E. coli* has only 14 tRNA genes associated with rRNA operons and of which only 4 are located immediate downstream of 5S rRNA gene (Dittmar *et al*., 2004) suggesting the huge variation and diversity in arrangements. In lactic acid bacteria all rRNA operons have a conserved 16S-23S-5S pattern with variations in location and types of tRNA genes within them. The number of tRNA genes following the 5S rRNA varies from 14-21 among different lactic acid bacteria (de Vries *et al*., 2006). The significance of such arrangements in different organisms and processing of polycistronic tRNA transcript is not evident. However structure determination of such polycistronic tRNA transcripts may provide clues for understanding their processing pathways.

In *E. coli* the optimal codons reflect the composition genomic tRNA pool. Optimal codons help in achieving faster and accurate translation and is based on the content of isoacceptors and the strength of interaction between codon and anticodon (Ikemura, 1981; 1982; Kanaya *et al*., 1999). The extent of codon bias is highly variable among genes in a given species (Comeron and Aguade, 1998). In fast growing organisms such as *E. coli* and yeast codon bias is highly dependent on the levels of isoacceptor tRNAs and level of gene expression to increase the translation efficiency (Ikemura, 1985;

Sharp and Li, 1987; Bulmer, 1991; Comeron and Aguade, 1998; Kanaya *et al*., 1999). Whereas organisms with slow growing rates or with small genomes, optimal codons are usually absent. It is still not clear whether codon usage led to tRNA evolution or tRNA abundance to codon usage. The proportion of isoacceptor tRNAs is the major factor in shaping up the codon usage patterns. It is known that the abundance of tRNA species differ among various genomes and sometimes within the same genome during different growth stages (Ermolaeva, 2001). The strong preference for codon is highly correlated with the composition of tRNA pool (Ikemura, 1981; Ikemura 1985; Ermolaeva, 2001). However, it is still unclear that codon usage is the cause or consequence of tRNA abundance. Recently experimental evidences have shown that mRNA with preferred codons is translated at higher rate than mRNA with rare codons (Robinson *et al*., 1984; Sorensen *et al*., 1989).

1.2 Classification of ribonucleases and phylogeny of concatenated tRNA's

Ribonucleases are the enzymes that participate in the processing and degradation of different RNA species. These are classified into exoribonucleases (digest RNA from one end) and endoribonucleases (cleaves RNA in the center). Exoribonucleases are grouped into six super families and various subfamilies based on the sequence, distribution and phylogenetic relation among different organisms (Zuo and Deutscher, 2001). Phylogenetic analysis of exo- and endo-ribonucleases among different bacterial species revealed that species with same factory of ribonucleases fall into same group. This kind of grouping of organisms with factory of ribonucleases is highly similar to the phylogenetic tree (Fig.1) constructed by aligning tRNA gene sequences with spacer region included (Tang *et al*., 2004).

According to their phylogenetic analysis of concatenated tRNA's with spacer regions from different prokaryotic organisms demonstrated the phylogenetic relationship between the different prokaryotes (Tang *et al.,* 2004) and grouping of such organisms indicates the possible existence of similar tRNA processing mechanisms. According to the recent bioinformatics study based on the availability of ribonucleases involved in tRNA processing, bacterial species with similar set of ribonucleases are grouped together (Li *et al*., 2005). According to the phylogram generated based on tRNA gene and spacer sequences, the organisms which are grouped together (Fig. 1) are also grouped according to the set of ribonucleases present suggesting the significant correlation between the availability of factory of ribonucleases and tRNA gene organization with spacer sequence between them. These studies will suggest the possible relationship between the tRNA gene organization and the existence of type of tRNA processing pathway in terms of factory of different ribonucleases present. Additionally some sequence and structural features which are evolutionarily conserved within the mature tRNA may influence tRNA processing pathway.

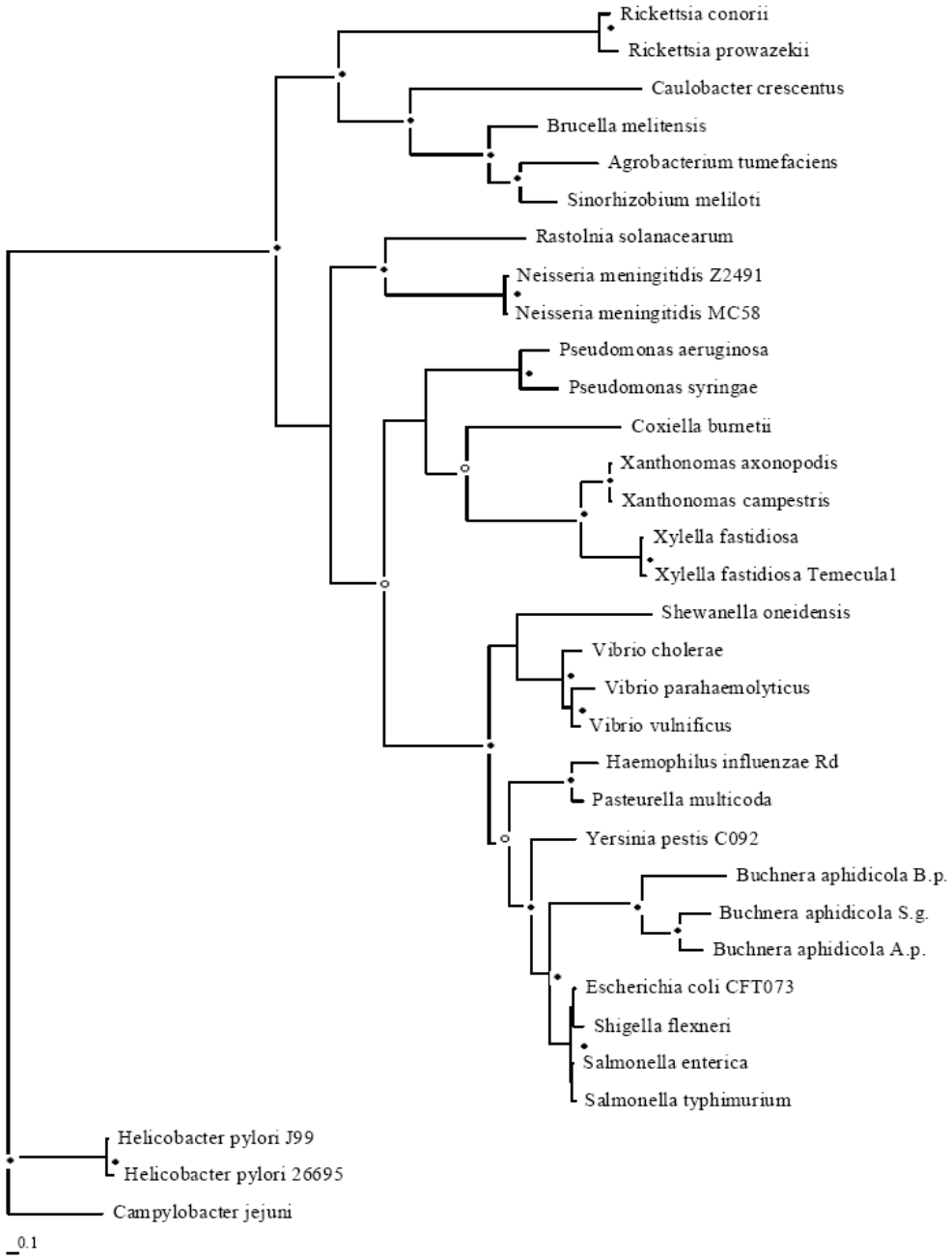

Figure 1. Phylogeny of concatenated tRNAs for the 38 bacterial species. Branch lengths are the maximum likelihood values for the consensus tree topology. (Tang *et al*., 2004).

1.3 tRNA processing

Living cells needs to produce and maintain functional transfer RNA (tRNA) pool constantly for efficient protein synthesis and cell viability (Ow and Kushner, 2002). In bacteria, the primary tRNA transcripts undergo processing at 5' and 3' end by several exo- and endo-ribonucleases and produce mature and functional tRNAs (Li and Deutscher, 1995, 1996, 2002). The processing defects in tRNA may lead to the formation of non-functional tRNAs which are subjected to quality control mechanisms (Li *et al*., 2002). tRNA processing deficiencies could lead to diseases (Holzmann and Rossmanith, 2009; Levinger *et al.*, 2004). In human mitochondrial genome, over 150 mutations have been reported to be associated with diseases and of them; a 100 are present in tRNA genes (Levinger *et al.*, 2004). *In vitro* studies revealed that these mutant tRNA transcripts were defective in the 3' end processing, CCA addition, and aminoacylation (Levinger *et al.*, 2004). These deficiencies may contribute individually or cumulatively to the progression of human mitochondrial diseases (Levinger *et al.*, 2004). However, as the 3' tRNA processing precedes the CCA addition and aminoacylation, deficiencies in tRNA 3' end processing may directly affect the CCA addition, aminoacylation, and result in disease.

1.3.1 Enzymes involved in tRNA processing

Ribonucleases are obligatory for cell viability and play an important role in the metabolism of RNA (Li and Deutscher, 2004). The catalytic action of ribonucleases involves processing of RNA precursors to their mature and functional forms and degrades those that are not needed for cellular activity (Li and Deutscher, 2004). To date 20 ribonucleases are present in *E. coli* that participate in the metabolism of different RNA

species includes tRNA, rRNA and mRNA (Li and Deutscher, 2004). These ribonucleases are categorized into two different classes based on their mode of action exo- and endo-ribonuclease. Exoribonucleases digest and release individual nucleotide residues in RNA from either 3’ or 5’ end (Li and Deutscher, 2004). Whereas endoribonucleases cleave RNA molecule internally and make RNA fragments of different sizes (Li and Deutscher, 2004).

Different sets of ribonucleases are involved in processing of 5’ and 3’ ends of tRNA. 5’ end processing is catalyzed by a ubiquitous endoribonuclease RNase P, a ribozyme with a RNA binding subunit and a 377 nt long RNA component. The protein component of RNase P called as C5 is 119 amino acids long and the combination of RNA and protein components constitutes the holoenzyme. It is well known that only RNA component can able to cleave tRNA precursor in the absence of C5 protein component *in vitro* (Takada *et al*., 1983). However under *in vivo* conditions C5 protein component enhances the cleavage reaction on tRNA precursors (Altman, 1990). Bacterial species have single RNase P RNA, with an exception of *B. subtilis* which has two RNase P RNA molecules which forms the dimer in holoenzyme.

Bacterial tRNA 3’ end processing is very complex and involves a factory of exo- and endo-ribonucleases. In *E. coli* 3’ end processing is initiated by an endoribonucleases RNase E and a set of Exoribonucleases such as PNPase, RNase II and RNase T, PH, BN and D. In *B. subtilis* 3’ end is processed by a single endoribonucleases RNase Z and is most common in majority of eukaryotes. RNase E is a multifunctional enzyme (Cohen and McDowall, 1997). It is a central component of RNA degradosome and involved in RNA degradation (Liou *et al*., 2001). RNase E contains multiple domains and N-terminal

domain having RNase activity is essential for cell viability and S1 domain is required for RNA binding but not essential for RNA cleavage (Bycroft *et al*., 1997; McDowell and Cohen, 1996). It cleaves in AU rich regions in 3' trailers of tRNA precursors.

Exoribonuclease RNase II belongs to RNR family of proteins which is the most active protein in *E. coli* and has 98% hydrolytic activity on poly(A) substrates (Cheng *et al*., 1998). It is specific to single stranded RNA and sensitive to secondary structures and its hydrolytic activity dramatically slows down on reaching double stranded DNA (Li and Deutscher, 2004). In tRNA processing it is involved in shortening longer 3' ends of tRNA precursors. Exoribonuclease PNPase belongs to PDX family proteins and is a part of RNA degradosome complex (Carpousis *et al*., 1994). PNPase catalyzes the degradation of RNA and in addition it can also act as a synthetic enzyme and in all reactions it requires a divalent Mg^{+2} ions (Li and Deutscher, 2004). In tRNA 3' end processing it is very important and in cells lacking PNPase tRNA precursors with long 3' trailers will accumulate to a significant level. Exoribonuclease RNase PH also belongs to the PDX family of proteins and acts as degradative enzyme in the presence of P_i (Kelly and Deutscher, 1992). The major function of RNase PH is the removal of last few residues and making mature tRNA 3' end. RNase T and RNase D both belong to DEDD family proteins (Li and Deutscher, 2004). RNase D is active on the residues present after CCA terminus and has less activity on mature tRNAs. It acts on tRNA molecules *in vivo* when it is expressed at elevated levels (Zhang and Deutscher, 1988). It functions as a backup enzyme for tRNA maturation when all tRNA maturation enzymes are missing (Li and Deutscher, 2004). RNase T participates in many metabolic processes of RNA and is essential for cell viability. RNase T for its catalytic activity requires a free 3' hydroxyl

group and actively works on single stranded substrates (Li and Deutscher, 2004). It has the ability to digest the single stranded RNA up to double strand region. It also involved in making mature 3’ ends of tRNA in *E. coli*.

1.3.2 tRNA processing pathways

In a well studied *E. coli* model, the primary polycistronic tRNA transcript undergo an initial endonucleolytic cleavage by RNase E a few nucleotides downstream of CCA terminus and generates individual pre-tRNAs with short or long 3’ trailers (Li and Deutscher, 2002). They form the substrate for the simultaneous action of both RNase P cleavage at 5’ end and 3’ exonucleolytic trimming. Pre-tRNAs with short and long 3’ trailers will undergo different exoribonuclease trimming pathways (Li and Deutscher, 1996). Long 3’ trailers will undergo an initial exonucleolytic trimming by RNase II, and PNPase which generates pre tRNAs with short 3’ trailers which is then followed by a series of exoribonuclease trimming action by RNase T, PH, D, II and BN amongst RNase T and PH plays an important role in removing the last few (2-4) nucleotides from CCA end to generate mature tRNA (Li and Deutscher, 1995, 1996) (Fig. 2).

An alternative tRNA processing pathway in *B. subtilis* has also been extensively studied, which involved the processing of both CCA-encoded and CCA-less tRNA transcripts (Pellegrini *et al*., 2003). CCA-less tRNA transcripts undergo an endoribonuclease cleavage by RNase Z at immediate downstream of discriminator base, followed by the addition of CCA sequence by tRNA nucleotidyl transferase (Fig. 2) (Pellegrini *et al*., 2003).

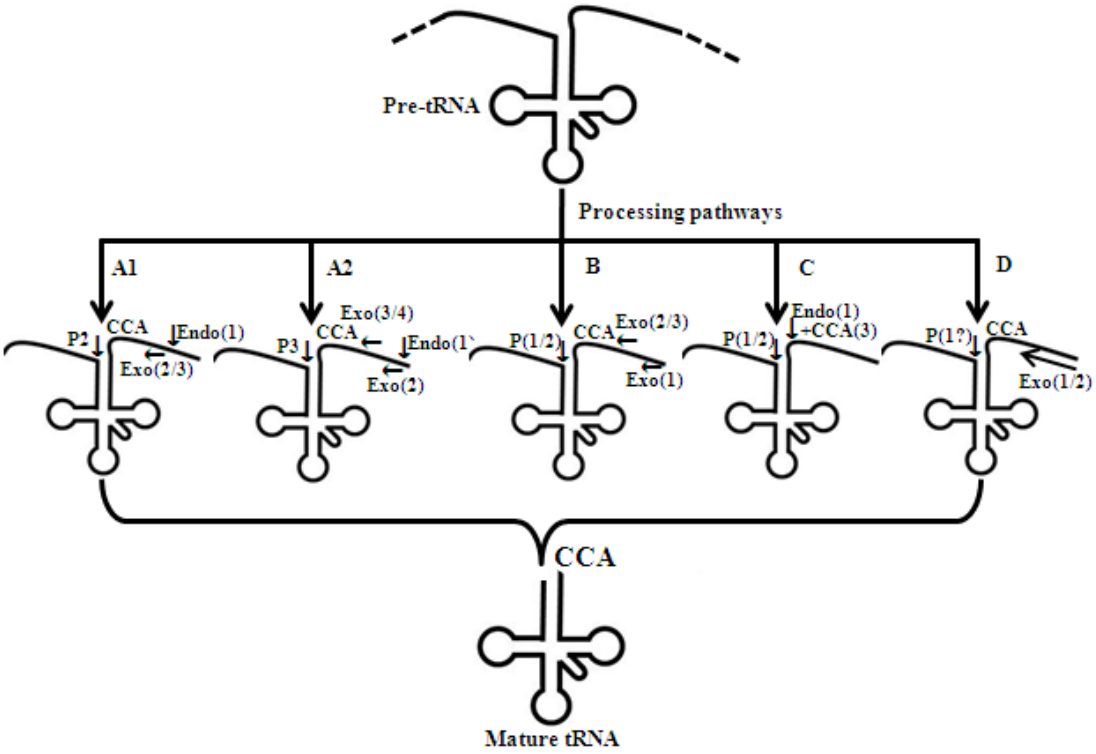

Figure 2. tRNA processing pathways in different bacterial species.(A1). tRNA processing pathway of *E. coli*, where short 3' trailers were processed.(A2). tRNA processing pathway of *E. coli*, where long 3' trailers were processed. (B). Processing of CCA-encoded tRNAs of *B. subtilis* by exoribonucleases. (C). Processing of CCA-less tRNAs of *B. subtilis* by endoribonuclease RNase Z. (D). tRNA 3' end processing of *M. genitalium* by RNase R. Vertical arrows on 5' leader and 3' trailer of RNA precursor represent the endoribonucleolytic cleavages and horizontal arrows represent the exoribonucleolytic trimming. P represent endoribonucleases RNase P, Endo in A1 and A2 represents the endoribonucleases RNase E. Exo in A1 represents RNase PH, T, BN and D, exo 2 in A2 represents RNase II and PNPase and exo 3/4 in A2 represents RNase PH, T, BN and D. In B, exo 2 represents PNPase and RNase R whereas exo 2/3 represents RNase PH. In C, endo represents RNase Z and in D exo represents RNase R. The numbers indicate the order of processing reactions and "/" indicate the alternative order of reactions while +CCA indicate the addition of CCA by tRNA nucleotidyl transferase.

However, the CCA-encoded tRNA transcripts undergo shortening of 3' trailers by exoribonucleases such as RNase R and PNPase and the fine trimming of last few residues by RNase PH, a process similar to *E. coli* (Fig. 2) (Pellegrini *et al*., 2003; Wen *et al*.,

2005). In *T. maritime,* the CCA-encoded tRNA transcript is processed at the 3' end by RNase Z cleavage at immediate downstream of CCA terminus (Minagawa, 2004). This is a single step mechanism for tRNA processing at 3' end by an endoribonuclease. However, the tRNA processing in organisms having a single exoribonuclease has not been studied extensively. A recent study demonstrated the involvement of RNase R in efficient removal of 3' trailers and maturation of tRNA 3' ends (Fig. 2) (Lalonde *et al*., 2007).

1.3.3 Processing of the 5' end of tRNA

RNase P is an important, ubiquitous ribozyme and the only 5' end processing endoribonuclease present in both prokaryotes and eukaryotes with few exceptions, where RNase P is absent (Willkomm *et al*., 2002). It is well known that RNase P RNA component's L15 region forms a Watson-Crick base pair with RCCA of tRNA 3' end and catalyzes the cleavage reaction (Kikovska *et al*., 2005; Wegscheid and Hartman, 2006) (Fig. 3). This interaction is essential both *in vivo* and *in vitro* for a precise cleavage (Wegscheid and Hartman, 2008). Importantly, disruption of any of the two base pairs results in reduced binding of RNase P RNA to tRNA precursor (Busch *et al*, 2000). Hyperthermophilic bacterium *Aquifex aeolicus* lacks both RNase P protein, and its RNA component; however, it makes the canonical 5' ends (Willkomm *et al*, 2002). Extracts of *A. aeolicus* revealed the presence of RNase E-like endoribonuclease, which cleaves in the AU rich elements in the spacer region of tandem pre-tRNAs and generates the mature 5' ends (Willkomm *et al*., 2002). Very recently, *Nanoarchaeum equitans* an archeon found without a universally conserved RNase P and bioinformatics studies revealed the existence of canonical 5' mature ends in their tRNAs located exactly at the transcription

start site which generates mature 5’ end without the need for RNase P (Randau et al 2008). It is important to note that RNase P RNA alone can cleave tRNA precursors at correct positions *in vitro* (Guerrier *et al.*, 1983).

B. subtilis which encodes both CCA and CCA less tRNAs and the processing of 5’ end with RNase P RNA may vary with CCA and CCA less tRNAs. A recent study demonstrated that 3’ CCA interaction with *B. subtilis* RNase P RNA is required for both *in vitro* and *in vivo* 5’ end processing suggesting that disturbances in this interaction inevitable for precise 5’ end processing (Wegscheid and Hartmann, 2007). However the 5’ end processing of CCA less tRNAs with RNase P RNA can occur with less efficiency. Previous studies demonstrated that *B. subtilis* contain two RNase P RNA and two RNase P protein molecules suggesting the diverse substrate recognition and processing mechanisms (Hansen *et al*., 2001). This can possibly provide the answer for the existence of two different mechanisms for 5’ end processing by RNase P RNA in *B. subtilis*. Previous studies demonstrated that $tRNA^{His}$ which is having ‘C’ at discriminator base position affect the interaction between discriminator C73 and U294 of M1 RNA resulting in mis-cleavage at -1 position and additionally replacement of U294 of RNase P RNA to G resulted in mis-cleavage suggesting the importance of U294 and discriminator base interaction in precise cleavage at 5’ end (Tallsjo *et al*., 1996; Brannvall and Kirsebom, 1999).

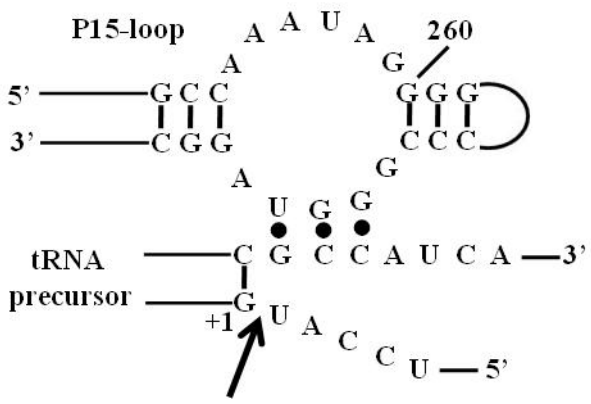

Figure 3. Illustration of UGG in P15 loop of RNase P RNA interaction with 3' RCCA of tRNA precursor. Arrow indicates the cleavage site and solid black dots indicate base pairings (Kikovska *et al*., 2005).

Bioinformatic studies revealed that 58 tRNAs in *E. coli* can potentially form base pair with discriminator base (Alluri and Li unpublished observations). $tRNA^{Arg}$ is the only species in *E. coli* K12 having two different discriminators A and G and among seven $tRNA^{Arg}$ five are encoded with wrong discriminator base A and the rest two with correct discriminator G (Alluri and Li unpublished observations). According to previous biochemical studies, ArgU tRNA contains discriminator G, whereas most other arginyl tRNA species contain discriminator A. These G or A discriminators can base pair with -1 nucleotide and affect the interaction of U294 and discriminator base resulting in miscleavage. Hence only one ArgX tRNA which cannot form base pair with functional discriminator G can undergo 5' end processing without miscleavage. Absence of such interaction between discriminator and U294 can results in miscleavage. According to discriminator analysis of *E. coli* K12 genome cysteinyl, histidinyl and glycinyl tRNA species possess discriminators U, C and U respectively which cannot base pair with U294 and hence mis-cleavage can occur in these tRNA species and among them $tRNA^{Cys}$ and

$tRNA^{His}$ are present in single copies (Alluri and Li unpublished observations). Recent biochemical studies demonstrated that additional base paring between discriminator and -1 result in the blocking of U294 and discriminator interaction and resulted in the 5' end cleavage at +1 in two steps (Brannvall *et al*., 2002). At first mis-cleavage occurs at -2 and divalent metal ions breaks the hydrogen bond between DB and -1 which results in the formation of base pair between U294 and DB and cleavage occurs at +1 resulting in mature 5' end (Brannvall *et al*., 2002). Those tRNAs which are not having complementary discriminator to U294 will be mis-cleaved and prone to degradation.

1.3.4 Mode of action of tRNA 3' end maturation enzymes

1.3.4.1 AU rich elements in the 3' trailer of a pre-tRNA are the sites of RNase E cleavage that initiates tRNA processing

Several sequence and structural features in tRNA affected the processing pathways. Previous studies demonstrated that the location of RNase E cleavage sites (AU rich regions) affected the processing pathways. RNase E cleavage sites are located in the AU rich elements (AUEs) present in the spacer region of primary tRNA transcript (Li *et al*., 2005). The location and abundance of AUEs may vary and determine the type of processing pathway. The abundance of AUEs is a prominent feature of bacterial group with RNase E and/G or their related proteins (Li *et al*., 2005). Extensive bioinformatics survey among diverse bacterial genomes revealed the abundance and conservation of AUEs within 10-nt from the downstream of 3' CCA and in lesser abundance in the succeeding regions in bacteria harboring RNase E enzymes (Li *et al*., 2005). Such pattern is absent in bacteria without RNase E, although the closely related RNase G may be present. The data suggest that RNase E initiate tRNA processing by cleaving at a AUE

site in the 3’ trailer in this subset of bacteria. Cleavage in this region by RNase E resulted in the production of individual pre-tRNAs for further processing. Primary tRNA transcript with AUEs located extreme downstream of CCA resulted in longer 3’ trailers, whereas the transcripts with AUEs located immediate downstream of CCA resulted in shorter 3’ trailers. The tRNA precursors with short 3’ trailers may prevent the formation of undesirable base pairings with 5’ leader sequence and helps in precise cleavage by RNase P at the 5’ end.

1.3.4.2 The 3’ terminal CCA sequence is an important determinant for correct 3’ end processing

Enzymes involved in the tRNA 3’ end maturation have specific sequences and structural preferences in the tRNA 3’ end in order to produce tRNAs with the CCA ends. In *E. coli*, RNase PH, and RNase T carried out the fine trimming of short 3’ trailers and the formation of mature 3’ CCA end (Li and Deutscher 1995, 1996). RNase PH trimmed off the 3’ trailers by phosphorolysis and released the nucleotide diphosphates. The precise mechanism how RNase PH stopped trimming at the CCA end is unclear. Recent studies have shown that the catalytic cleft of RNase PH protein can accommodate only a 4-nucleotide long single stranded RNA. This suggests one of the possible reasons for the termination of trimming action immediately after RCCA end. Crystal structure of RNase PH from *A. aeolicus* revealed that it resembled RNase P protein subunit suggesting that these two proteins may use common structural features for recognizing the tRNA 3’ end.

RNase T of *E. coli* is another 3’ end maturation enzyme, which has the ability to digest RNA up to first base pair, which is not the usual characteristic feature of other exoribonucleases (Zuo and Deutscher, 2002). Recent studies on RNase T specificity on

several RNA homopolymers and oligoribonucleotides revealed that it was able to discriminate pyrimidine residues and in particular, C residue. Studies demonstrated that RNase T activity was reduced by >100-fold by a single 3' C residue. More importantly 2-terminal 3' C residues completely abolished the enzyme activity (Zuo and Deutscher, 2002). RNase T specificity towards C residue might be due to the presence of phenylalanine side chains in the active site, which make van Der Walls interaction with A, U, or G but not with C residues (Jones *et al.*, 2001). Recent studies on crystal structure of RNase T-DNA complex revealed that RNase T dimer ideally binds to a duplex with a short 3' overhang and generate a duplex with a 2-nt or 1-nt 3' overhang. RNase T is able to screen out 3' – terminal cytosine residues, which caused disruptive conformational changes in the active site (Hsiao *et al*., 2011), which abolished the enzyme activity. In *B. subtilis* and other eukaryotes, tRNA 3' end is processed by RNase Z, which cleaved immediately after the discriminator base followed by the addition of CCA by tRNA nucleotidyl transferase. The CCA sequence located downstream of discriminator base inhibited RNase Z cleavage and most of the inhibition is due to the first C residue (Pellergini *et al*., 2003). All these studies demonstrated the importance of C residues at the 3' end of tRNA and strikingly, most of the tRNA 3' end maturation enzymes were inhibited by C residues.

1.3.4.3 The aminoacyl acceptor stem plays a major role in stopping exonucleolytic processing reactions at the mature 3' end

Acceptor stem also plays an important role in both 5' and 3' end tRNA processing (Levinger *et al*., 1995; Park *et al*., 2000; Li *et al*., 1998; Li and Deutscher, 2004). Previous studies in drosophila demonstrated that mis-folding of tRNA resulted in

reduced processing (Levinger *et al*., 1995). They also demonstrated that single base substitutions in acceptor stem resulted in reduced processing at both 5’ and 3’ ends; however, changes in anticodon stem does not affect processing, suggesting the importance of acceptor stem for both 5’ and 3’ end processing. It is also important to note that in *Drosophila*, both RNase P and 3’-tRNase appear to require similar substrate structure to maintain the catalytic fit (Levinger *et al*., 1995). *E. coli* $tRNA^{Phe}$ having single mismatch in the acceptor stem generated both correct and miscleavage products at the 5’ end by RNase P (Park *et al*., 2000). In addition, it was found that the terminal double-stranded stem structure present in the precursors of many stable RNA species is essential for exonucleolytic processing to stop correctly at the mature 3' end (Li *et al*., 1998; Li and Deutscher, 2004).

1.3.5 Purines are highly conserved at discriminator base position of tRNA among bacteria

Discriminator base is one of the major determinants for the addition of correct amino acid to the 3’ end of tRNA. Here we aim at analyzing the type of discriminator base and their conservation between two different bacterial species we are interested in. tRNA gene sequence information for this analysis was obtained from “Genomic tRNA Database” (Chan and Lowe, 2009). All tRNA gene sequences analyzed manually for discriminator base and are listed in a tabular form in Table 4. Analysis revealed that discriminator base in all tRNA species across the two bacterial species is highly conserved with A and G present in 17 tRNA species, C, and U in only 3 tRNA species. List of all tRNA genes and the conserved discriminator base for both *E. coli* and *M. genitalium* are listed in Table 2. The data provided here shows the conservation of

purines (A/G) at discriminator base position among the two bacterial species studied *E. coli* and *M. genitalium*. Importantly, only three tRNA species have been shown to have pyrimidines at discriminator base position. It is well known that in majority of aminoacylation systems discriminator base is an essential element for recognition by synthetase (Giege *et al*., 1998). Discriminator base in tRNA is highly essential for aminoacylation of tRNA in *E. coli*. Crystallographic studies revealed that, the specificity of discriminator base in aminoacylation is due to direct interaction with synthetase (Nagan *et al*., 2000). The other mechanism is by changing the confirmation of acceptor stem and facilitates aminoacylation (Puglisi *et al*., 1994). Studies on tRNA 5' end processing by RNase P have shown the importance of discriminator base for precise processing (Kikovska *et al*., 2005). However no study has shown its influence on 3' end processing. This data will helps in studying the role of discriminator base on 3' end processing and helps to evaluate why purines are highly conserved at this position. Future studies will also help to understand its significant conservation at evolutionary level.

Table 2. List of tRNA species with conserved discriminator base in *E. coli* and *M. genitalium*. In the Table, number beside the tRNA species represents the number of the respective genes present in the genome

Bacteria	***E. coli***				***M. genitalium***			
Discriminator Base	**A**	**G**	**C**	**U**	**A**	**G**	**C**	**U**
tRNAs	Ala-5 Ileu-3 Thr-5 Met-8 Leu-8 Lys-6 Val-7 Tyr-3 Pro-3 Phe-2	Asp-3 Arg-7 Gln-4 Ser-5 Asn-4 Glu-4 Trp-1	His-1	Cys-1 Gly-6	Ala-1 Ileu-1 Thr-3 Met-3 Leu-4 Lys-2 Val-1 Tyr-1 Pro-1 Phe-1	Asp-1 Arg-4 Gln-1 Ser-4 Asn-1 Glu-1 Trp-1	His-1	Cys-1 Gly-2

1.3.6 An extended base pairing from the aminoacyl acceptor stem of pre-tRNA alters the order of processing reactions

The influence of extended acceptor stem on the type of tRNA processing pathway and the order of ribonuclease actions involved has been well studied in *E. coli* (Li *et al*., 1998; Li and Deutscher, 2002). The primary transcript with additional base pairings undergoes an initial RNase E cleavage followed by RNase P and then a series of exoribonuclease trimming actions (Fig. 4). Whereas transcripts with no additional base pairings undergo an initial cleavage by RNase E, which is then simultaneously processed by RNase P and a set of exoribonucleases depending upon the length of 3' trailer (Fig. 4). Extensive base pairing between 5' leader and 3' trailer hindered the recognition of RNase P and inhibit processing (Ziehler *et al*., 2000). In *E. coli,* RNase P protein subunit recognized the unpaired 5' leader and RNA subunit interacted with 3' CCA and maintained the cleavage site (Stams *et al*., 1998). Studies have shown that tRNA precursors with long 5' leader sequences are the poor substrates for RNase Z cleavage in *B. subtilis,* demonstrating that some tRNA species may undergo initial RNase P cleavage followed by RNase Z (Pellegrini *et al*., 2003).

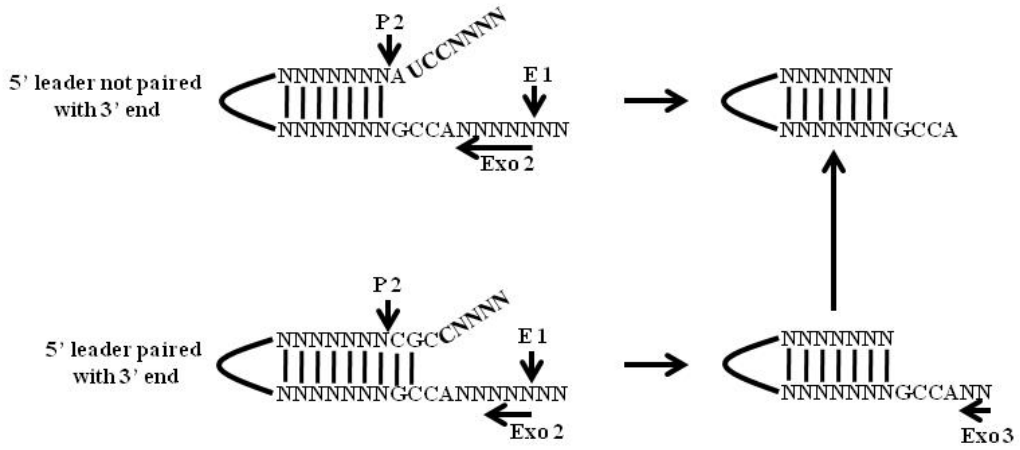

Figure 4. Influence of additional base pairing at acceptor stem on type of tRNA processing and order of ribonuclease reaction. Vertical arrows represent the endoribonucleolytic cleavages and horizontal arrows represent the exonucleolytic trimming. P and E represent endoribonucleases. The numbers indicate the order of processing reactions (Li and Deutscher, 2002).

1.3.7 Existence of extended base pairings in bacterial tRNA precursors: A bioinformatics analysis

Additional base pairings at acceptor stem region has significant effect on both 5' and 3' end processing and on the factory of ribonucleases involved. The influence of extended acceptor stem on the type tRNA processing pathway has been well studied in *E. coli* (Li *et al*., 1998 and Li and Deutscher, 2002). In brief, the primary transcript with additional base pairings undergoes an initial RNase E cleavage followed by RNase P and a series of exoribonuclease trimming actions. Whereas the transcripts without additional base pairings, undergo initial cleavage by RNase E which is then simultaneously processed by RNase P and a set of exoribonucleases depending on the length of 3' trailer (Fig. 4). tRNA primary transcript sequences from *E. coli* and *B. subtilis* genome were analyzed manually for additional base pair formation between 5' leader and 3' trailer

sequence. Additional base pairs between different base positions in tRNA primary transcripts in *E. coli* K12 strain and *B. subtilis* are listed in Tables 3 and 4. In brief, analysis of *E. coli* tRNA transcriptome revealed the presence of 26 tRNA genes without any additional base pairings, which accounts for 30% and the rest of the 60 tRNA genes, formed additional base pairs (Table 3). These tRNA genes can form either continuous or discontinuous additional base pairings. Very interestingly 14 tRNA genes were found to-

Table 3. **List of *E. coli* K12 tRNA species with additional base pairings between 5' leader and 3' trailer sequences**. In the belowTable, -1, -2, -3 and -4 represents the upstream nucleosides to the mature tRNA 5' end. DB represents discriminator base.

Base pair between	**Number of tRNAs**	**tRNA genes**
No base pairs	26	alaW, argX, glyW, glyV, ileV, ileU, ileT, lysW, lysY, lysQ, lysV, thrV,tyrU, leuZ, leuP, lysT, metW, metV, metY, selC, thrW, glyT, ileY, valT, valZ, hisR
-1 and DB	39	argU, argW, cyst, gltU, gltV, glyX, glyY, ilex, leuT, leuQ, lysZ, metU, proK, proM, serW, serX, trpT, tyrV, argQ, argZ, argY, argV, asnT, asnW, asnU, asnV, glyU, metT, pheV, pheU, serU, valV, alaV, alaU, alaT, glnW, leuW, serT, valW
-1, -2 and DB, first C of CCA	14	aspV, glnX, leuV, lysT, proL, serV, thrT, tyrT, valX, valY, alaX, glnV, gltW, gltT
-1, -2, -3, and DB, two CC of CCA	4	aspU, aspT, leuU, leuX
-2, -3 first and second C	2	glnU, metZ
-1,-3,-4 and DB, second C and A of CCA	1	thrU

-be potentially form two and 4 tRNA genes with 3 continuous additional base pairings. Interestingly a large number of 39 tRNAs were found to form a single additional base pair (Table 3). In *B. subtilis*, the 37 tRNA genes form a single additional base pairing and only 4 tRNA species with continuous 2 additional base pairs (Table 4). The bioinformatics data provided here on additional base pairings will helps in understanding the type of tRNA processing the tRNAs will undergo according to their classification.

Table 4. List of *B. Subtilis* CCA encoding tRNA species with additional base pairings between 5' leader and 3' trailer sequences. In the figure legend -1, -2, -3 and -4 represents the upstream nucleosides to the mature tRNA 5' end. DB rerepresents discriminator base

Base pair between	Number of tRNAs	tRNA genes
No base pairs	18	O-Ala, A-Ala, J-Lys, J-Gly, I-Gly, SL-Glu2, S-Lys, E-Arg, E-Gly, D-Phe, D-Gly, SL-Gly1, B-Gly2, B-Phe, B-Gly1, B-Lys, Y-Asp, Y-Glu
-1 and DB	37	O-Ile, SL-Ser1, A-Ile, SL-Met1, J-Val, J-Thr, J-Arg, J-Pro, J-Ala, I-Arg, I-Pro, I-Ala, SL-Val1, S-Asn, S-Ser, E-Met, E-Asp, D-Asn, D-Ser, D-Val, D-Met, D-Asp, D-Trp, D-His, D-Leu1, B-Ser, B-Ile2, B-His, B-Asp, B-Met2, B-Ser1, B-Met3, B-Met1, B-pro, B-Arg, B-Thr, B-Val
-1, -2 and DB, first C of CCA	4	SL-Tyr1, S-Gln, D-Tyr, B-Asn
-2, -3 and CC of CCA	NIL	NIL
-1, -2, -3 and DB, two CC of CCA	NIL	NIL
-1 ,-3,-4 and DB, second C and A of CCA	1	B-Leu1

Bioinformatics analysis revealed that there are 18 tRNA species in *E. coli* which can potentially form 2 and 3 continuous additional base pairings at acceptor stem which involve base pairing of 5' leader sequence with discriminator and CC of CCA. Among these four tRNA species aspU, aspT, leuU and leuX will form three continuous additional base pairings at acceptor stem with discriminator and CC of CCA, which blocks the watson crick base pairing with P15-loop of RNase P RNA with discriminator and CC residues and may affects 5' end processing. Biochemical analysis of such tRNA species for 5' end processing by RNase P was not studied yet. According to a recent biochemical study the binding and cleavage efficiency of RNase P is affected by replacement of G+1, C+72 with U+1 A+72 (Kikovska *et al*.,2005). According to the data provided (Table 3) 14 tRNAs in *E. coli* are with UA/AU at +1 and + 72 positions respectively and hence 5' end processing of these tRNAs may be affected by RNase P due to inefficient binding and cleavage. Previous studies demonstrated that $tRNA^{His}$ which is having 'C' as discriminator affect the interaction between discriminator C73 and U294 of RNase P RNA resulting in miscleavage at -1. Also replacement of U294 of RNase P RNA to G resulted in miscleavage suggesting the importance of U294 and discriminator base interaction in precise cleavage at 5' end (Tallsjo *et al*., 1996; Brannvall and Kirsebom, 1999). According the data provided 58 tRNAs (Table 3) in *E. coli* can pair with discriminator base. Absence of interaction between discriminator and U294 of RNase P RNA can results in miscleavage. According discriminator analysis of *E. coli* K12 genome, cysteinyl, histidinyl and glycinyl tRNA species possess discriminators U, C and U respectively which cannot base pair with U294 and hence miscleavage can occur in these tRNA species and among them $tRNA^{cys}$ and $tRNA^{his}$ are present in single copies.

Hence extensive bioinformatics analysis of tRNA species among different organisms will reveal the existence of different tRNA processing pathways.

1.4 tRNA quality control

Structural and sequence variations in tRNA precursor can lead to hypo or hyper-processing and generate aberrant tRNAs which will undergo degradation by exoribonucleases via polyadenylation by polyadenylate polymerase (PAP) (Li *et al*., 2002) (Fig. 5). Accumulation of defective, nonfunctional tRNAs can cause deleterious effects on cell growth and thus degradation or repair of defective tRNAs is an inevitable process.

The processing of tRNAs by exo- and endoribonucleases generates fully matured and functional tRNAs, however due to some structural or sequence (mutations) variations some tRNAs may not be processed or processed less efficiently. In general these aberrant tRNAs which are not functional and has to be degraded or corrected in order to maintain the quality of tRNAs for error free translation and to protect the cell from its deleterious effects. Organisms must have developed mechanisms to degrade or repair such tRNAs. Recent studies demonstrated that aberrant tRNAs get polyadenylated by poly (A) polymerase (PAP) which forms the signaling feature of aberrant tRNA to subsequently undergo degradation by PNPase (Li *et al*., 2002) and by RNase R (Deutscher, 2003). A previous study demonstrated that Hfq protein interacts with PAP and stimulates RNA polyadenylation (Mohanty *et al*., 2004) and which can undergo degradation by exonucleases indicating its indirect role in RNA degradation. Another study has shown that Hfq binds poly (A) and protect RNA from RNase E and exonucleolytic degradation (Folichon *et al*., 2003). Role of helicases in the degradation of RNA is evident however

its role in tRNA degradation has not been studied in prokaryotes. Recent study in eukaryotes demonstrated that helicases play an important role in degradation of hypo-modified polyadenylated tRNA in which it helps in the unwinding of structured tRNA (Wang *et al*., 2008). According to the model developed by Li *et al*., 2002, tRNA precursors can undergo degradation at different processing steps via polyadenylation by PAP and can even undergo degradation directly by exoribonucleases without polyadenylation (Fig. 5).

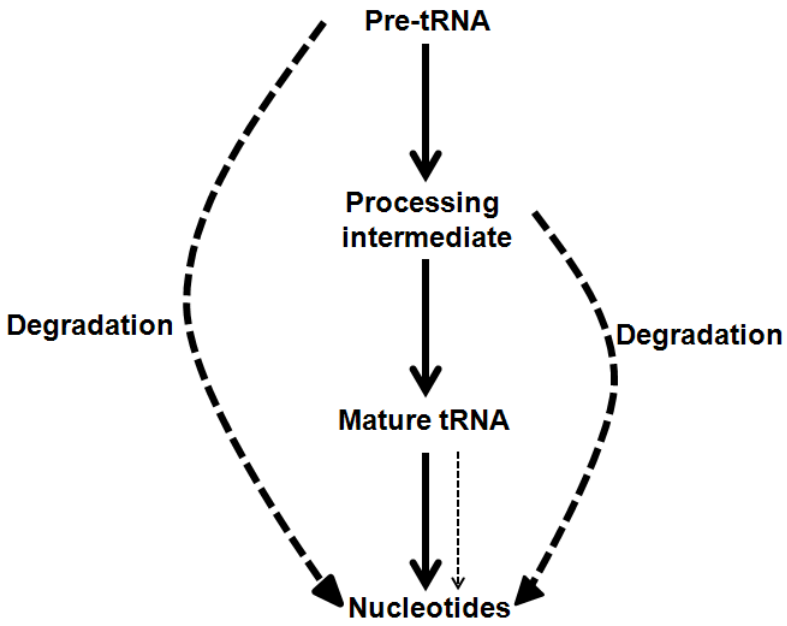

Figure 5. **Pre-tRNA degradation pathways, a model for quality control of tRNA precursors.** Defective tRNA precursors are polyadenylated by poly(A) polymerase, and subjected to degradation at relatively faster rate by PNPase and other RNases. The processing intermediates are also subjected to degradation by the same pathway. However the mature tRNAs maybe degraded at a low efficiency (indicated by thin dashed arrow). In the figure dashed arrows indicates the degradation steps and the thickness of arrows indicates the relative rates of degradation process. This figure is modified from the source, Li *et al*., 2002.

tRNAs with unusual secondary structures and confirmations can block precise cleavage sites for processing enzymes and may allow other alternative sites for cleavage.

This can result in miscleavage and production of aberrant tRNAs prone to degradation. A previous study in *B. subtilis* demonstrated that tRNAs with altered confirmations are processed by RNase P RNA which resulted in specific RNA fragments by a process called “hyper-processing” (Hori *et al*., 2001). A similar kind of report demonstrated that conformational changes in the secondary structure of tRNA can result in the hyper-processing activity of *B. subtilis* RNase P RNA which cleaves 5’ end at mature site and further cleaves internally leading to fragmentation which is similar to the action of *E. coli* M1 RNA (Hori *et al*., 2001). A recent study demonstrated that mitochondrial like (mt-like) tRNAs in *E. coli* which forms unusual secondary structures with altered anticodon and D-loop structures which undergo hypo-processing at their 5’ end and get cleaved internally (Bourdeau *et al*., 2001) and these can be targets for polyadenylation and subsequent degradation. Recent studies demonstrated that double mutants of tRNA modifying enzymes resulted in reduced levels of tRNA suggesting the rapid degradation of hypo-modified tRNAs indicating the importance of nonessential modifications for maintaining tRNA stability and otherwise they can be subjected to degradation pathway (Alexandrov *et al*., 2006). tRNA defects such as a mutation which destabilizes it resulted in significant increase in the amount of rRNA which has effect on protein synthesis (Slagter-Jager *et al*., 2007). tRNAs with mismatches at acceptor stem can lead to miscleavage by RNase P RNA which may be partly due to lack of cleavage sites and generate aberrant tRNAs which then undergo degradation. Supporting to this idea a study has been done on the effect of RNase P on tRNA with a single mismatch at acceptor stem which resulted in the generation of cleavage products with +1 and -8 cleavage (Park *et al*., 2000). Based on previous reports these - 8 cleavage products which are aberrant can

undergo degradation and moreover the rate of generation of +1 cleavage products will be reduced and may have an influential effect on mature tRNA turnover.

Mechanisms of tRNA degradation have been understood to a certain extent but the area of aberrant tRNA repair is poorly studied. One of such study demonstrated the repair mechanism of hyper-processed tRNAs in which RNase T can cleave A residue from CCA sequence which allow the fall off of CC and later repaired by CCA adding enzyme tRNA nucleotidyltransferase (Zuo and Deutscher, 2002). Another study demonstrated the repair of further truncations at 3' end caused by exoribonuclease activity in metazoan mitochondria in which loss of nucleotides upstream of CCA terminus by exoribonucleases were added upon incubation with the mitochondrial protein extract (Reichert and Morl, 2000) suggesting the existence of repair mechanism.

All these previous findings suggest that the tRNA quality control is more complex and involves several enzymes and exo- and endoribonucleases. These also suggest that tRNA structural variations, processing defects, mutations, mismatches at acceptor stem and hypo-modifications can results in fragmentation or miscleavage of tRNA which may undergo polyadenylation and degradation by exoribonucleases.

1.5 Oxidative stress and RNA quality control in *E. coli*

tRNA can be damaged under oxidative stress conditions. However, little is known about oxidation of any RNA species in general, and for tRNA specifically. Therefore, I will introduce RNA oxidation and quality control as a general problem in this section, and discuss tRNA relevant information when it is available.

Oxidative stress is an imbalance between ratio of oxidant and antioxidant where oxidant levels are higher leading to cell damage (Sies, 1991). Free radicals are chemical

molecules with unpaired electrons in their outer orbit and these are highly reactive and play an important role in many biological reactions. These free radicals include oxygen species such as superoxide (O_2^-), hydroxyl radical ($^{\bullet}OH$), and nitrogen species such as nitric oxide (NO). These free radicals also play a major role in many major age-related and neurodegenerative diseases such as Parkinson's (PD) (Sayre *et al*., 2001; Jenner, 2003), Alzheimer's (AD) (Nunomura *et al*., 2001; Lovell *et al*., 1999; Koppele *et al*., 1996), atherosclerosis (Singh and Jialal, 2006; Vogiatzi *et al*., 2009) etc. Cancers are also due to the action of free radicals with DNA, which cause mutations that might lead to malignancy (Hussain *et al*., 2003). Among all free radicals, superoxide (O_2^-) is a highly reactive molecule, which is produced as a byproduct of mitochondrial respiration. However, most of the organisms have isoforms of superoxide dismutase enzyme, which catalyze the dismutation of superoxide into H_2O_2 and oxygen. H_2O_2 upon interaction with Fe^{+2} produces a highly reactive hydroxyl radical ($^{\bullet}OH$) and hence, lethal to cells. Catalase catalyzes the decomposition of H_2O_2 to H_2O and O_2 molecules and prevents the destructive effects of H_2O_2. Phagocytes produce nitric oxide free radical as a product of immune response and these are highly diffusible and have long half-life apart from specific reactivity. These nitric oxide free radicals can also react with superoxide and produce highly reactive peroxinitrite (ONOO-), which can directly react with cellular components (Pacher *et al.*, 2007).

1.5.1 RNA oxidative damage

Recent studies were focused on RNA oxidation due its significant effect on several cellular processes. Earlier, it was speculated that cellular RNA is more prone to oxidative damage than DNA due to its single stranded nature, less association with

proteins, its availability in cytoplasm, close proximity to the mitochondria and the lack of oxidized RNA repair mechanisms (Radak and Boldogh, 2010; Li *et al*., 2006). Oxidative damage to RNA may even affect its function, may alter its structure, and causes obstructions in interaction between RNA and other macromolecules (Li *et al*., 2006). Oxidative damage to RNA and DNA and in particular mitochondrial DNA will play a major role in aging and neurodegeneration and associated neuronal loss (Nunomura *et al*., 1999; Melov, 2004; Beal, 2005). Comparative studies in human lung epithelial cells on the levels of oxidative damage to DNA and RNA revealed that RNA has 14-25 times higher oxidized guanosine adducts than in DNA (Hofer *et al*., 2005). Studies in astrocyte and neuronal cultures demonstrated that upon proteasome inhibition, RNA undergoes higher levels of oxidation than that of DNA (Ding *et al*., 2004). Recent studies also demonstrated that RNA oxidation occurred primarily in distinct neurons, which later undergo degeneration suggesting that RNA oxidation is an early event that precedes the cell death (Shan *et al*., 2007).

1.5.2 Types of RNA oxidative damages and methods to determine RNA oxidative damage

Recent studies found that more than 20 oxidized lesions were observed in DNA (Cooke *et al*., 2003). Oxidized forms of guanine such as 8-hydroxydeoxyguanine (8-oxo-dG) (Fig. 6) and 8-hydroxyguanine (8-oxo-G) are more prevalent in RNA and deleterious to the cells (Ames and Gold, 1991). 8-oxo-G has the ability to pair with adenine and thymine with a higher affinity along with cytosine, which results in mis-incorporation during replication and transcription and leads to translational errors (Li *et al*., 2006; Shibutani *et al*., 1991; Taddei *et al*., 1997). Apart from base damage under oxidative

stress, base excision is also a common event that occurs as a direct effect of oxidative damage to RNA/DNA or by removal of oxidized base in DNA via DNA N-glycosidases as an intermediate in the repair mechanism. These sites without bases are called abasic sites or apurinic sites (as most of them are purines) (Tanaka *et al*., 2011). Oxidative damage to RNA also cause strand breaks (Singh *et al*., 2004) and RNA cross-linking apart from base modifications.

Very few methods have been developed to determine the oxidative damage to RNA both qualitatively and quantitatively. Among these, quantification of oxidative lesions such as 8-oxo-G in RNA can be done by HPLC using an electrochemical detector (ECD) (Floyd *et al*., 1989). An immunohistochemical method was used to detect the *in situ* levels of 8-oxo-G in the brain sections of Alzheimer's patients (Nunomura *et al*., 1999) using monoclonal antibodies specific for 8-oxo-G. A northwestern approach was used to detect 8-oxo-G levels in mRNA species isolated from frozen postmortem brain tissues using monoclonal anti-8-OHG antibodies (Shan *et al*., 2003). The monoclonal antibodies 15A3 and IF7 have high affinity and specificity to 8-oxo-G (Park *et al*., 1992; Yin *et al*., 1995).

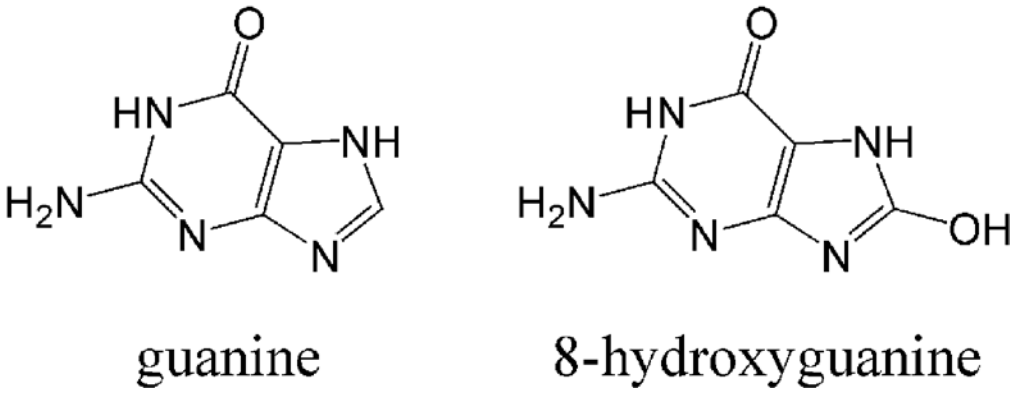

Figure 6. The structure of guanine and 8-hydroxyguanine (Li *et al*., 2006)

An ELISA (enzyme linked immunosorbent assay) method is also used to detect the extent of DNA damage in terms of 8-oxo-dG (Yin *et al*., 1995). Very recently, a method has been developed to efficiently quantify the extent of oxidative damage to RNA in terms of number of abasic sites. This approach used biotinylated Aldehyde Reactive Probe (ARP) that contained an amino oxy group, which specifically binds to abasic sites in RNA. This complex is further conjugated with streptavidin conjugated HRP (horseradish peroxidase) and quantified using enhanced chemiluminiscence (ECL) detection method (Tanaka *et al*., 2011).

1.5.3 RNA oxidation and role of metal ions

ROS originated because of a reaction between molecular oxygen with redox-active metals such as copper and iron (Halliwell and Gutteridge, 1999). Studies have shown that an elevated level of copper and iron in the brain tissue is the consequence of normal aging in mice (Morita *et al*., 1994; Maynard *et al*., 2002). Cu^{+2} and Fe^{+3} ions induced protein aggregation (Atwood *et al*., 1998) and these metal ions were present at higher concentrations in brain regions susceptible to neurodegeneration. Amyloid- β plaques in AD brains were found to have significantly higher concentration of Cu (400μM), Zn (1 mM), and Fe (1 mM) (Lovell *et al*., 1998; Smith *et al*., 1997). Previous studies have demonstrated that ribosomal RNA provides a binding site for metal ion binding such as redox-active iron. This forms the redox center in the cytoplasm of vulnerable neurons in AD and is a sign of neurodegeneration (Honda *et al*., 2005). According to earlier speculation, RNA is more prone to oxidation due to its single stranded nature. Recent studies from our laboratory also demonstrated that structure of rRNA, and tRNA promotes higher oxidation; however, their denatured forms have

significantly lower levels of 8-oxo-G (Liu *et al*., 2012). This could be because stable RNA structure can accommodate more metal ions than their denatured forms, which facilitate the chemical induced oxidation to a higher level (Honda *et al*., 2005).

1.5.4 Consequences of RNA oxidation

Effect of oxidized mRNAs on translation has been reported and demonstrated that it can cause translational errors. Studies found that when human cells were transfected with oxidized mRNA encoding luciferase protein, short polypeptides were observed which were increased with increase in 8-oxo-G content (Tanaka *et al*., 2007). These short polypeptides were also found when *in vitro* oxidized mRNA used in cell free translation system (Tanaka *et al*., 2007). Formation of short polypeptides might be due to premature termination of translation or by proteolytic degradation of the full-length protein. Specific mRNA species are more susceptible to oxidative damage than others and the protein production corresponding to the oxidized mRNA was significantly reduced due to stalling of ribosomes on oxidized bases in mRNA (Shan, 2007). Under chemically induced oxidative stress by H_2O_2, Met-misacylation increases by 10-fold (Netzer *et al*., 2009) and poses problems on the fidelity of tRNA aminoacylation. Impairment of ribosomal function in cortical areas of Alzheimer's disease is linked to increased RNA oxidation and reduced levels of rRNA and tRNA (Ding *et al*., 2005). In yeast cells, upon treatment with H_2O_2, 86% of the ribosomal proteins were oxidized and the pull down assays revealed the cross-linking of oxidized proteins with RNA molecules having ribose residue with 2', 3'-hydroxyl groups (Mirzaei and Regnier, 2006).

1.5.5 Quality control of oxidized RNA

This idea of oxidized RNA quality control is supported by the fact that 8-oxo-G levels of RNA drops dramatically after removal of oxidative stress insult. Studies have shown that pulse treatment of cultured human lung epithelia cells with H_2O_2 resulted in quick elevation of 8-oxo-G levels and their levels decreased after 24 h (Hofer e*t al*., 2005). HeLa cells when subjected to a pulse H_2O_2 treatment 8-oxo-G levels increased and dropped by 50% in 60 min and gradually reached to baseline (Wu and Li, 2008). It is also important to know that when *E. coli*, cells subjected to H_2O_2 treatment, a sharp increase in 8-oxo-G level will drops to the base level when the cells are transferred to fresh medium (Liu *et al*., 2012). These results indicate that cells have developed a mechanism to keep the levels of oxidized RNA under control especially by degrading it and the exact mechanisms are still unclear.

It is well known that multiple RNases are involved in removing the aberrant RNA as a quality control mechanism and it is common to propose that the same RNases might be responsible for removing the oxidized RNA. In *E. coli*, ribonucleases, poly (A) polymerase, and RNA helicases may help in removal of oxidatively damaged RNA. Previous studies on *E. coli* PNPase, an exoribonuclease, and an integral component of RNA degradosome complex demonstrated that it binds with specific affinity to 8-oxo-G containing synthetic RNA (Hayakawa *et al*., 2001). A similar study on *E. coli* PNPase was also demonstrated that it binds with oxidized RNA with higher affinity in a dose-dependent manner (Wu *et al*., 2009). Interestingly, PNPase affinity towards oxidized RNA is not dependent association with the degradosome or with RhlB. They also found that cells lacking PNPase are sensitive to oxidative stress caused by H_2O_2. However,

introduction of *pnp* gene rescued cells from H_2O_2 induced stress. Very interestingly, in cells lacking PNPase, 8-oxo-G containing RNA accumulated to a significant level suggesting its possible role in removing the oxidized RNA (Wu *et al*., 2009). Human PNPase (hPNPase) over expression reduced the levels of 8-oxo-G in RNA and increased the cell viability of HeLa cells, which were exposed to H_2O_2. They have also shown that knockdown of hPNPase resulted in accumulation of 8-oxo-G containing RNA and reduces the cell viability (Wu and Li, 2008).

Recent studies from our laboratory have shown the role of RNase II, R, and PAP in controlling the oxidized RNA levels under oxidative stress (unpublished observations). However, it is still unknown how proteins recognize oxidized RNA and steps involved in its degradation. Studies have shown that individual ribonucleotides can be oxidized by ROS attack directly or by degradation of oxidized RNA and can be incorporated into the RNA during transcription. It is interesting to know that under oxidative stress conditions leucocytes produced higher levels of 8-oxo-G containing nucleotides (Shen *et al*., 2000). Incorporation of oxidized ribonucleotides into the newly synthesizing RNA is limited due to mechanisms exist that reduce the incorporation of damaged ribonucleotides into RNA (Hayakawa *et al*., 1999). *E. coli* DNA repair protein such as MutT prevents the incorporation of 8-oxo-GTP into RNA by degrading it to 8-oxo-GDP and GMP (Taddei *et al*., 1997). However, *E. coli* RNA polymerase can incorporate 8-oxo-GMP into RNA at a much lower efficiency (Taddei *et al*., 1997). These studies demonstrated the existence of quality control mechanism against oxidized RNA and the importance of deciphering the precise mechanisms.

1.6 Objectives of the present study

In conclusion, in bacterial species the tRNA processing is very complex and depends on several factors from tRNA gene arrangements to availability of ribonucleases. Structural and sequence features within tRNA and in the spacer regions are also very important determinants of tRNA processing. tRNAs which are aberrant are prone to degradation by ribonucleases and mostly by poly(A) polymerase pathway and additionally mature tRNA also undergo degradation but at very low efficiency. In general several RNA species undergo quality control under different cellular stress conditions. Importantly under oxidative stress conditions RNA species undergo oxidative damage and are specifically degraded by quality control mechanisms. Several known proteins such as PNPase having high affinity to oxidized RNA are involved in the degradation of oxidized RNA. The role of other unknown proteins having the same affinity to oxidized RNA has to be elucidated.

The first objective of my study is to understand how a single exoribonuclease, RNase R of *M. genitalium*, carries out tRNA 3' end processing. Additionally we also interested to study and unravel the structural and sequence determinants of RNase R in tRNA 3' end processing. This will help us to understand and explore how different bacterial species with minimal genome accomplish tRNA metabolism at tRNA processing perspective.

The second objective we are focusing my study is to understand the characteristics of tRNA damage under oxidative stress conditions and to decipher the factors which influence the higher oxidation levels of tRNA. This will help us to better

understand the structural features within different RNA species which aid in RNA oxidative damage.

The third objective of my study is to elucidate the role of a novel *E. coli* tRNA modification enzyme TruD in cell viability under oxidative stress conditions. Previous studies in our laboratory found TruD protein having high affinity to oxidized RNA. Our present studies focus on understanding the relation between oxidized RNA binding and cell viability and to decipher the molecular mechanisms behind it.

2. Materials and Methods

2.1 Materials

Oligodeoxynucleotides were synthesized by Integrated DNA Technologies Inc. (Coralville, IA). α-[^{32}P]UTP was purchased from GE Healthcare Inc. (Pittsburgh, PA). Genomic DNA of *M. genitalium* G37 was obtained from American Type Culture Collection (Manassas, VA). Taq DNA polymerase was the product of 5 Prime (Fisher Scientific, Pittsburgh, PA). T7 RNA polymerase and RNase inhibitor were obtained from New England Biolabs (Ipswich, MA). RNA 5' polyphosphatase was from EPICENTRE® Biotechnologies (Madison, WI). The plasmid pET15b harboring the gene encoding *M. genitalium* RNase R (pET-mgR) and the expression in *E. coli* strain Rosetta-gami 2(DE3)/pLysS were described previously. SequaGel for denaturing urea-polyacrylamide gel electrophoresis was the product of National Diagnostics (Atlanta, GA). All other chemicals and reagents were analytical grade. alamarBlue® from Invitrogen Life technologies (Grand Island, NY), GeneScreen Plus® hybridization transfer membrane from Perkin Elmer (Waltham, MA), MicroSpin G-25 columns from GE Healthcare (Piscataway, NJ), T4-polynucleotide kinase from NEB (Ipswich, MA). Biotinylated ARP (N'-aminooxymethylcarbonylhydrazino D-biotin), Odyssey Blocking Buffer from Li-COR (Lincoln, NE), Strepatavidin-Horse radish peroxidase from Rockland (Gilbertsville, PA), ECL Plus western blotting detection reagents from GE Healthcare (Piscataway, NJ).

QIAquick Gel Extraction Kit from QIAGEN (Valencia, CA), QIAprep Spin Miniprep plasmid isolation Kit from (Valencia, CA), and PURExpress® *In Vitro* Protein Synthesis Kit from NEB (Ipswich, MA). Methionine L-[^{35}S] was from Perkin Elmer (Waltham, MA).

2.2 Over expression and purification of *M. genitalium* RNase R

In order to prepare *M. genitalium* RNase R free of *E. coli* RNase R and II, a mutant of Rosetta-gami 2(DE3)/pLysS devoid of RNase R and RNase II was constructed by sequential P1 transduction of the *rnb::kan* and *rnr::kan* alleles (Li and Deutscher, 1996; Datsenko and Wanner, 2000). Expression and purification of *M. genitalium* RNase R were carried out as described (Lalonde *et al*., 2007) with minor modifications. Briefly, pET-mgR was transformed into Rosetta-gami 2(DE3)(*rnb*,*rnr*)/pLysS. Transformed cells were grown in LB medium at 37°C to OD_{600}=0.6, followed by induction using 1 mM isopropyl β-thiogalactopyranoside (IPTG) overnight at room temperature. Cells were chilled on ice, harvested, re suspended in buffer A (20 mM Tris-Cl, pH 7.5, 10% glycerol, 1 mM DTT), flash frozen in liquid nitrogen and stored at −80°C until further use. Frozen cell suspension was thawed on ice and lysed using French press at 12,000 psi in the presence of protease inhibitors and 10 μg/mL DNase I. All purifications steps were carried out at 4°C. The clarified crude extract was first applied to an AffiGel Blue column (GE Healthcare Inc.) equilibrated with Buffer A and eluted stepwise with increasing amounts of NaCl from 0.1 M to 1 M. Fractions containing MgR were pooled and applied to hydroxylapatite column (Bio-Rad Inc.) equilibrated with Buffer A containing 1 M NaCl. The MgR containing fractions are passed through desalting column (GE Healthcare Inc.) and flow through was applied to Superdex S200 column (GE Healthcare

Inc.). MgR protein was concentrated using Microcon centrifugation (Millipore Inc.) to 9 mg/ml, flash frozen in liquid nitrogen and stored at −80°C. For activity assays, small portion of protein was diluted to 0.5 mg/ml in storage buffer containing 10 mM Tris-Cl (pH 7.5), 25 mM NaCl, 40% glycerol, 0.5 mM DTT, and 12.5 μM EDTA and stored at −20°C. Purified RNase R was at least 99% pure based on a SDS-polyacrylamide gel electrophoresis analysis. The activity of the purified RNase R protein was confirmed by poly(A) degradation assays (Lalonde *et al*., 2007).

2.3 Synthesis of tRNA precursors

PCR product encoding the precursor to $tRNA^{Gly}_{1}$ under the control of a T7 promoter was generated using Taq DNA polymerase, *M. genitalium* genomic DNA template, and primers. The pre-$tRNA_1^{Gly}$ generated by run-off transcription starts at the mature 5' end of the tRNA and contains a 21–nt 3' trailer sequence (5'-ACTTGTGTGTCCTCCGTCTAT-3'). PCR products encoding derivatives of pre-$tRNA_1^{Gly}$ were generated using mutagenic primers and the DNA for pre-$tRNA_1^{Gly}$ as the template. Labeled precursors to $tRNA^{Gly}_{1}$ were made by *in vitro* transcription using these PCR products, T7 RNA polymerase, and α-[^{32}P]UTP as described previously (Lalonde *et al*., 2007) with 0.5 mM of the four nucleoside triphosphates. *In vitro* transcribed pre-tRNAs were purified using RNeasy®MinElute® Cleanup kit (QIAGEN, Valencia, CA).

2.4 Preparation of 5'-monophosphorylated RNA

In vitro transcribed pre-tRNAs containing 5'-triphosphate were treated with RNA 5' polyphosphatase which sequentially removes γ and β phosphates and produces 5'-monophosphate. Reactions were conducted according to the manufacturer's protocol. In brief, 5 μg of pre-tRNA transcript was incubated with 30 units of RNA 5'

polyphosphatase and 20 units of RNase inhibitor at 37°C for 30 min. Treated RNA was purified using RNeasy®MinElute® Cleanup kit.

2.5 *In vitro* tRNA processing reactions by purified RNase R

In vitro tRNA processing was carried out as described (Lalonde *et al*., 2007). After incubation at 37°C for 5 or 30 min, the reactions were stopped by the addition of two volumes of loading buffer (96% formamide and 1 mM EDTA). The products were separated on an 8% urea-polyacrylamide denaturing gel. The products in the gel were detected by autoradiography. Alternatively, the products were detected by Personal Molecular Imager (Bio-Rad, Hercules, CA) and were quantified using the accompanying Quantity One® software.

2.6 λDE3 lysogenization and verification of λDE3 Lysogens

Host strain to be lysogenized was grown in LB media supplemented with 0.2% maltose, 10 mM $MgSO_4$ and with appropriate antibiotics at 37°C to an OD_{600} of 0.5. At this point cells can be stored at 4°C up to 24 hrs until needed. To 1-10 µl of host cells 10^8 pfu of λDE3, 10^8 pfu of Helper Phage, and 10^8 pfu of Selection Phage Lyasates were added, mixed and incubate at 37°C for 20 min to allow the phage to adsorb to the host cells. Spread the mixture evenly onto the LB plates and incubated at 37°C overnight. Almost most of the surviving colonies will be λDE3 lysogens. Host strains to be tested for λDE3 lysogenization in grown LB supplemented with 0.2% maltose, 10 mM $MgSO_4$ with appropriate antibiotics at 37°C up to an OD_{600} of 0.5. Tester phage was diluted to 1–2×10^3 pfu/ml in 1X phage dilution buffer (20 mM Tris-Cl, pH 7.4, 1M NaCl, and 100 mM $MgSO_4$). In duplicate tubes 100 µl of the host cells were mixed with 100 µl of the

diluted phage and incubate at room temperature for 10 min. To the incubated mixture, 3 ml of molten top agarose (1% Tryptone, 0.5% NaCl (W/V), and 0.6% Agarose) kept at 47°C was added to each tube and poured one of the contents onto an LB plate and other onto LB plate supplemented with 0.4 mM IPTG which induces T7 RNA polymerase. Plates were left undisturbed for a few minutes and then incubate at room temperature overnight.

2.7 Competent cell preparation and transformation by heat shock

E. coli competent cells were prepared by standard $CaCl_2$ method. In brief, cells were grown up to 0.4 OD at 37 °C and centrifuged at 5,000 g for 5 min followed by washing the cells in 80 mM $MgSO_4$ and 20 mM $CaCl_2$. All reactions are carried out at 4 °C unless specified. Cells were pelleted by centrifugation and re-suspended in 0.1 M $CaCl_2$ and incubated in ice for 30 min. 75 µl of cells were mixed with plasmid of interest and incubated on ice for 30 min followed by a heat shock at 42°C for 90 sec. The mixture was kept on ice water immediately for about 2 min and 750 µl of fresh YT/LB media was added and incubated at 37 °C for 45 min and later, plated on YT/LB agar plates with respective antibiotics.

2.8 Construction of TruD active site mutants in plasmid vector pTRC99A

The TruD active site mutants D80N and D80T were constructed in pTRC99A were not expressed and sequencing results revealed the presence of stop codon at an active site region leading to the production of short peptide. In order to construct new active site mutants in pTRC99A vector we used the megaprimer PCR approach using site-specific mutagenic primers. We used the wild type TruD construct in pTRC99A vector as backbone DNA template for succeeding PCR amplifications. The first PCR

product was generated to the left end (5’ end) of plasmid which covers the start codon AUG and active site region using the primer combinations pTRC99A left primer: GGAAACAGATCATGATTGAGTTTGA which is having restriction sites for NcoI and D80N-B2: AGCATGTTTGTTTTTTTGCCCAGC (for D80N mutant); D80T-B2: AGCATGTTTGGTTTTTTGCCCAGC (for D80T mutant). The second PCR product was generated for right end (3’ end) of plasmid which covers the active site region and terminator using the prier combinations pTRC99A right primer: TAGAGGATCCCTTTGCGCAGCGT which is having the restriction site for BamHI and D80N-A2: GCTGGGCAAAAAAACAAACATGCT (for D80N mutant) and D80T-A2: GCTGGGCAAAAAACCAAACATGCT (for D80T mutant). The primers are designed in such a way that both PCR products have a common overlapping region of 50 bp covering the active site mutation region. The two PCR products were mixed in 1:1 ratio by volume and used as template for megaprimer PCR using primer combinations pTRC99A left primer and pTRC99A right primer. The PCR product generated were double digested with NcoI and BamHI and purified by PCR purification kit (QIAGEN) according to manufacturers’ protocol. The empty plasmid vector pTRC99A was also digested with same set of restriction enzymes, purified by gel extraction kit method (QIAGEN). Digested PCR product and digested plasmid were ligated in 3:1 ratio in nanograms by standard laboratory method. Ligation mix was transformed into DH5α competent cells using standard heat shock method and the resulting recombinant clones were further confirmed by DNA sequencing.

2.9 Preparation of S-100 bacterial cell extracts

50 ml of *E. coli* cells were grown overnight until saturation. This culture was scaled upto 1 liter of LB media and grown until the OD_{550} reached to an O.D of 1.0. Cells were collected by centrifugation at 4,500 g for 5 min at 4°C. Cells were re-suspended and washed twice with 300 ml of saline solution. Finally cells were weighed and for each gram of wet cells approximately 4 ml of S-100 cell extraction buffer (20 mM TrisAc pH7.5, 5 mM $MgAc_2$, 60 mM KAc, 1 mM EDTA, 1 mM DTT, and 5% Glycerol) was added and French-pressed at 1100 psi twice. The lysate was centrifuged at 30,000g for 30 min at 4°C. The supernatant was collected and centrifuged again at 100,000 g for 2 hrs at 4 °C. The resulting supernatant (S-100) was divided into aliquots, flash frozen in ethanol/dry ice bath, and stored at -80 °C.

2.10 RNA-protein binding assays using S-100 cell extracts

The 50-mer RNA oligonucleotide was oxidized *in vitro* at 37°C for 1 hr in a buffer containing 20 mM H_2O_2, 100 mM sodium phosphate buffer pH 6.8, 30 mM ascorbic acid and 3 µM Cu_2SO_4. Oxidized RNA was purified by ethanol precipitation and covalently linked to adipic acid dihydrazide agarose beads as described previously (Caputi *et al.*, 2004) with little modifications. In brief, 4000 picomoles of normal and *in vitro* oxidized 50-mer RNA oligonucleotide were treated with 5 mM sodium M periodate and 100 mM NaAc pH 5.0 for 1 hr at dark at room temperature. 250 µl of agarose beads were washed four times with 100 mM NaAc pH 5.0 by centrifugation at 300 rpm for 2 min and re-suspend in 1 ml of 100 mM NaAc pH 5.0. Periodate-treated RNA was mixed with washed agarose beads and incubated on a rotating shaker overnight at 4 °C. Unbound RNA washed 2X with 2M NaCl and 3X with buffer D (20 mM HEPES-KOH

pH 7.6, 5% (v/v) glycerol, 100 mM KCl, 0.2 mM EDTA and 0.5 mM DTT). To the RNA bound agarose beads 250 µl of S-100 cell extract was added and incubate at 30 °C rotating shaker for 30 min at 300 rpm. Nonspecifically bound proteins were washed 4X with buffer D by centrifugation at 2000 rpm for 2 min at room temperature. To the purified immobilized RNA-protein complex, 70 µl of 2X protein sample buffer was added and heated at 90°C for 10 min, spun down at top speed and supernatant was collected and 35 µl of sample ran on 10% SDS PAGE at 300 V for 40 min at 4°C. Gel was fixed for 1 hr with the fixing solution (50% methanol and 7% acetic acid) and stained with SYPRO Ruby overnight and visualized under transilluminator.

2.11 P1 transduction for mutagenesis

P1 lysate for transduction was prepared by mixing 250 µl of overnight grown cells with 12.5 µl of 100 mM 100 mM $CaCl_2$, and 1ul of starter P1 lysate and incubated at 37 °C for 15 min without shaking. To the mixture 25 ml of fresh YT along with antibiotics and $CaCl_2$ was added to 5 mM and continued shaking at 37 °C until cells lysed. 1 ml of chloroform was added to 10 ml of lysed cells vortexed and kept in ice several times and spun at 5000 rpm for 5 min and the supernatant which is P1 lysate was store at 4 °C. Cells to be transduced were grown in YT media overnight and 0.5 ml of culture and 0.5 ml of 0.015 M $CaCl_2$ and 0.03 M $MgSO_4$ along with 20 µl of P1 lysate were added and incubated at 37 °C for 20 without shaking. Cells were washed twice with 5 ml of fresh YT by centrifugation and re-suspended in 1 ml of YT with 20 mM sodium citrate and incubated at 37 °C for 1 hr. Spin down the cells and spread onto YT plates with antibiotics.

2.12 Total RNA isolation for 8-oxoG and abasic site measurements

Total RNA was isolated according to previous reports (Li *et al*., 1999) with modifications. In brief, cells were grown up to 0.5 OD at 550 nm and centrifuge 2 ml of cells at 13,000 rpm for 2 min at room temperature. The pellet was resuspended in 50 µl of lysis buffer (10 mM Tris-Cl pH7.4, 10 mM Na_2EDTA pH 7.4, 1% SDS, 10% glycerol and freshly prepared 10 mM DFOM). 500 µl of phenol: chloroform (9:1) and 450 µl of Chelex 100-treated DEPC H_2O were added and vortex for 20 sec and incubated at room temperature for 10 min with occasional vortexing. The lysate was centrifuge at 13,000 rpm for 5 min at room temperature and to the supernatant, 50 µl of 3 M Potassium Acetate (KOAc) and 400 µl of isopropanol mix were added and incubated at -20 °C for 2 hrs. The supernatant was spun at 20,000 g for 15 min at 4 °C and the RNA pellets were washed with 75% ethanol, twice. The pellet was dried under vacuum for 5 min and re-suspended in RNA digestion buffer for 8-oxo-G measurement and Chelex 100-treated H_2O for abasic site determination.

2.13 Preparation of tRNA and long RNA

50 ml of cells were grown up to 0.5 OD_{550} and pellet the cells by centrifugation at 5,000 g for 10 min at 4°C followed by re-suspending cells in 500 µl of 0.9% ice cold NaCl. 500 µl of 90% aqueous phenol (one volume) was added and incubated on a rotator shaker at 300 rpm at room temperature for 30 min. To this mixture, 50 µµl of chloroform was added and mixed for an additional 15 min at room temperature. The lysate was centrifuge at 22,000 g for 15 min and supernatant was transferred into a new tube containing 50 µl of 20% KOAc and 1.25 ml of ethanol mix and incubated at -20 °C for 2 hrs. RNA was pelleted by centrifugation at 22,000 g for 15 min at 4 °C and washed twice

with 75% ethanol. The pellet was air dried and re-suspended in 500 µl of 0.4 M NaAc, pH 7.0, at room temperature. This is the total RNA. To precipitate long RNA, 270 µl of isopropanol (0.54 volumes) was added to 500 µl of total RNA, mixed and centrifuged at 22,000 g for 15 min at 4°C. The pellet was the long RNA fraction, which can be washed and re-suspended in DEPC H_2O. To the supernatant, 220 µl (0.98 volumes combining) of isopropanol was added and incubated at -20 °C for 2 hrs followed by centrifugation at 22,000 g for 20 min and the pellet was re-suspended in DEPC H_2O, which contained tRNA.

2.14 DNA isolation for measuring abasic sites

Overnight grown *E. coli* cells (5 ml) were centrifuged and suspended in 600 µl of DNA lysis buffer (0.6% SDS, 1.2 µg/ml proteinase K and 20µg/ml RNase A in TE buffer). The suspension was incubated at 65 °C for 30-45 min. To the suspension, 100 µl of 5 M NaCl was added and mixed thoroughly. Secondly, 80 µl of CTAB/NaCl solution was added, and mixed, and incubated for 15 min at 65 °C. The mixture was extracted once with phenol:chloroform and once with chloroform:isoamylalcohol. The supernatant was mixed with one volume of isopropanol, and washed twice with 75% ethanol and re-suspended in H_2O.

2.15 *In vitro* oxidation of tRNA

tRNA was oxidized *in vitro* in 100 µl reaction volume containing 40 µg of tRNA, 10 µM of L-ascorbic acid, 10 mM sodium phosphate buffer pH 6.8, 1 µM $CuS0_4$ and 1 mM H_2O_2. Reaction mixture was incubated at 37°C for 1 hr and precipitated by 3 volumes of absolute ethanol and $1/10^{th}$ volume of 3 M KAc followed by 75% ethanol wash.

2.16 tRNA denaturation with heat

For heat denaturation of tRNA, all the contents of *in vitro* oxidation reaction mixture except H_2O_2 were heated in a thermal cycler (Mastercycler gradient-Eppendorf) with the heated lid at 95°C for the respective times points (1, 2, 4 and 8 min) and kept in ice water immediately to prevent renaturation of denatured tRNA.

2.17 Detection of 8-oxo-G levels by HPLC

Cells were grown in YT media up to 0.5 OD at 550 nm and treated with various concentrations of H_2O_2 and cells were collected at different time points as indicated. Total RNA was isolated as described previously (Li and Deutscher, 1995). Total RNA pellet was re-suspended in a mixture containing P1 nuclease and 25 mM NaAc and incubated at 37 °C for 1 hr. P1 nuclease digested RNA was then treated with bacterial alkaline phosphatase and then subjected to HPLC. 8-oxo-G levels were detected with EC detector at potential of +600 mV and guanosine was detected with UV absorbance at 254 nm.

2.18 ARP assay to detect abasic sites in RNA

Abasic sites in RNA have been detected as described before (Tanaka *et al*., 2011) with little modifications. In brief, 10 µg of total RNA was incubated with 2 mM biotinylated ARP (2 mM N'-aminooxymethylcarbonylhydrazino D-biotin) in TE buffer for 1 hr at 37°C followed by terminating the reaction with 50 mM formaldehyde. RNA was precipitated with 0.1 vol of 3M NaOAc pH 5.2 and 3 vol of absolute ethanol and incubated at -20 °C for 1 hr followed by ethanol washes and re-suspend in TE buffer. 1 µg of RNA was spotted on GeneScreen Plus membrane, air dried and cross linked with UV light at 600 mJ/cm^2 for 2 min, followed by pre-incubation in blocking solution (Li-

COR, Lincoln, NE) for 30 min at room temperature. Further membrane was incubated with streptavidin-Horseradish peroxidase (Rockland, Gilbertsville, PA) at 1: 20000 in blocking solution for 1 hr at room temperature. Membrane was washed 4X, 5 min each with PBS containing 0.05% Tween20. Develop the membrane with ECLPlus (GE Healthcare) chemiluminiscent reagent for 5 min according to manufacturer's protocol. Image was captured on x-ray film and using Licor CCD camera and the accompanying software provided by Licor was used to quantify the signal intensities.

2.19 *In vivo* site-directed mutagenesis of the D80 position of TruD protein

CA244 WT strains with the recombineering plasmid PC136 was grown in LB media at 30 °C overnight. Overnight grown culture was diluted at 1:100 ratio and continued shaking at 30 °C until the OD reaches 0.5-0.6. The cells were heat shocked at 42 °C in water bath for exactly 15 min to induce the PC136 plasmid and swirled in ice water slurry for 2 min and kept in ice water for 10 min. Cells were transferred to pre-cooled centrifuge tubes and spun at 8,000 rpm for 5 min at 4 °C. The supernatant was remove and the cells were re-suspended in 1 ml of ice cold sterile H_2O and transferred to 2 ml Eppendorf tube using cut tips. Cells were washed 2X with ice-cold sterile H_2O by centrifugation at 9,000 rpm for 30 sec. Finally cells were suspended in ice-cold sterile H_2O to$1/200^{th}$ of initial culture volume and immediately followed by electroporation. For electroporation, 100-200 ng of mutagenic DNA oligonucleotide was added to 40 µl of induced competent cells, mixed gently, and later, added to pre-chilled and dried electroporation cuvettes. Electroporation was carried out with 1.75 KV at 200 ohms and 25 microfarads with time constants between 4 and 4.8 microseconds. Immediately after electroporation 1 ml of LB media was added and cells were grown at 30 °C for 45 min

and cells were diluted to 10^{-6} and plated and incubated at 30 °C overnight. Positive clones were confirmed by colony PCR and sequencing.

2.20 Determination of cell viability by growth curve

Single colony was inoculated in LB media with antibiotics included until the OD_{600} reaches 0.5. Primary cultures were then diluted to 0.1 OD in fresh LB media with and without oxidants such as TBHP and H_2O_2 and without antibiotics and OD readings were recorded at time points as indicated.

2.21 Isolation and analysis of aminoacylated tRNA

Charged tRNAs are isolated according the previous reports (Kohrer and Rajbhandary, 2008) with slight modifications. In brief, cells were grown in LB media at 37 °C to 0.5 OD at 550 nm and cells are treated with 5 mM H_2O_2 and samples were collected for RNA isolation at time points 15, 30, and 60 min after treating cells with H_2O_2 and 0 min being without H_2O_2 treatment. 5 ml of cultures collected at indicated time points were centrifuged at 5000 rpm for 2 min at 4°C in Beckman Coulter centrifuge. Unless specified, all steps are performed at 4°C. Cell pellet was re-suspend in 500 µl of sodium acetate buffer (0.3 M sodium acetate pH 4.5-5.0, 10 mM Na_2EDTA) and one volume of phenol equilibrated with sodium acetate buffer was added. Contents were mixed by occasional vortexing for 15 seconds and kept in ice for 15 min with repeated vortexing once for every 5 min. Centrifuge at 12,000 g for 15 min and transfer the aqueous phase to new tube. RNA was precipitated with 2.5 volumes of ice-cold ethanol and kept at -20 °C for 2 hr and centrifuged at 12,000 g for 30 min followed by 70% ethanol wash. The pellet was air-dried on ice and re-suspended in 10 mM sodium acetate pH 4.5–5.0. Pellets were

then quickly frozen and stored at -80 °C until use or may be used immediately without freezing.

tRNAs and aminoacylated tRNAs are separated by acid gel electrophoresis according to previous reports (Kohrer and Rajbhandary, 2008). In brief, 6.5% polyacrylamide gel with 8M urea and 0.1 M NaOAc pH 5.0 was prepared with gel dimensions 0.4 mm × 20 cm × 45 cm. RNA samples were mixed with one volume of urea loading buffer (0.1 M sodium acetate pH 5.0, 8 M urea, 0.05% bromophenol blue and 0.05% xylene cyanol). Gel was pre-ran for 30 min at 4 °C in running buffer (0.1 M sodium acetate pH 5.0). 2-5 µg of RNA samples were loaded without heating and ran at 500 V for 15-18 hrs until the bromophenol blue dye reached to the bottom of the gel. After electrophoresis, RNA from gel was transferred to GeneScreen Plus membrane by electroblotting in transfer buffer (40 mM Tris–Cl pH 8.0, 2 mM Na_2EDTA) at 40V for 4 hrs. Membranes were treated by UV cross-linking using a UVP CL-1000 ultraviolet crosslinker at 600 mJ/CM^2 for 2 min, followed by Northern blotting analysis.

2.22 Northern blotting

Oligonucleotide probes were labeled at the 5' end with ^{32}P according to standard protocol. In brief, a mixture of 10 picomoles of probe in 1X T4 PNK buffer (NEB), 25 µCi of γ-[^{32}P] ATP, and 10 units of T4 polynucleotide kinase, in a 10 µl reaction volume was incubated at 37°C for 1 hr. Later, the reaction was stopped by heating at 65°C for 20 min. Purification of end-labeled reaction mixture was performed using the illustra MicroSpin G-25 Column according to manufacturer's protocol. In brief, the resin was re-suspended in the G-25 column by vortexing, and the column placed in a collection tube spin at 735 g for 1 min. About 20 µl of DEPC H_2O was added to the 10 µl of end labeled

reaction mixture, mixed and added to the center of the column matrix placed in new collection tube and spun at 735 x g for 2 min. The purified probe was stored at -20°C until further use. Northern blot of tRNA was performed according to previous reports with modifications. In brief, 2-6 µg of total RNA was loaded on to 8% urea polyacrylamide gel and was transferred to GeneScreen Plus® membrane by electroblotting using BioRad electroblotting apparatus in 1X TBE buffer at 40 V for 4 hr at 4 °C. The membrane was then cross linked in UVP CL-1000 ultraviolet crosslinker at 600 mJ/cm^2 for 2 min. Membrane was pre-hybridized at 42 °C for 4 hrs in pre-hybridization buffer (4X SSC, 0.5% SDS, 1X Denhardt's solution and 0.1 µg/µl of denatured salmon sperm DNA). Later hybridization was carried out in the presence of radiolabeled probe in hybridization buffer (6X SSC, 0.1% SDS, 1X Denhardt's solution and 0.1 µg/µl of denatured salmon sperm DNA) at 42 °C overnight. Post-hybridization membrane was washed one time with 1X SSC and 0.1% SDS and washed for the second time with 0.5X SSC and 0.1% SDS at 42 °C for 10 min each. Excess moisture was removed from the membrane and exposed to X-ray film or phosphor imager screen.

2.23 *In vitro* translation using NEB pure system

NEB pure translation system contains all the components necessary for protein synthesis with the amino acids mixture added separately. *In vitro* translation reaction was carried out with manufacturer's protocol. Briefly, 3 µg of *in vitro* oxidized tRNA was added additionally to pure system and in another reaction same amount (3 µg) of untreated tRNA was used. Positive control reaction was setup without addition of external supply of tRNA. Reactions were carried out with manufacturer's protocol using DHFR gene harboring plasmid as a template along with labeled ^{35}S methionine. The

reactions were set up at 37 °C for 2 hrs. Protein samples were run on 10% SDS polyacrylamide gel followed by fixing (45% methanol and 10% acetic acid), drying and exposure to X-ray film and/ or phosphor imager screen and quantified signal intensities by quantity-one software.

2.24 Western blot analysis with HEP conjugated anti-His antibody

Pulled down protein from each lysate were separated on a 10% SDS PAGE gel. The proteins were transferred by electroblotting to Protran nitrocellulose membrane (Schleicher and Schuell Inc.). The membrane was stained with 0.1%W/V Ponceau S in 5% V/V acetic acid (Sigma-Aldrich) for 1 min, and then destained with 25ml of 0.1M NaOH for 1min to show membrane-bound proteins. The membranes were blocked with 5% non-fat dry milk in TBST (20 mM Tris-Cl, pH 7.6, 136 mM NaCl, 0.1% Tween 20) for 2 hrs, briefly washed with TBS (omitting Tween 20 from TBST), and incubated overnight with HRP conjugated anti-his antibody (His-probe HRP, Santa Cruz Biotechnology) at 1:5000 dilution in TBST. After three 10-min washes with TBST containing 5% non-fat dry milk and one 5-min wash with TBS, the membrane was treated with ECL^{TM} system (GE Healthcare). The chemiluminescent signals were either collected by Odyssey® Fc (LI-COR) imaging system or by exposure to an X-ray film.

3. Results and Discussion

3.1 A Novel one-step mechanism for tRNA 3'-end maturation by the exoribonuclease RNase R of *Mycoplasma genitalium*

Essentially in all organisms, tRNA species are made from primary transcripts containing extra sequences. These extra sequences are removed by nucleolytic processing activities. The 5′-leader sequences in tRNA precursors are removed ubiquitously by RNase P. At the 3′-end, the extra sequences are removed by a variety of different mechanisms. In bacteria, tRNA 3′-processing may be accomplished by the actions of endo- or exoribonucleases or both (Condon, 2003; Li *et al*., 2005). In *Escherichia coli*, the primary tRNA transcript undergoes an initial cleavage by RNase E in its 3′-trailer downstream of the CCA sequence (Li and Deutscher, 2002; Ow and Kushner, 2002), followed by stepwise trimming reactions of the extra residues by multiple exoribonucleases, including RNases T, PH, D, II, and BN and polynucleotide phosphorylase (Li and Deutscher, 1994; 1996). In *Bacillus subtilis*, pre-tRNAs with an encoded CCA sequence are matured by exonucleolytic action at the 3′-end, whereas CCA-less tRNA precursors are cleaved by RNase Z after the discriminator base, followed by CCA addition (Pellegrini *et al*., 2003). In other bacteria such as *Thermotoga maritima*, the 3′-ends of tRNA are matured by a single endoribonucleolytic cleavage

after CCA by RNase Z (Minagawa *et al*., 2004). These data demonstrate the existence of diversified mechanisms of tRNA 3′-end maturation in bacteria.

Mycoplasma genitalium is the second smallest known bacterium and is considered as a model for an organism with a minimal genome. Exhaustive data mining revealed the existence of endoribonucleases RNases P, III, M5, and H3 and a single exoribonuclease, RNase R (Zuo and Deutscher, 2001; Condon and Putzer, 2002). It is unknown how this organism carries out RNA metabolism, a process usually requiring the action of numerous RNases in other bacteria. Surprisingly, none of the RNases listed above for tRNA 3′-maturation was identified in *M. genitalium* and related species (Li *et al*., 2005; Zuo and Deutscher, 2001; Condon and Putzer, 2002). Recently, we demonstrated that purified RNase R of *M. genitalium* exhibits 3′ → 5′ exoribonuclease activity that is somewhat different from the activities of its *E. coli* homologues RNases R and II (Lalonde *et al*., 2007). Interestingly, *M. genitalium* RNase R alone is able to remove 3′-trailers efficiently and to generate the mature tRNA 3′-end (Lalonde *et al*., 2007). In contrast, *E. coli* RNase R degrades pre-tRNA and other structural RNAs (Lalonde *et al*., 2007; Cheng and Deutscher, 2003; Vincent and Deutscher 2009), whereas *E. coli* RNase II generates mature tRNA poorly (Li and Deutscher, 1994; Lalonde *et al*., 2007). These observations suggest that in the presence of a limited number of RNases, *M. genitalium* RNase R may have acquired a unique exonucleolytic tRNA 3′-processing function.

To carry out tRNA 3′-maturation, *M. genitalium* RNase R must be able to recognize pre-tRNA and precisely remove the trailer sequences to form the mature 3′-end. Several sequence and structural features of tRNA have been previously shown to be

important for tRNA 3′-processing by other enzymes. For instance, the *E. coli* tRNA 3′-maturation exoribonuclease RNase T is strongly inhibited by C residues in the 3′-CCA sequence, suggesting a role for these C residues in stopping digestion of tRNA by this enzyme once the mature 3′-end is generated **(**Zuo and Deutscher, 2002). *B. subtilis* RNase Z cleaves CCA-less tRNA precursors after the discriminator base. However, its activity is inhibited if a C residue is present immediately downstream of the discriminator base (Pellegrini *et al*., 2003). In addition, it was found that the terminal double-stranded stem structure present in the precursors of many stable RNA species is essential for exonucleolytic processing to stop correctly at the mature 3′-end (Li *et al*., 1998; Li and Deutscher, 2004).

In this work, we report that *M. genitalium* RNase R demonstrates novel specificity for the nucleotide sequence and structure of a pre-tRNA, enabling tRNA 3′-maturation by one-step exonucleolytic removal of a relatively long 3′-trailer. This represents a unique mechanism of tRNA 3′-maturation by which organisms of minimal genome employ only a single exoribonuclease.

3.1.1 *M. genitalium* RNase R generates a mature 3′-end from pre-tRNA$_1^{Gly}$ containing a long 3′-trailer

The 95-nt pre-tRNA$_1^{Gly}$ construct starts with triphosphate at the mature 5′-end of the tRNA and contains a 21-nt trailer sequence with an –OH group at the 3′-end. Upon incubation with RNase R purified from *M. genitalium*, a 74-nt product corresponding to the size of the mature tRNA$_1^{Gly}$ was produced after 5 min and increased at 30 min (Fig. 1A, lanes 2 and 3). This product terminates at the mature 3′-end of tRNA$_1^{Gly}$ because it co-migrated with the 74-nt transcript of the same tRNA (Fig.7A, lane 7), and the 3′-

terminal sequence was previously confirmed by 3′-rapid amplification of cDNA ends (Lalonde *et al*., 2007). In contrast, incubation with buffer alone did not cause any change to the pre-tRNA (Fig. 8A and B, lanes 1 and 2). Formation of the mature tRNA by RNase R demonstrates that this enzyme alone is able to remove the entire 3′-trailer by an exonucleolytic action.

A 77-nt product was present in small amounts in some pre-$tRNA_1^{Gly}$ preparations (Fig. 7A, lane 4), presumably due to pre-termination of T7 RNA polymerase. This 77-nt product was also generated by incubation with RNase R, suggesting that it is a true processing intermediate of RNase R. In addition, a 72-nt product corresponding to tRNA lacking the terminal CA residues at the 3′-end was also produced by RNase R (Fig. 7A, lanes 2 and 3), indicating that this exoribonuclease is capable of removing nucleotide residues from the mature 3′-end.

We have also incubated the 74-nt transcript with RNase R. Interestingly, this RNA form was not digested by RNase R even after 30 min of incubation (Fig. 7B, lanes 2 and 3). This result suggests that the 72-nt product from pre-$tRNA_1^{Gly}$ (Fig. 7A, lanes 2 and 3) was probably generated from a longer 3′ terminus by processive exonucleolytic action of RNase R. Once the tRNA with a mature 3′-end is released from RNase R, it may become resistant to further trimming by the enzyme.

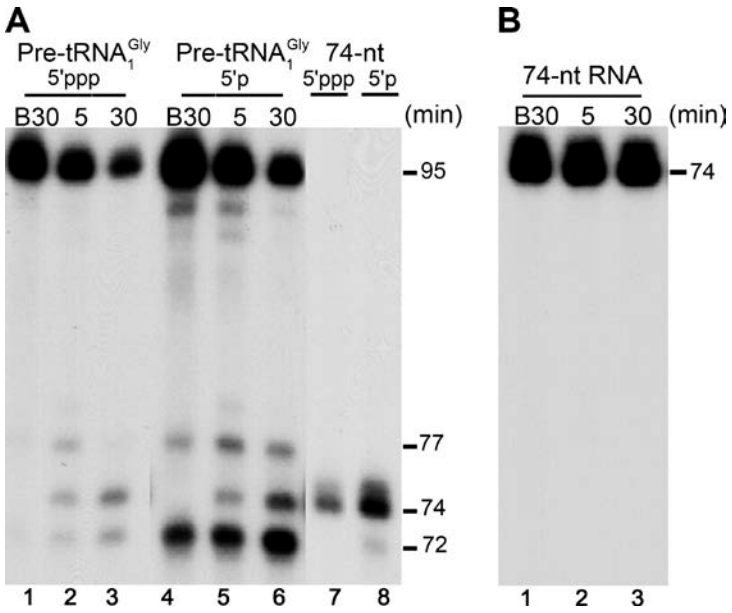

Figure 7. RNase R processes pre-tRNA$_1^{Gly}$ but not mature tRNA independent of 5' phosphorylation status. 5'ppp represents 5' triphosphate, and 5'p represents 5' monophosphate. The RNA substrates were uniformly labeled with ^{32}P, and were treated with RNase R for the length of time indicated at the top of the lanes. RNA products were separated and detected as described in Experimental Procedures. The sizes of RNA are marked on the right showing length in nucleotides. (A). The 95-nt pre-tRNA$_1^{Gly}$ constructs containing 5' tri- or mono-phosphate and a 21-nt 3' trailer were treated with RNase R. A 74-nt RNA corresponding to the mature tRNA$^{Gly}_1$ was included as size marker. (B). The 74-nt RNA transcript corresponding to the tRNA with mature 3' end was treated with RNase R. "B" denotes incubation with buffer for 30-min. Sizes of RNA products are labeled on the right

tRNA normally contains a 5′-monophosphate. To examine whether the 5′-triphosphate present in the *in vitro* transcript affects 3′-processing by RNase R, the pre-tRNA was treated with RNA 5′-polyphosphatase to generate a 5′-monophosphate (Fig. 7A, lane 4). Polyphosphatase treatment also produced a major 72-nt product along with some other minor products, probably due to contamination by a nuclease activity. When the 5′-monophosphate pre-tRNA$_1^{Gly}$ was treated with RNase R, the 77-, 74-, and 72-nt products were produced (Fig. 7A, lanes 5 and *6*) in a manner similar to those from the pre-tRNA with 5′-triphosphate, suggesting that the 5′-triphosphate does not have a

detectable effect on RNase R-mediated 3′-processing. Pre-tRNA constructs containing 5′-triphosphate were used in the subsequent experiments.

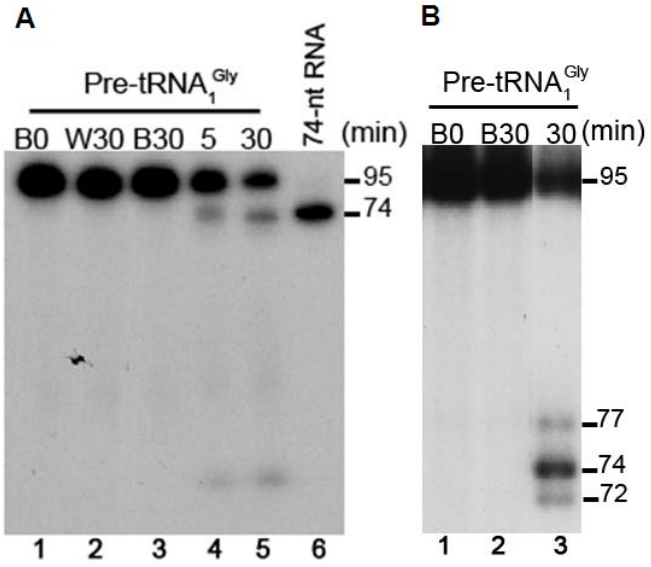

Figure 8. Pre-tRNA$_1^{Gly}$ was converted to shorter products by RNase R and was stable in reaction buffer. [^{32}P]-labeled pre-tRNA$_1^{Gly}$ was incubated with water, with reaction buffer, or with RNase R in reaction buffer. The length of time of incubation with RNase R is marked on top of the gel. B0 and B30 indicate incubation with buffer for 0 and 30 min respectively. W30 indicates incubation with water for 30 min. (A). The products were separated in a short 8 M urea/6% acrylamide gel and were detected by autoradiography. The 74-nt RNA was included as size marker. (B). The products were separated to single-nucleotide resolution.

3.1.2 Acceptor stem stops RNase R trimming at 4 nucleotides downstream of the double strand

Stable bacterial RNA species that undergo 3′-exonucleolytic processing share a common feature of having a stable double-stranded stem formed between the 5′ and 3′ termini, followed by 2–4 unpaired nucleotides at the mature 3′-end (Li *et al*., 1998). This feature supports the notion that stable stems function as “rulers” to stop exonucleolytic

trimming at the downstream mature 3′-ends. Being a processing exoribonuclease, *M. genitalium* RNase R may recognize the same terminal stem to stop at the mature 3′-end of tRNA.

To test this idea, a pre-tRNA construct (DS+3) containing a 3-bp extension in the acceptor stem (Fig. 9A) was treated with RNase R. This construct would produce a tRNA of 80 nt if RNase R stops 4 nt downstream of the stem. As shown in Fig. 9B (lanes 5 and 6), the expected 80-nt RNA and a minor 82-nt product formed after 5 min of incubation with RNase R and became more abundant after 30 min. Therefore, RNase R stops at similar distances downstream of the acceptor stem of DS+3 and pre-$tRNA_1^{Gly}$. The lack of the 2-nt shorter product from DS+3 is probably due to a higher stability of the extended stem and the presence of a new adenine discriminator in this construct (see below). Similar behavior was observed previously when a pre-tRNA containing 2 extra bp in the acceptor stem was treated with RNase R (Lalonde, 2006).

If the acceptor stem impedes RNase R digestion, disruption of the stem may fail to stop RNase R. This idea is well supported by the results in Fig. 2. Incubation of a 2-bp disruption construct (DS−2) with RNase R resulted in complete degradation of the pre-tRNA (Fig. 9B, lanes 8 and 9), demonstrating an essential role for a stable acceptor stem in stopping RNase R at the CCA terminus. Fig. 9C further demonstrates that base pair disruption at different positions in the acceptor stem resulted in different products, all at much reduced levels.

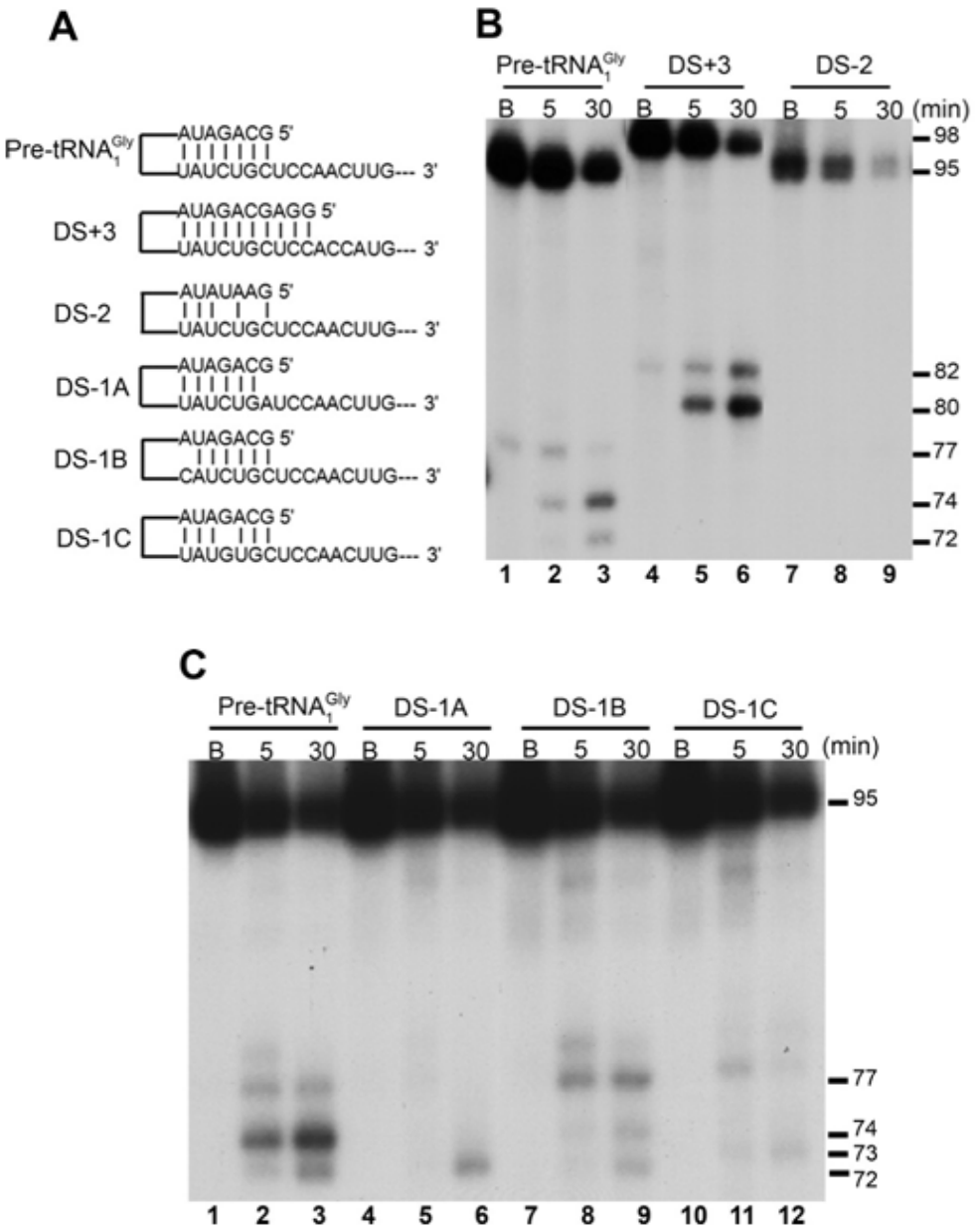

Figure 9. Processing of pre-tRNA$_1^{Gly}$ constructs containing variations in aminoacyl-acceptor stem. (A). Diagrammatic representation of pre-tRNA$_1^{Gly}$ and its derivatives containing extension or disruption in the acceptor stem. (B). Processing products of pre-tRNA$_1^{Gly}$ variants containing acceptor stem extension or 2-bp disruption by RNase R. (C). Processing products of pre-tRNA constructs containing 1-bp disrupted acceptor stem by RNase R. Time of incubation with RNase R or is marked on top. "B" denotes incubation with buffer for 30-min. Sizes of RNA products are labeled on the right.

Treatment of DS−1A (Fig. 9A) produced only the 72-nt product (Fig. 9C, lane 6), indicating that the terminal base pair is important for preventing the CCA terminus from being trimmed by RNase R. Similarly, a 73-nt RNA was generated at trace levels from DS−1C (Fig. 9C, lane 12), which lacks the middle base pair, probably due to a lowered stability of the stem.

Disruption of the base paring distal from the CCA terminus in DS−1B caused the least degradation and the formation of 74-nt RNA, albeit at a low level (Fig. 9C, lane 10). Apparently, 1-bp disruptions caused partial degradation and altered the positions where RNase R trimming stopped.

3.1.3 A and G are preferred discriminator bases for RNase R to stop at the mature 3′-end of tRNA

The discriminator base has been recognized as an important determinant for charging tRNA with its cognate amino acid (Giege *et al*., 1998) and for maturation of the 5′-end by RNase P (Kikovska *et al*., 2005). Here, we attempted to investigate the possible role of the discriminator residue in tRNA 3′-processing by RNase R. Figure. 10 shows the processing products of pre-tRNA constructs with the four different discriminators. Variations in the discriminator base caused a major change in the ratios of the 74- and 72-nt products and slightly affected the production of these products in combination from the pre-tRNAs. Pre-$tRNA_1^{Gly}$ containing the encoded discriminator U yielded a major 74-nt mature tRNA and a less abundant 72-nt RNA after incubation with RNase R (Fig. 10, lanes 2 and *3*). Substitution of the discriminator U with A or G increased the amount of mature tRNA (Fig. 10, lanes 5, 6, 8, and 9). In contrast, replacement of U with C produced increased levels of the shorter 72-nt product (Fig. 10, lanes 11 and 12). These

results indicate that purines are the preferred discriminator bases to prevent the digestion of the CCA terminus by RNase R.

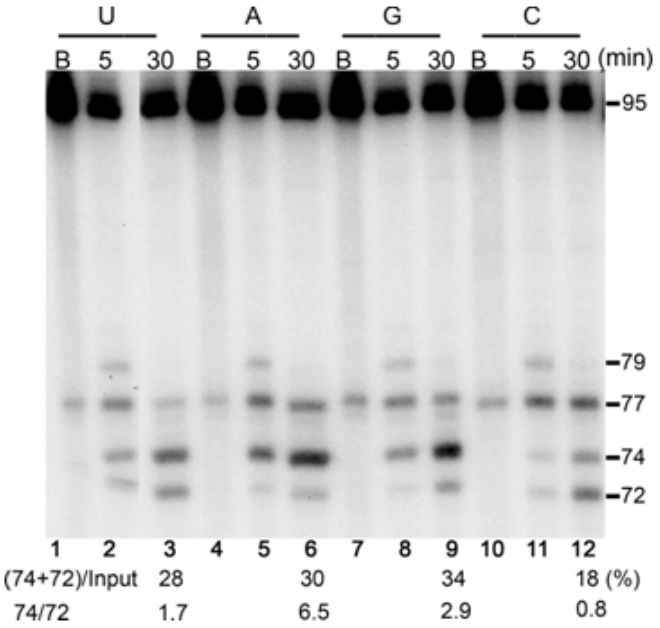

Figure 10. Processing of pre-tRNA$_1^{Gly}$ constructs containing various discriminator bases. Pre-tRNA$_1^{Gly}$ contains U as the discriminator encoded in *M. genitalium* genome. Discriminator variations are indicated on top. Incubation conditions and RNA sizes are marked as in previous figures. The products were quantified using a phosphoimager as described in Experimental Procedures. The percentage of the 74-nt and 72-nt products out of the input pre-tRNA (marked as "(74+72)/input") was calculated by the sum radioactivity of the two products divided by the total input radioactivity, normalized by the number of labeled U residues. The ratio of the 74-nt and 72-nt products (marked as "74/72") is also shown on the bottom of the gel. "B" denotes incubation with buffer for 30-min. Sizes of RNA products are labeled on the right

3.1.4 C residues in the CCA terminus play important roles in stopping RNase R at the mature 3′-end

Because the 3′-terminal CCA sequence has been implicated in tRNA 3′-maturation under a number of circumstances and because the trimming of CCA by RNase R was observed in this work, we studied whether the CCA sequence is a determinant for

RNase R-mediated tRNA processing. As shown in Fig. 11A (lanes 6 and 12), substitution of one or both C residues with A or G increased production of the 72-nt product. Substitution of the first C had more effect than that of the second C on conversion of 74-nt RNA to 72-nt RNA (Fig. 11A, lanes 3, 6, and 9). Notably, substitution of both C residues with purines resulted in a 10-fold increase in the 72-nt product (Fig. 11A, lanes 12 and 15).

In contrast, substitution of these cytidines with uridines caused little change in the relative amount of mature and 2-nt shorter products, although a moderate increase in the 72-nt product was observed by substitution at the first position (Fig. 11B). A similar effect of U substitutions was also observed when the pre-tRNA containing an A discriminator was treated with RNase R (Fig. 12). In addition, pre-tRNAs containing G, C, or U at the 3′ terminus generated more 74-nt RNA than the parent pre-$tRNA_1^{Gly}$ (Fig. 11*C*), suggesting that A is not the preferred nucleotide at the mature 3′-end for RNase R to stop correctly.

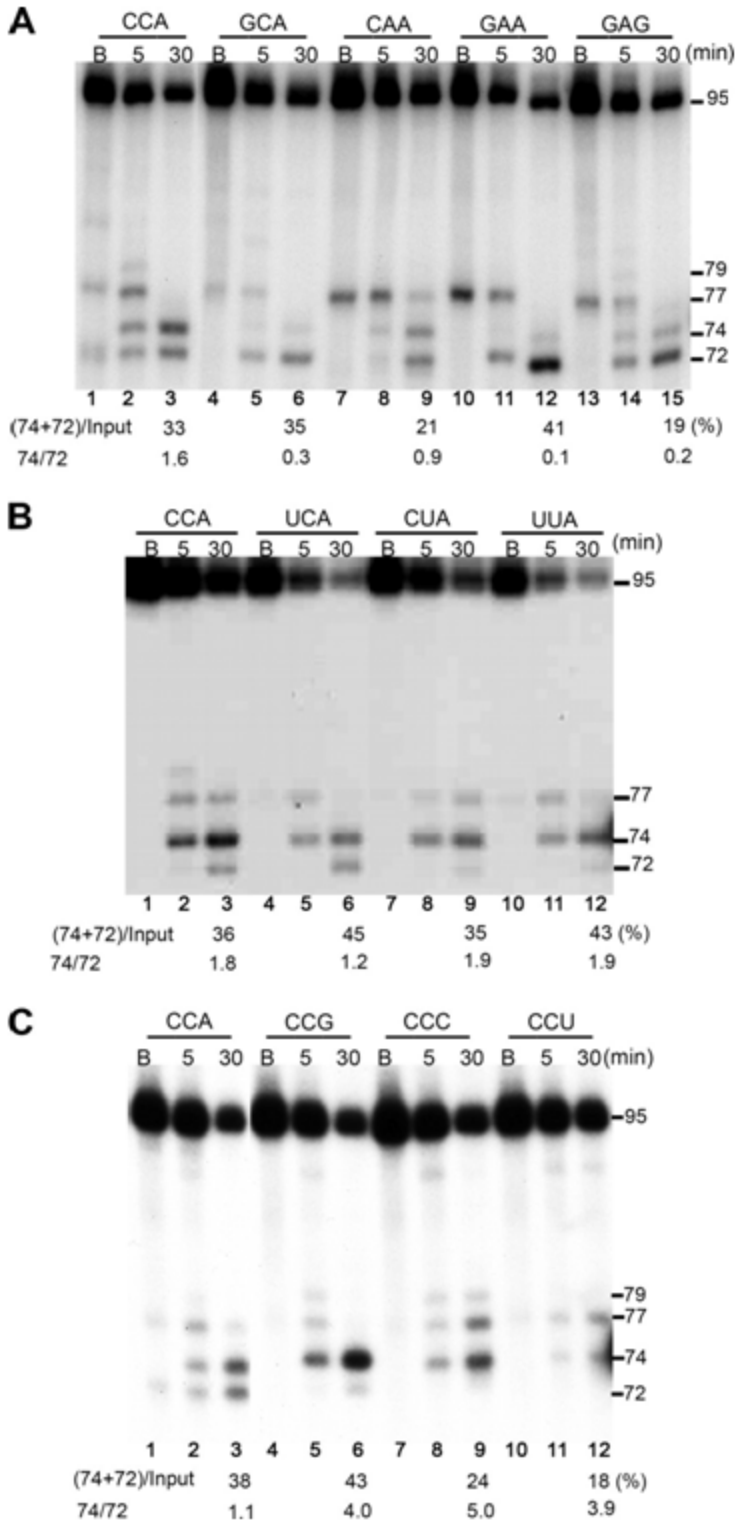

Figure 11. Processing of pre-tRNA$_1^{Gly}$ and its derivatives having substitutions in 3' CCA. Pre-tRNA$_1^{Gly}$ (CCA) and its CCA variants were incubated with RNase R for the indicated length of time on the top of the lanes. The lengths of the pre-

tRNAs and products were marked on the right. (A). Processing products of pre-tRNAs containing purine substitutions of one or more residues in the CCA sequence. (B). Processing products of pre-tRNAs containing substitutions of C by U in the CCA sequence. (C). Processing products of pre-$tRNA_1^{Gly}$ constructs containing substitutions in the 3' terminal A residue. The percentage of 74 and 72-nt products out of input substrates and the ratio of the 74 and 72-nt products are labeled on the bottom of the gel. “B” denotes incubation with buffer for 30-min. Sizes of RNA products are labeled on the right

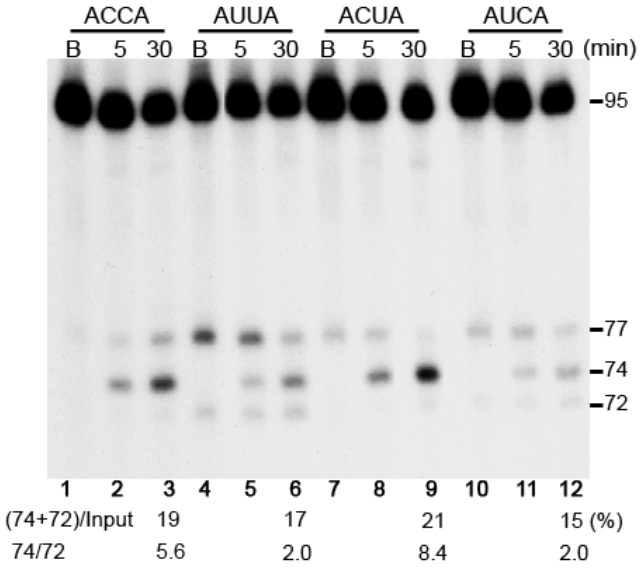

Figure 12. Processing products of pre-$tRNA_1^{Gly}$ constructs containing an adenine discriminator and C to U substitutions in the 3' terminal CCA sequence. Labeled pre-tRNAs were incubated with RNase R for 5 or 30 min or with buffer for 30 min (marked as “B”). The sizes of RNA substrates and products are marked on the right. The percentage of 74 and 72-nt products out of input RNA and the ratio of the 74-nt and 72-nt products are labeled on the bottom of the gel.

On the basis of the above observations, we also studied if the CCA sequence *per se* impedes RNase R degradation by examining pre-$tRNA_1^{Gly}$ derivatives with additional CCA sequences in the 3′-trailer (Fig. 13A). None of these constructs formed a predicted stable structure in the 3′-trailer. In all cases, the mature 74-nt tRNA and the 72-nt form were the main products (Fig. 13B), showing little variation among the pre-tRNAs. The downstream CCA sequences did not stop RNase R at their respective specific locations.

However, a +15-nt RNA was produced from constructs harboring one or two separated CCA sequences (Fig. 13B, lanes 5, 6, 8, and 9), and a +5-nt RNA formed from constructs with one or two tandem CCA sequences (lanes 11, 14, and 15). Interestingly, the +15- and +5-nt products terminate at the 3′-end of C-rich regions in these constructs, suggesting a possible role for C-rich sequence in resisting RNase R digestion.

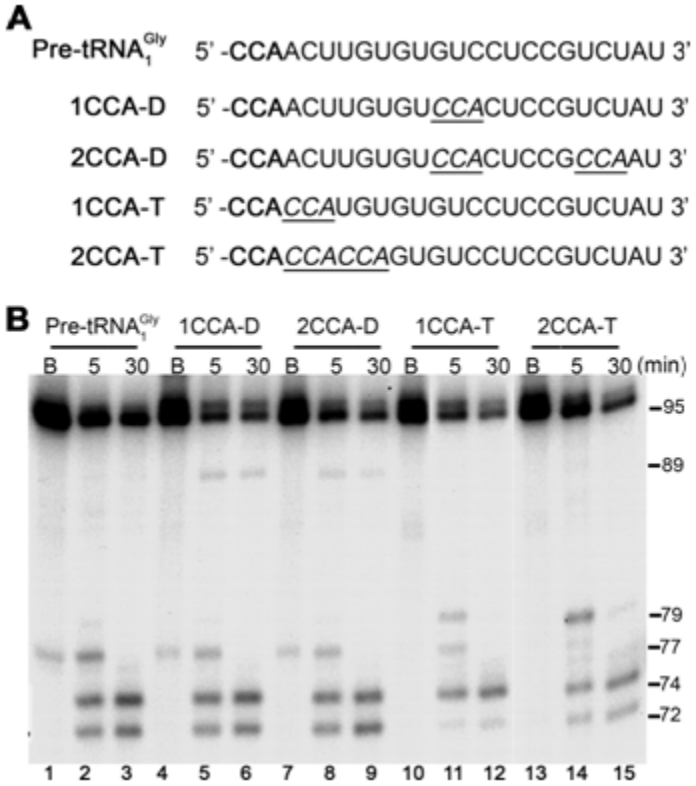

Figure 13. Processing products of pre-tRNA$_1^{Gly}$ constructs containing additional CCA sequence(s) in the 3' trailer. (A). 3' trailer sequences of the pre-tRNA constructs showing additional CCAs as underlined text. (B). Processing products of pre-tRNA$_1^{Gly}$ and additional CCA constructs.

3.1.5 Discussion

We have shown that the sole exoribonuclease identified in *M. genitalium*, RNase R, is able to generate mature tRNA from a transcript that contains a relatively long 3′-trailer sequence. The results in this study demonstrate a delicate mechanism of tRNA 3′-

maturation by which the entire 3′-trailer is removed in a single-step exonucleolytic action (Fig. 14). It is likely that RNase R acts processively on tRNA precursors. The precise removal of the 3′-trailer appears to depend on the ability of RNase R to recognize several sequence and structural features of the tRNA. RNase R processing activity is strongly inhibited by the aminoacyl-acceptor stem, stopping mainly 4 nt downstream of the stem to form the mature 3′-end. The discriminator residue and the terminal CCA sequence also play important roles in preventing further trimming of the mature 3′-end by RNase R. These findings suggest that RNase R is able to carry out tRNA 3′-maturation in *M. genitalium*. However, the results do not rule out the possibility that other factors may also play a role in tRNA 3′-end processing *in vivo*.

This unique mode of action of RNase R distinguishes this enzyme from exoribonucleases participating in tRNA processing in other bacteria (Condon, 2003; Li *et al*., 2005; Li and Deutscher, 2004). In *E. coli*, for example, the shortening of the long 3′-trailer in a tRNA precursor and the generation of the mature 3′-end are carried out by different RNases. The endoribonuclease RNase E and the processive exoribonucleases RNase II and polynucleotide phosphorylase can efficiently remove the long 3′-trailer, leaving a few extra residues at the 3′-end (Li and Deutscher, 2002). The last few 3′ extra residues are removed by any of the five exoribonucleases RNases T, PH, D, II, and BN, with T and PH being the most efficient enzymes.

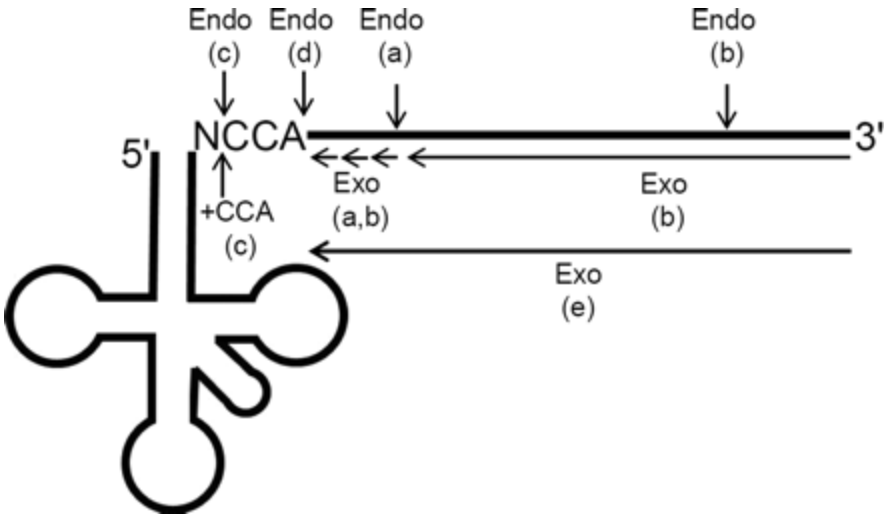

Figure 14. Mechanisms for removal of the 3′-trailer of bacterial tRNA precursors. The structure of a tRNA precursor containing an extra sequence at the 3′-end is shown. *Endo* and *Exo* represent endo- and exoribonucleases, the activities of which are marked by *vertical* and *horizontal arrows*, respectively. *Letters in parentheses* represent mechanisms by which the 3′-trailer can be removed. (a). The 3′-trailer is shortened by endonucleolytic cleavage at a few nucleotides downstream of CCA. The few extra residues are then removed exonucleolytically in a stepwise manner. This mechanism is represented in *E. coli* by the action of the endoribonucleases RNases E and P and by exoribonucleases RNases T, PH, D, II, and BN. (b). the 3′-trailer is shortened by exonucleolytic digestion, leaving a few nucleotides downstream of CCA that can be removed by the same exonucleolytic activities shown in (a). An endonuclease cleavage downstream of the 3′-trailer may precede the exonucleolytic digestion. In *E. coli*, the exonucleolytic shortening of the 3′-trailer is carried out by the processive exoribonucleases RNase II and polynucleotide phosphorylase. (c). the 3′-trailer of a precursor to CCA-less tRNA is removed endonucleolytically after the discriminator, and CCA is added by tRNA nucleotidyltransferase. An example of this mechanism is the endonucleolytic action of RNase Z in *B. subtilis*. (d). the 3′-trailer is removed by a single-step endonucleolytic cleavage after CCA, represented by the action of RNase Z in *T. maritima*. (e). the 3′-trailer is removed by a single-step exonucleolytic digestion, represented by the action of RNase R in *M. genitalium*.

RNases T, PH, D, and BN are highly specific for 3′-processing of tRNA and other stable RNA species, and they are inactive on most other RNA substrates (Li and Deutscher, 2004). Importantly, *M. genitalium* RNase R is able to carry out both shortening of the

long 3′-trailer and generation of the mature 3′-end. This represents a novel mechanism for tRNA 3′-maturation that has not been found in other organisms (Fig. 14) (Li *et al.*, 2005).

M. genitalium RNase R and its *E. coli* homologues RNases R and II are members of the RNR exoribonuclease family (Zuo and Deutsccher, 2001). In contrast to *M. genitalium* RNase R, *E. coli* RNase R completely degrades a tRNA precursor, whereas RNase II generates the mature 3′-end of tRNA at very low efficiency (Li and Deutscher, 1994; 1996; 2004; Lalonde *et al*., 2007). Such functional differences may be explained by their different sensitivities to higher order structures in RNA. RNase II degrades single-stranded RNA efficiently but stalls at RNA duplex regions (Coburn and Mackie, 1996). A clamp-like assembly in the RNA-binding domain of RNase II possibly allows single-stranded RNA 3′-ends to enter the catalytic center and blocks double-stranded RNA. During RNA digestion *in vitro*, RNase II progressively slows down at double-stranded structures, resulting in products that usually contain an average 7–9-nt single-stranded overhang at the 3′-end (Zuo *et al*., 2006). In contrast to RNase II, *E. coli* RNase R is able to degrade double-stranded RNA effectively starting from a single-stranded 3′-overhang. *E. coli* RNase R binds single-stranded RNA tightly within the nuclease domain channel. This helps the separation of the double-stranded RNA region immediately outside of the channel and leads the resulting single-stranded RNA to the channel for degradation (Vincent and Deutscher, 2009). *E. coli* RNase R also possesses a RNA helicase activity in its CsdA domain that contributes to the degradation of double-stranded RNA (Awano *et al*., 2010). *M. genitalium* RNase R is able to degrade highly structured rRNA; however, it is sensitive to the aminoacyl-acceptor stem of tRNA and to RNA 2′-*O*-methylation (Lalonde *et al*., 2007; this work). The structural features of *M.*

genitalium RNase R responsible for its selective sensitivity to different RNA structures remain to be elucidated.

M. genitalium RNase R has some interesting properties that are similar to those of *E. coli* RNase T with respect to tRNA 3′-maturation reactions. First, *M. genitalium* RNase R stops at the mature 3′-end of tRNA most efficiently when the terminal sequence is RCCN. Alterations of the discriminator and CCA sequences may result in removal of the 3′-terminal CA residues by this enzyme. Second, RNase R appears to be sensitive to C-rich sequences (Fig. 13B), which may help it to stop at the 3′-CCA end. Interestingly, *E. coli* RNase T is also able to remove part of the terminal CCA sequence in tRNA, demonstrates similar sensitivity to C-rich sequences, and prefers a CCN terminus for 3′-maturation of tRNA (Zuo and Deutscher, 2002). RNase T is also able to trim residues that are immediately downstream of a stem structure in stable RNAs (Li *et al*., 1998). However, unlike *M. genitalium* RNase R, *E. coli* RNase T does not degrade long 3′-trailer sequences in tRNA precursors (Li and Deutscher, 1994; Mohanty and Kushner, 2010; Maes *et al*., 2012).

The preference of a purine discriminator for tRNA 3′-maturation seems to be unique for *M. genitalium* RNase R because this has not been shown for any other exoribonucleases. It should be noted that 31 of 36 *M. genitalium* tRNAs contain an A or a G discriminator (unpublished observations). RNase R may have evolved to recognize a 3′-terminal RCCN sequence for more efficient processing of most tRNA species in *M. genitalium*. Recognition of the same sequence has been described for the 5′-end processing enzyme RNase P in *E. coli* (Kikovska *et al*., 2005). The RNA subunit of RNase P contains a UGG sequence in its P15 loop that forms perfect base pairing with

the RCC sequence for correct cleavage at the 5′-end. Strikingly, *M. genitalium* RNase P also contains the same UGG motif, which presumably recognizes the RCC sequence in its pre-tRNA substrates. Therefore, it is likely that both RNases P and R of *M. genitalium* have evolved to make use of the same RCCN sequence in a pre-tRNA for maturation.

In this work, we observed that pre-tRNAs with altered acceptor stems and 3′-terminal sequences are partially or completely degraded by RNase R. This suggests a possible role for this enzyme in the quality control of tRNA. In summary, *M. genitalium* RNase R has a combination of properties found in several other exoribonucleases, making it a unique RNase that may carry out diverse reactions in tRNA processing, RNA degradation, and quality control. This multifunctional enzyme is extremely important for RNA metabolism in *M. genitalium* because of its limited genome size. It remains to be determined if RNase R has a broad role in RNA processing and degradation in *M. genitalium* and other related bacteria.

3.2 Characterization of tRNA damage under oxidative stress in *E. coli*

Many studies have revealed that DNA damaging agents also cause RNA damage (Li *et al*., 2006; Wurtmann and Wolin, 2009). Reactive oxygen species (ROS), which become more abundant under oxidative stress (OS), are common nucleic acid damaging agents. In the few cases when oxidative damages to DNA and RNA were compared by measuring the content of 8-hydroxyguanosine (8-oxo-G), oxidation was much greater in RNA than in DNA in mammalian cells and tissues, especially when exogenous oxidants such as hydrogen peroxide (H_2O_2), were introduced to cause oxidative stress (Fiala *et*

al., 1989; Shen *et al*., 2000; Hofer *et al*., 2005, 2006). In a study using reverse-transcriptase PCR to measure the damage of *Escherichia coli* 16S rRNA, H_2O_2 treatment caused RNA damage that stopped reverse transcription up to 50% in 1 kilobase distance (Gong *et al*., 2006). These findings suggest that RNA oxidation is a pre-dominant feature under conditions of ROS attack.

There is increasing evidence regarding RNA dysfunction caused by oxidation. mRNA oxidized *in vitro* causes a reduction in protein synthesis and the formation of aggregated protein products (Shan *et al*., 2003, 2007). Oxidative damage of mRNA could cause ribosome stalling during translation elongation (Shan *et al*., 2007). Consistent with these observations, truncated proteins were made from oxidized mRNA (Tanaka *et al*., 2007). Oxidation also causes ribosome dysfunction (Ding *et al*., 2005; Honda *et al*., 2005). Cells must have developed various mechanisms that control the quality of RNA and minimize the deleterious effect of RNA oxidation. RNA surveillance activities could reduce the incorporation of damaged nucleotides into RNA (Taddei *et al*., 1997; Hayakawa *et al*., 1999; Ishibashi *et al*., 2005) and degrade or repair damaged RNA (Li *et al*., 2006; Wurtmann and Wolin, 2009, Kong and Lin, 2010). Consistent with this notion, an important RNA degrading exoribonuclease, polynucleotide phosphorylase, was shown to reduce RNA oxidation and protect *E. coli* and HeLa cells under oxidative stress (Wu and Li, 2008; Wu *et al*., 2009).

Despite the increasing interest in studying RNA oxidative damage and quality control, little is known about the level of RNA damage under oxidative stress and whether different RNA species and structures are differentially oxidized by ROS. In a growing *E. coli* cell, highly structured rRNA and tRNA account for nearly 80% and 15%

of the total RNA, respectively. In addition, most of the rRNA molecules are present in ribosomes where rRNAs are tightly bound with ribosomal proteins. One would expect that RNA would be protected from oxidation by the presence of highly folded structures or by association with proteins. In contrast to the abovementioned postulation, we have recently shown that RNA structure and its association with proteins do not seem to protect RNA from oxidative damage. After *Escherichia coli* cells were exposed to hydrogen peroxide (H_2O_2), RNA isolated from ribosomes often contained higher levels of 8-oxo-G than RNA from the non-ribosomal fraction (Liu et al., 2012). In addition, highly structured RNA species are not protected from oxidation *in vitro* (Liu et al., 2012). These observations prompted us to investigate the potential relationship between RNA structure and levels of RNA oxidation.

3.2.1 tRNAs undergoes oxidative damage both *in vivo* and *in vitro*

In order to study the effect of oxidative stress caused by H_2O_2 on tRNA, *E. coli* cells (CA244 I-) are treated with 1, 2, 3, 5, and 10 mM H_2O_2 as indicated in figure 15A. tRNAs (Samll RNA fraction) were isolated from cells, as described in materials and methods, at 15 min after treatment with H_2O_2 and 8-oxo-G levels were measured by HPLC-ECD method. Results demonstrated that 8-oxo-G levels are increased in a dose dependent manner (Fig. 15A) and with 10 H_2O_2 mM treatment 8-oxo-G levels reached to a maximum of 28 8-oxo-G/10^5G demonstrating that tRNAs were prone to damage *in vivo* by H_2O_2 treatment. Very interestingly, large (ribosomal) and small RNA (tRNA) fractions isolated from *E. coli* cells under normal conditions revealed that small RNA fractions have significantly higher levels of 8-oxo-G compared to that of large RNA fractions (Fig. 15B). This observation was consistently evident from six independent experimental

results. This suggests that under normal conditions ribosomal RNAs are damaged less than tRNAs.

In vivo oxidation results made us to study the effect of oxidative damage to tRNA *in vitro*. tRNAs isolated from *E. coli* cells under normal conditions were subjected to *in vitro* oxidation with H_2O_2 as described in material and methods. tRNAs were treated with 0.001, 0.01, 0.1, 1 and 10 mM H_2O_2 and the results demonstrated that 8-oxo-G levels of tRNA are increased in a dose dependent manner (Fig. 16) suggesting that tRNAs are prone to oxidative damage *in vitro*.

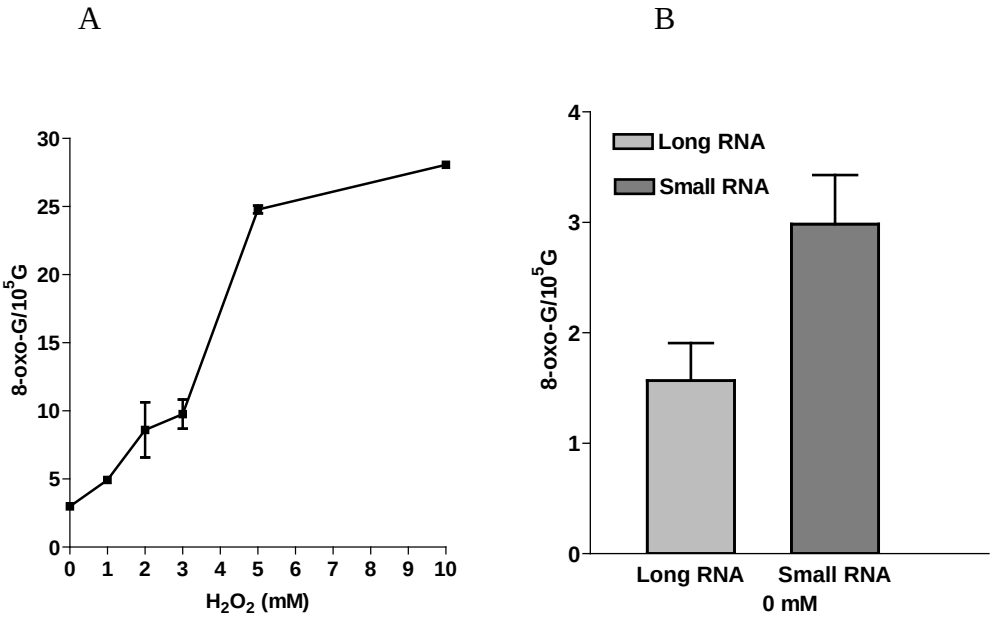

Figure 15. The levels of 8-oxo-G in various cellular RNA species under normal conditions and in response to H_2O_2 treatment. (A). 8-oxo-G levels in small RNA fractions of total RNA isolated from cultures that were treated without and with 1, 2, 3, 5 and 10 mM H_2O_2. (B). 8-oxo-G levels in long and small RNA fractions isolated from exponentially grown cells under normal conditions without any H_2O_2 treatment.

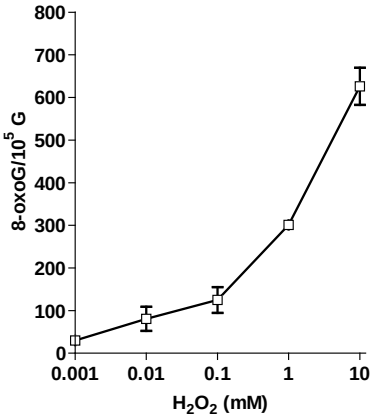

Figure 16. The 8-oxo-G levels of *in vitro* oxidized small RNA fraction. Small RNA fraction was isolated from exponentially grown cultures under normal conditions and RNA was in vitro oxidized by treating with 0.001, 0.01, 0.1, 1 and 10 mM H_2O_2 and 8-oxoG levels are determined as described.

3.2.2 Structure of native tRNA do not protect but enhances oxidative damage

It was assumed that higher levels of RNA oxidative damage over DNA might be due to its linear nature and its abundance in the cytoplasm. In order to examine if tRNA structure has any protective role against oxidation, we have determined the levels of 8-oxo-G generated by H_2O_2 treatment *in vitro* of tRNA in either native or denatured forms. Such treatment introduces hundreds of 8-oxo-G per 10^5 G using mM levels of H_2O_2. Surprisingly, native tRNA contains more 8-oxo-G than denatured tRNA at every concentration (0.01, 0.1, 1 and 10 mM) of H_2O_2 used in this experiment (Fig. 17). At 10 mM concentration of H_2O_2, 8-oxo-G levels were elevated to nearly two-fold in native tRNA compared to that of denatured tRNAs (Fig. 17). This clearly demonstrates that the structure in tRNA do not protect but enhances oxidative damage.

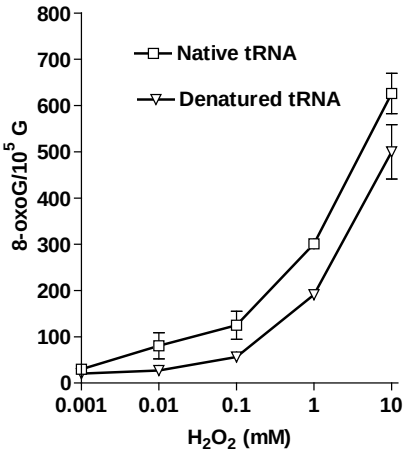

Figure 17. Native tRNA structures do not protect RNA from H_2O_2-mediated oxidation *in vitro*. tRNA was isolated from total RNA by isopropanol differential precipitation. Native and denatured tRNA samples were incubated with indicated concentrations of H_2O_2 *in vitro* and 8-oxo-G levels were determined as described in the Materials and methods section. The mean and standard error of at least three replicates were plotted.

3.2.3 Oxidation of tRNA is inversely correlated to the extent of denaturation

We demonstrated from the above experiment that native tRNAs having intact structure enhance the oxidative damage. In order to test if the preferential formation of 8-oxo-G in tRNA is related to its highly structured feature, native and heat-denatured tRNA were oxidized *in vitro* and 8-oxo-G levels were determined. As shown in Fig. 18A, H_2O_2-induced 8-oxo-G level is higher in native tRNA than in denatured tRNA. Longer heat treatments result in lower 8-oxo-G levels, presumably due to more complete denaturation of tRNA. In the control reactions without H_2O_2, heat treatment *per se* did not have much effect on 8-oxo-G levels. These results clearly demonstrated a role of RNA structures for promoting 8-oxo-G formation. The effect of RNA structures may account for the production of at least ~60% of 8-oxo-G comparing the levels of 0 and 8 min denaturation (Fig. 18A). Because the RNA was denatured by heating prior to incubating with H_2O_2, it

is likely that some of the denatured RNA molecules may renature during oxidation, making it likely that the actual level of structural effect is even higher than shown here.

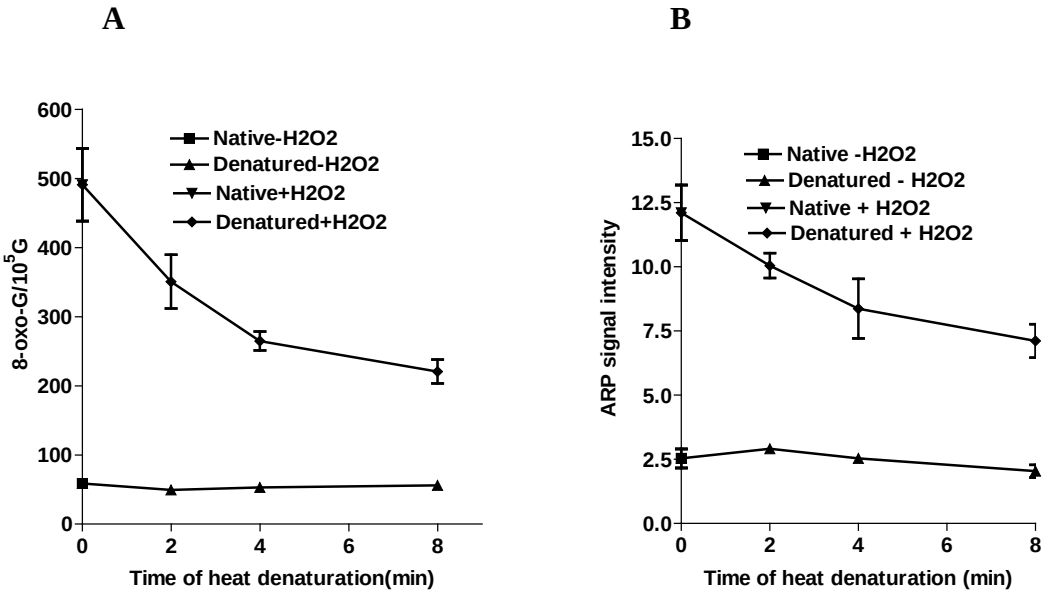

Figure 18. Oxidation of tRNA is inversely correlated to the extent of denaturation. tRNA were prepared from total RNA as described in Materials and Methods. The tRNA samples were dissolved in the buffer for *in vitro* oxidation without H_2O_2. RNA denaturation was carried out by incubating at 95 °C for the indicated amount of time and then immediately chilled in an ice water bath. The heat-denatured RNA was then immediately oxidized by the addition of H_2O_2 to a final concentration of 1 mM in a 100 µl mixture containing 20 µg tRNA. (A). 8-oxo-G levels and (B) abasic sites were determined as described in Materials and Methods. The mean and standard error of at least three replicates were plotted. 8-oxo-G levels generated in rRNA and tRNA are shown in A and B, respectively.

Apart from 8-oxoG, we also measured the levels of abasic sites in RNA, which are formed because of direct effect of oxidative damage by ROS. There are no previous reports on the role of RNA structure and basic sites in RNA. If the structure of tRNA enhanced 8-oxo-G levels, the same structure may or may not influence the abasic site formation upon oxidative treatment. Here, we also studied the levels of abasic sites from the aliquots of tRNA samples used for measuring 8-oxo-G levels. Very interestingly,

abasic sites levels were also decreased upon denaturation and tRNAs heated for 8 min has lowest levels of abasic sites (Fig. 18B). This exactly followed the same pattern as that of 8-oxo-G levels. These results evidently demonstrate that the structure in RNA promotes oxidative damage in the form of 8-oxo-G and abasic sites.

3.2.4 Metal ions (Cu^{+2}) catalyze and enhance oxidative damage *in vitro*

According to the previous study (Honda *et al*., 2005), it is known that metal ions such as Fe^{+2} are associated with structural RNA such as rRNA and tRNA and among them rRNA harbors more metal ions. They demonstrated that this could be the reason behind the higher levels of *in vivo* 8-oxo-G levels in rRNA compared to tRNA. They also demonstrated that denatured forms of RNA harbors fewer metal ions (Fe^{+2}) than their native rRNA and tRNA. However, they have not performed any *in vitro* oxidation studies on denatured and native tRNAs and their associated levels 8-oxo-G. Here we made an attempt to study how copper ions used in our *in vitro* oxidation reactions affect 8-oxo-G levels of native and denatured forms of tRNA.

It is also important to note that addition of Cu^{+2} in reaction buffer without H_2O_2 also slightly enhanced 8-oxo-G formation both in native and denatured forms of tRNA. This could be due catalysis of Cu^{+2} with the available oxygen to form reactive oxygen species. Very importantly treatment of tRNAs with H_2O_2 in the absence of Cu^{+2} resulted in approximately 6 fold increase in 8-oxo-G level (Fig. 19) suggesting that other metal ions such as Mg^{+2} which are associated with tRNA during isolation might have played a role. However, as expected, treatment of tRNAs with both Cu^{+2} and H_2O_2 resulted in elevation of 8-oxo-G levels by 16- fold in native, and 11-fold in denatured tRNAs (Fig.

19). These results demonstrate that metal ions associated with tRNA enhance oxidative damage.

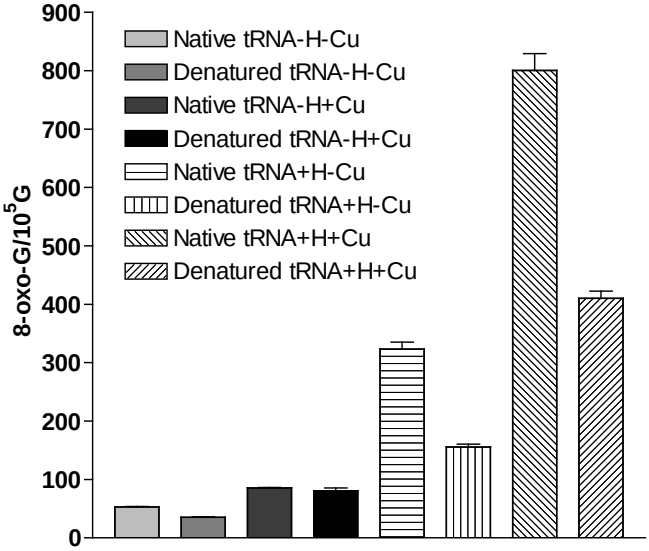

Figure 19. 8-oxo-G levels of native and denatured tRNA with and without Cu^{+2} and H_2O_2. In the figure legend +H and –H represents with and without H_2O_2, +Cu and –Cu represents with and without Cu. tRNAs isolated and in vitro oxidized with and without Cu as described in materials and methods and 8-oxo-G levels are determined by HPLC-ECD method.

3.2.5 Discussion

In this work we have demonstrated that cellular tRNAs are quickly and highly oxidized under oxidative stress, as indicated by the rise of 8-oxo-G levels in RNA, which is dependent on H_2O_2 dosage. Oxidation occurs to all RNA species. RNA structures do not appear to be able to protect RNA from being oxidized by H_2O_2. Fenton reaction during preparation, storage and processing causes spurious oxidation of nucleic acids, resulting in variations of reported basal levels of oxidized nucleobases in the order of magnitude (ESCODD *et al*., 2005). This variation could also greatly interfere with the results in response to oxidants (de Souza-Pinto and Bohr, 2002). In order to reduce

spurious oxidation in our experiments, we have adopted procedures to minimize exposure to oxygen and to reduce the level of contaminating metal ions (Shen et al., 2000; ESCODD et al., 2005; Hofer et al., 2006; Wu et al., 2009). However, it is likely that the true basal level of 8-oxo-G is lower than reported in this work because spurious oxidation might not be completely avoided during HPLC analysis (ESCODD et al., 2005). Nonetheless, our results demonstrated 8-oxo-G levels that respond well to all dosages of H_2O_2. Importantly, under normal conditions longer RNAs (mainly rRNAs) isolated from the cells contain much lower levels of 8-oxo-G than the cellular tRNA (Fig. 15B), suggesting that rRNAs are normally kept with low oxidative damage. This phenomenon could be important for optimal ribosome function to support cell growth because oxidative damage might hinder protein synthesis or generate errors in the protein products.

An unexpected observation was that tRNAs are not protected by their structures (Fig. 17). The inability of tRNA structure to protect tRNA from oxidation was further shown *in vitro* by exposing purified tRNA to H_2O_2 (Fig. 18A). These findings are surprising because one would expect that RNA structure and protein binding would limit the accessibility of RNA to ROS. Apparently, ROS can reach the bases in these RNAs efficiently. One possible explanation for the lack of protection is the association of the highly structured RNAs with Fe^{2+}, the ion known to generate oxidative chemicals and free radicals from H_2O_2 by Fenton chemistry (Wardman and Candeias, 1996). Indeed, such association of rRNA with Fe^{2+} has been reported to play a role in promoting rRNA oxidation and inactivation in translation (Honda et al., 2005). Our results with extent of heat denaturation of tRNA on 8-oxo-G and abasic site levels revealed that, native tRNA

with intact secondary structure retained more 8-oxo-G (Fig. 18A) and abasic sites (Fig. 18B), compared to denatured form. It is interesting to know that ROS might have attacked preferentially secondary structures (hot spots) in tRNA and resulted in elevated levels of 8-oxo-G (Fig. 18A) and abasic sites (Fig. 18B).

Previous studies reported significant differences in iron binding between rRNA and tRNA, however under their denaturation conditions, iron binding capacity decreased significantly (Honda *et al*., 2005). Moreover no significant differences in iron binding were observed among denatured tRNA and rRNA (Honda *et al*., 2005). They also demonstrated that upon oxidation by Fenton reaction rRNA generated 13 fold higher 8-oxo-G levels compared tRNA, which is due to the fact that rRNA provides largest sites for iron binding which promotes higher oxidation levels (Honda *et al*., 2005). This explains the fact that specific metal binding motifs are present in RNA tertiary structure may enhances the levels of oxidation. This demonstrates why our studies with native tRNA promote higher oxidation levels than their denatured forms.

According to previous reports, the major groove of tandem G-U pairs and in particular major groove edge of guanosine forms the ligand for magnesium bound water (Pyle, 2002). This motif forms a cavity and provides the best ligand for metal ions binding (Cate and Doudna, 1996) which may enhances the metal ion mediated oxidation by oxidant/H_2O_2. Unpublished results from our laboratory have demonstrate that higher level of 8-oxo-G formation from RNA:DNA duplex compared to single stranded RNA might be due to its ability to have many metal ion binding sites and preferentially higher oxidation levels (Liu *et al*., unpublished observations). tRNA has less complex tertiary structure than rRNA, which forms the basis for lower oxidation levels in tRNA

compared to rRNA (Liu *et al*., unpublished observations). However it is difficult to evaluate and corroborate how different structural features in these RNA species affect their ability to be oxidized.

In summary, the results of this study suggest a surprising role for higher-order structure of RNA in promoting oxidative damage. Such structural features may include, but are not limited to, double-stranded structures. Compared to RNA single strand, double strand may recruit ROS more efficiently or react with ROS at higher rate. Other structural feature and sequence context may also affect oxidation of RNA, making it possible for "hot spots" of ROS target to exist. For the same reason, some RNA molecules may contain higher levels of oxidative lesions than others, causing differential effect on RNA function under OS. The exact nature how each of the sequence and structural features affect the formation of various oxidative damages in RNA deserve to be studied in the future. The observation that tRNA is highly oxidized shortly after the cells' exposure to H_2O_2 suggests that preferential oxidation of highly structured RNA may also happen *in vivo*. Because highly structured rRNA and tRNA constitute the majority of cellular RNA, high levels of oxidation of these RNAs would present a major challenge to any living organism. Efficient RNA surveillance mechanisms may play pivotal roles in cell survival under OS, but such important mechanisms remain to be elucidated.

3.3 The tRNA pseudouridine synthase TruD binds oxidized RNA specifically and plays an important role in protecting *E. coli* cells against oxidative stress

The *E. coli* tRNA pseudouridine synthase TruD was identified as one of the 11 pseudouridine synthases (ΨS) present in *E. coli* that specifically catalyzes the

pseudouridylation of U13 of $tRNA^{Glu}$ (Kaya *et al*., 2004). Recent functional studies on *truD* deletion mutant showed no significant growth differences either in rich or minimal media from 25°C to 42°C or even with competition experiments with wild type in rich medium (Kaya and Ofengand, 2003). This suggests that the Ψ13 may not be important for the function of $tRNA^{Glu}$ under normal conditions. Previous studies have also shown that under normal growth conditions, there is no difference in the aminoacylation levels of $tRNA^{Glu}$ between wild type and a *truD* deletion mutant (Kaya, 2006). As Ψ is considered generally important for RNA structural stability, it might be essential for $tRNA^{Glu}$ stability in *E. coli* (Kaya and Ofengand, 2003). It is assumed that the effect of *truD* deletion may be manifested only under specific conditions where Ψ13 of $tRNA^{Glu}$ may become limiting factor for some unknown metabolic processes (Kaya and Ofengand, 2003). Conceivably, TruD may become essential for growth under those conditions when Ψ13 of $tRNA^{Glu}$ becomes important. Alternatively, TruD may be crucial for certain unknown cellular activity which is totally unrelated to the modification of $tRNA^{Glu}$, and this point needs to be included in our studies.

TruD belongs to the fifth family of ΨS with 349 amino acids and has a molecular weight of 39 KDa. The four families of ΨS have a conserved Asp and Tyr in catalytic site and are crucial for catalysis. TruD differ from the rest of the ΨS in not having conserved the Tyr. TruD homologues are widespread and conserved among other bacteria, archaea, and eukaryotes (Kaya and Ofengand, 2003). Recently reported crystal structure of TruD has a V-shaped catalytic domain (Fig. 20B) and a novel TRUD domain (Fig. 20A) (Hoang and, Ferre-D'Amare, 2004; Kaya *et al*., 2004; Ericsson *et al*., 2004).

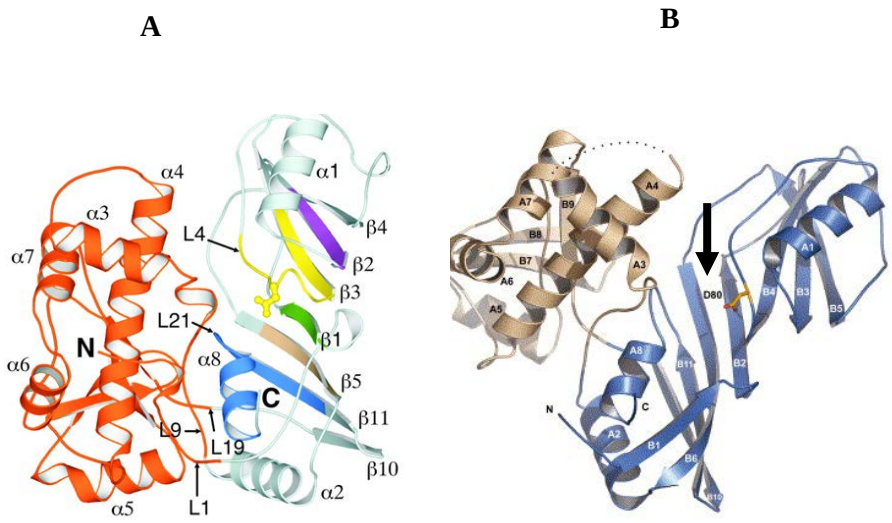

Figure 20. Crystal structure of TruD. (A). A ribbon representation of TruD protein with catalytic domain C represented in light blue color and a novel domain (N) named as TRUD domain specific to TruD represented in orange color. The Ψ synthase structural motifs are highlighted in purple-motif-I, yellow-motif-II, peach-IIa, dark blue-motif III and green-motif IIIa. (B). Crystal structure of TruD (Ericsson *et al*., 2004) with Aspartic acid 80 (D80) in active site indicated by vertical black arrow.

TRUD domain has a novel three-dimensional structure that has not been found in any known organism with the available databases. It is speculated that this novel TRUD domain may be involved in substrate recognition and possibly a new RNA binding domain (Kaya *et al*., 2004). The mechanism of pseudouridine formation by TruD has recently been demonstrated (Fig. 21) (Chan and Huang, 2009). According to their proposed mechanism, the conserved D80 of TruD remove uracil from the ribose sugar by nucleophilic attack on C10 of ribose sugar. The detached uracil base is rotated and reattached to the ribose sugar by E31 of TruD with the formation of C5-C10 bond between uracil base and ribose sugar. The conserved E31 of TruD abstracts a proton from C5 of the uracil base and completes the reaction.

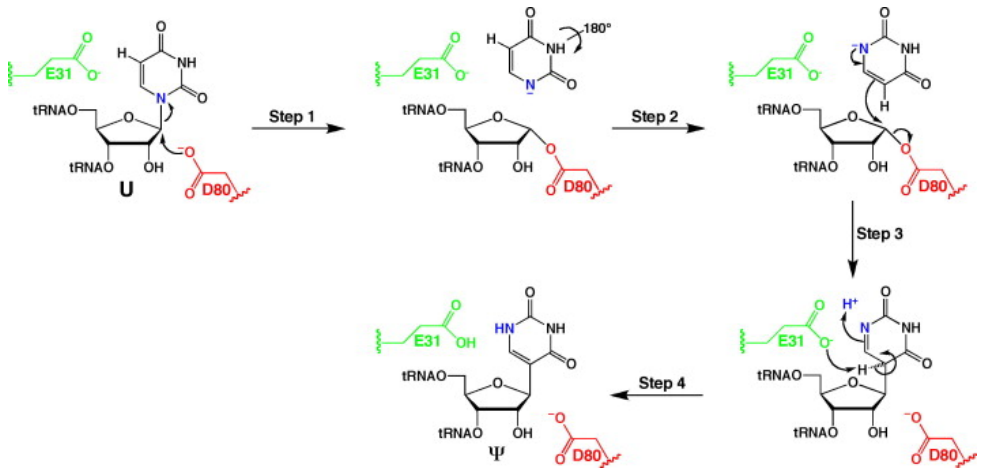

Figure 21. Proposed mechanism of pseudouridine formation by TruD. The conserved glutamate (E31) in TruD is likely be the general base involved in the abstraction of the proton attached to C5 of the base and leading to the formation of product Ψ (Chan and Huang, 2009).

Previous studies on TruD active site mutations demonstrated that negatively charged aspartic acid at 80 position is crucial for catalytic activity (Kaya *et al*., 2004; Chan and Huang, 2009). Replacing aspartic acid (D80) with uncharged amino acids threonine (D80T) and asparagine (D80N) resulted in completed loss of catalytic activity (Kaya *et al*., 2004; Chan and Huang, 2009). Studies have also shown that the binding affinity of these active site mutant proteins to synthetic full length $tRNA^{Glu}$ was reduced by four fold (Kaya, 2006). This demonstrates the importance of aspartic acid in RNA binding affinity. However no further information is available on their binding affinities to different RNA species.

Recently, studies from our laboratory have shown that TruD as one of the potential protein having high affinity binding to oxidized RNA compared to normal RNA (Jiang *et al*., unpublished observations). This suggests a possible role for TruD in quality control of oxidized RNA, and in protecting cells against oxidative stress. We propose that

high affinity binding of TruD with oxidized RNA may protect cells under oxidative stress presumably by controlling the levels of oxidized RNA. In this work, we demonstrated the role of TruD in cell viability and quality control of RNA under oxidative stress conditions.

3.3.1 TruD binds oxidized RNA with high affinity

According to previous studies PNPase binds specifically with oxidized RNA with higher affinity and protect cells under oxidative stress by degrading the oxidized RNA (Hayakawa *et al*., 2001; Wu *et al*., 2009). These studies prompted us to identify the other potential proteins having higher affinity to oxidized RNA. Protein pull down experiments using S-100 cell extracts with normal and oxidized RNA revealed that TruD protein as one of the proteins having higher affinity to oxidized RNA but not to normal RNA (Jiang *et al*., unpublished observations) (Fig. 22, lanes 1 and 2). Additionally we did not find any TruD protein band in S-100 cell extracts of *truD* deletion cells both with normal or oxidized RNA demonstrating that it is, indeed, the TruD protein (Fig. 22, lanes 3 and 4). Mass spectroscopy analysis also confirmed that the band is TruD (Jiang *et al*., unpublished observations).

This high affinity binding of TruD to oxidized RNA implies its potential role under oxidative stress, controlling the levels of RNA oxidative damage. This characteristic feature of TruD also entails its possible role in protecting *E. coli* cells under oxidative stress.

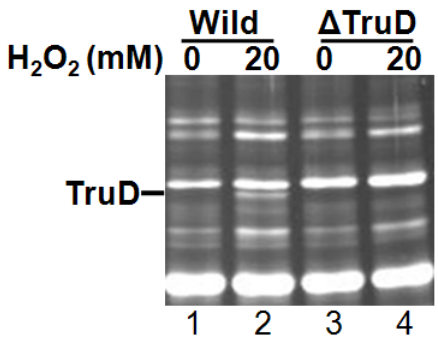

Figure 22. TruD binds oxidized RNA with high affinity. Crude cell extracts were incubated with conjugated RNA-agarose beads. After washing, bead-bound proteins were eluted, separated by SDS–PAGE, and visualized with SYPRO Ruby. The S100 extracts from wild type and a mutant lacking TruD were used. RNA used is 50-mer RNA oligonucleotide which was *in vitro* oxidized with 20 mM H_2O_2 as described in materials and methods.

3.3.2 *truD* deletion mutants are hypersensitive to oxidative stress

In order to study the role of TruD protein under oxidative stress, we used *E. coli* strains CA244 and CA244Δ*truD*. *truD* deletion mutant was constructed in CA244 wild type strain background by P1 transduction by removing the entire *truD* gene and replacing it with kanamycin cassette. Overnight grown CA244 and CA244Δ*truD* cultures were diluted at 1:100 ratio in fresh LB media and grown up to 0.1 OD_{600} and challenged with various dosages of oxidants such as H_2O_2 and TBHP. Samples were collected at various time points and OD_{600} readings are recorded. Growth curve results have shown that under controlled conditions where no oxidant was added, both CA244 and CA244Δ*truD* cells grow at similar level (Fig. 23A), suggesting no difference in growth under normal conditions. Interestingly, when cells are treated with various dosages of TBHP such as 0.4 mM (Fig. 24B), 0.65 mM (Fig. 24C), and 0.9 mM (Fig. 23D), wild type cells were recovered from the oxidative stress at faster rate than *truD* deletion cells.

It is important to note that, greater growth differences were observed in a dose dependent manner as the concentration of oxidant increased. Very interestingly when cells were treated with 0.65 mM TBHP, it appears that most of the CA244Δ*truD* cells were killed and the wild type CA244 cells are affected the least and also recovered at a very faster rate.

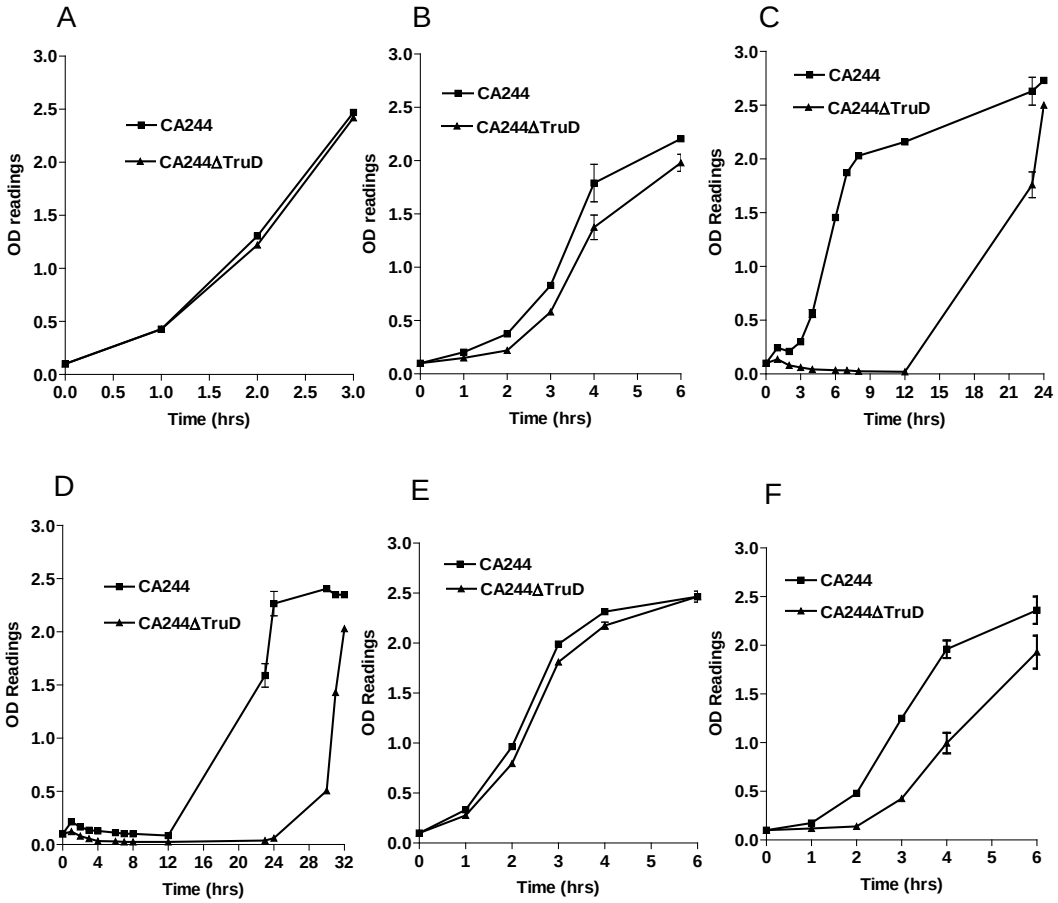

Figure 23.Growth curve of wild type CA244 and CA244Δ*truD* mutants. *E. coli* cells were grown up to to OD_{600} 0.1 in LB media and challenged with oxidants. OD readings were recorded at time points as indicated. (A). Control growth curves without any oxidant. (B), (C) and (D) are growth curves generated by treating cells with oxidant TBHP at 0.4, 0.65 and 0.9 mM respectively. (E) and (F) are the growth curves generated by treating cells with H_2O_2 at 2 and 5 mM respectively. Duplicate samples were taken at each time points for generating error bars.

Similar results were obtained when cells treated with 2 mM (Fig. 23E) and 5 mM (Fig.23 F) H_2O_2. It appears that with lower concentration (2 mM) of H_2O_2 no significant difference between wild type CA244 and CA244Δ*truD* mutant was observed (Fig. 23E). However, when cells were treated with 5 mM H_2O_2, greater difference was observed between wild type CA244 and CA244Δ*truD* mutant (Fig. 23 F). These results demonstrated that *truD* deletion mutants are not deficient under normal conditions; however they are hypersensitive to oxidative stress in a dose dependent manner. Because TruD binds to oxidized RNA with high affinity and its deletion resulted in hypersensitivity to oxidative stress suggest a role for TruD in protecting cells under oxidative stress by controlling the levels of oxidized RNA.

3.3.3 Aminoacylation of $tRNA^{Glu}$ is not affected under OS in *truD* deletion mutant

Because the only known biochemical function of TruD is the pseudouridylation of $tRNA^{Glu}$, we have studied if lack of pseudouridylation is related to growth defects of *truD* deletion mutant observed under oxidative stress. In this work, we have studied the aminoacylation levels of $tRNA^{Glu}$ under normal and oxidative stress conditions. CA244 and CA244Δ*truD* cells were treated with 5 mM H_2O_2 and total RNA was isolated under acidic conditions as described in materials and methods in a time course after addition of H_2O_2. Total RNA was prepared under a condition that aminoacyl group is retained on tRNA, and the RNA samples were subjected to acid gel electrophoresis and northern blotting with $tRNA^{Glu}$ probe. Results have shown that $tRNA^{Glu}$ remains charged in both wild type and *truD* cells in the entire time course. Uncharged $tRNA^{Glu}$ was not observed in either in wild type or *truD* cells at any given condition (Fig. 24). This suggests that aminoacylation of $tRNA^{Glu}$ was not affected under oxidative stress condition.

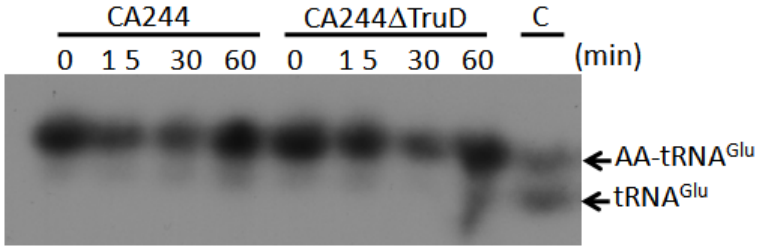

Figure 24. Northern blot analysis of charged tRNA^{Glu}. Total RNA was isolated under acidic conditions as described in materials and methods at indicated time points after treating cells with 5 mM H_2O_2. Charged tRNA seperated by acid gel electrophoresis and porobed with radiolableed tRNA^{Glu}. 'C' represents the control tRNA which was isolated by normal method (not under acidic condition) which contains both charged and uncharged tRNAs as indicated in figure.

We observed a significant drop in the levels of charged tRNA at the 15 and 30 min time points in both wild type and *truD* cells (Fig. 24). This raised a question if the tRNA was degraded in response to H_2O_2 treatment. Therefore, we have analyzed the level of tRNA^{Glu} under normal and oxidative stress conditions. The previously mentioned H_2O_2-treated cultures were used to prepare total RNA using a normal RNA isolation method. The level of tRNA^{Glu} was analyzed by Northern blotting at all time points, using 5S rRNA for normalization (Fig. 25). Results have shown that steady state levels of tRNA^{Glu} did not change upon H_2O_2 treatment at any given point of time either in wild type or in *truD* mutant (Fig. 25). The relative signal intensity values generated with 0 min being 1.0, shows no significant change at any given point of time. These results suggested that tRNA^{Glu} lacking pseudouridine modification at 13th position are stable even under oxidative stress condition.

These results demonstrate that aminoacylation and stability of tRNA^{Glu} are not affected by the lack of Ψ13, although we do not have information about the functionality

of Ψ13 of $tRNA^{Glu}$ during translation. On the other hand, it is likely that the growth defect of the *truD* cells under oxidative stress is caused by a more direct role of this protein in controlling RNA oxidation due to its high affinity to oxidized RNA.

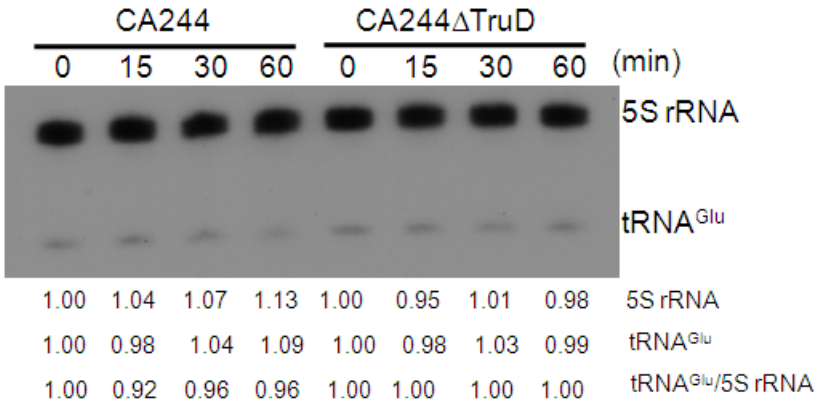

Figure 25. Norther blot analysis of $tRNA^{Glu}$ and 5S rRNA. Exponentially grown wild type CA244 and CA244Δ*truD* cells were challenged with 5 mM H_2O_2. Total RNA was isolated at indicated time points and subjected to northern blot with 5S rRNA and $tRNA^{Glu}$ probes . The value of 5S rRNA and $tRNA^{Glu}$ provided below the figure represents the relative intensities of respective bands with 0 min value being set as 1.00. The relative values of tRNA at each time point normalized by 5S rRNA are provided as ratio of $tRNA^{Glu}$/5S rRNA with the value at 0 min set as 1.00.

3.3.4 Wild type TruD, but not the inactive mutants D80N and D80T, shows high affinity to oxidized RNA

The aspartate residue at the 80th position (D80) in TruD is very important for the enzyme's catalytic activity. Replacing D80 with asparagine (D80N) or threonine (D80T) resulted in complete loss of catalytic activity (Kaya *et al*., 2004). Apart from losing catalytic activity, these mutants also display a decreased binding affinity to full length synthetic $tRNA^{Glu}$ by four folds compared to wild type TruD (Kaya, 2006). Importantly,

we have shown that TruD binds oxidized RNA with high affinity. Therefore, we are interested to learn if D80 is also important for TruD's high affinity to oxidized RNA.

In order to study whether D80 is important for TruD to specifically bind oxidized RNA, we have overexpressed the wild type, D80N and D80T TruD proteins as described in methods. The S-100 fractions of the cell extracts containing the overexpressed TruD proteins were normalized to the same TruD protein level by diluting them with the S-100 of a *truD* cell extract. These normalized S-100s contain the same level of TruD proteins at high concentration, and they were further diluted with *truD* S-100 to medium concentration (1:10 dilution) and low concentration (1:50 dilution) of TruD proteins, respectively. RNA-binding experiments were performed as described in materials and methods. Additionally, we have included S-100s from wild type and *truD* cells as positive and negative controls for RNA binding.

As expected, oxidized RNA pulled down much more TruD protein from the wild type S-100 than the control RNA, suggesting that TruD binds oxidized RNA with higher affinity than it does to control RNA (Fig. 26, lane 1 and 2). The TruD band was missing in the *truD* cell extracts (Fig. 26, lane 4). Interestingly, overexpressed TruD proteins showed various abilities for RNA binding. At high concentration of TruD in S-100, the wild type TruD binds both control and oxidized RNA equally well (Fig. 26, lanes 5 and 6), probably due to saturation of binding to both RNA substrates irrespective of its oxidative status when too much TruD protein is available. At the medium (1:10 dilution) and low concentration (1:50 dilution), wild type TruD binds oxidized RNA selectively (Fig. 26, lanes 11, 12, 17, 18). Note that at the low concentration, the amount of TruD protein that was pulled down by oxidized RNA is still much higher than that of the

endogenous TruD from wild type (compare Fig. 26, lane 18 vs. lane 2). Under the same condition, no TruD protein was pulled down by the control RNA, strongly indicating high selectivity of TruD for binding oxidized RNA.

In contrast, D80N and D80T shows RNA binding patterns different from that of the wild type TruD. Surprisingly, D80N had shown weaker binding to oxidized RNA compared to binding to normal RNA at both high and medium concentrations (Fig. 26, lane 7, 8, 13 and 14). At low concentration, no D80N was pulled down by any RNA (Fig. 26, lane 19 and 20). D80T was pulled down by both control and oxidized RNA only when the protein is available at high concentration (Fig. 26, lane 9, 10, 15, 16, 21 and 22). The preferential binding of the D80N construct to control RNA is completely opposite to the behavior of wild type TruD which prefers to bind oxidized RNA. Additionally, from the results of high and medium concentrations, it is also evident that D80N binds to normal control RNA equally well as wild type TruD does (Fig. 26, lanes 5, 7, 11, 13). Therefore, D80N appears to have completely lost the ability to specifically bind oxidized RNA (Fig. 26, lanes 14, 20). D80T was pulled down by both control and oxidized RNA equally well when the protein is available at high concentration (Fig. 26, lane 9, 10). At medium and lower concentrations, D80T did not show binding to either normal or oxidized RNA (Fig. 26, lanes 15, 16, 21 and 22), suggesting that binding to both normal and oxidized RNA was affected by the threonine substitution at this position.

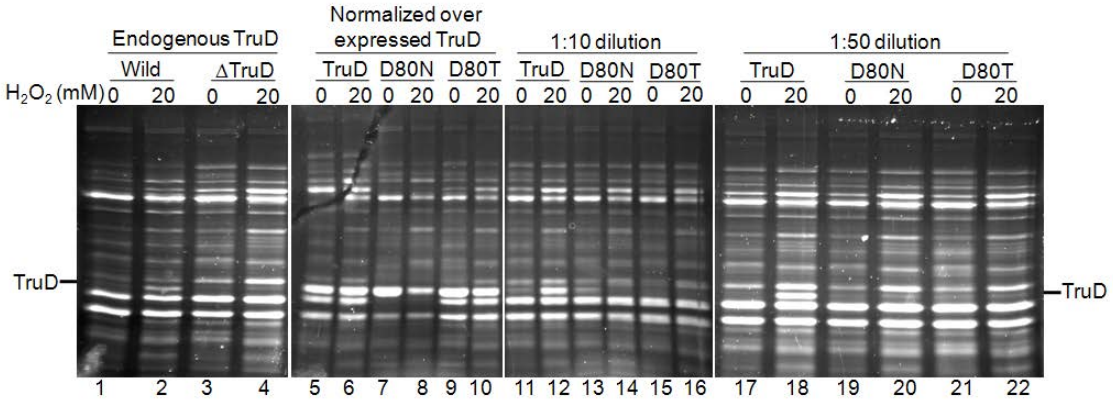

Figure 26. **D80 is required for TruD to bind oxidized RNA with high affinity.** Crude cell extracts (S-100 fractions) were incubated with RNA that was cross-linked to agarose beads. After washing, RNA-bound proteins were eluted, separated by 10% SDS–PAGE, and visualized after SYPRO Ruby staining. S-100 extracts of wild type and *truD* deletion mutant were used as controls with or without endogenous TruD. S-100s containing overexpressed wild type, D80N or D80T TruD constructs were normalized to the same level of TruD content by diluting the extracts with S-100 of the *truD* deletion mutant (data not shown). Medium and low concentrations of TruD S-100s were prepared by 1:10 or 1:50 dilutions of normalized overexpressed S-100s with S-100 from *truD* cells. The 50-mer RNA samples were treated with H_2O_2 at either 0 mM (for normal control RNA) or 20 mM (for oxidized RNA) that were marked on top of the lanes.

These results suggest that at physiological concentrations within a cell, TruD is able to differentially bind to oxidized RNA at high affinity. D80 residue plays a pivotal role in the specific binding to oxidized RNA. Substitution with other amino acids at this position abolishes the protein's high affinity to oxidized RNA and may also affect binding of normal RNA. These results led us to study how cells harboring these inactive TruD mutants survive oxidative stress, and whether binding to oxidized RNA is responsible for the protective function of TruD.

3.3.4.1 Western blot analysis confirms the identity of TruD protein

In order to prove the identiy of TruD protein that the band we observed is truly a TruD protein, we used His-tag version of TruD overexpression cell lysates. Experiment

was performed as described above and in brief cell lysates were normalized and diluted at 1:10 and 1:50 ratios. SDS page gel have shown similar results as expected that only wild type TruD has diferential affinity to oxidized RNA but not D80N and D80T (Fig. 27, lanes 17-22). These results are in agreement with our previous observations and concretely supports the idea. Western blot analysis with anti-His-antibody evidently shows that the protein band we expected to be TruD is a truly a TruD protein (Fig. 28, lanes 1-12). Purified his-tagged TruD proteins were also shown signals with anti-His-antibody and they ran at the same level with pulled out TruD in cell lysates (Fig. 28, lanes 13-15). These results demonstrates that only wild type TruD has differential binding affinity to oxidized RNA.

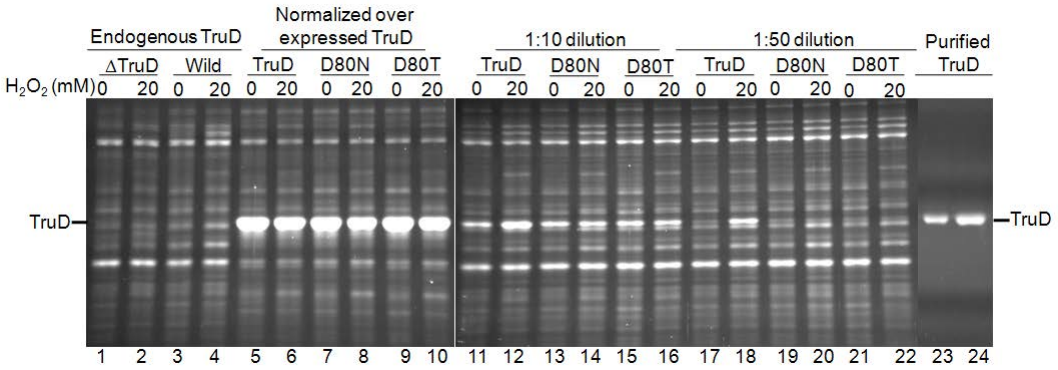

Figure 27. D80 is required for TruD to bind oxidized RNA with high affinity. Crude cell extracts (S-100 fractions) His-tag versions were incubated with RNA that was cross-linked to agarose beads. After washing, RNA-bound proteins were eluted, separated by 10% SDS–PAGE, and visualized after SYPRO Ruby staining. S-100 extracts of wild type and *truD* deletion mutant were used as controls with or without endogenous TruD. S-100s containing overexpressed wild type, D80N or D80T TruD constructs were normalized to the same level of TruD content by diluting the extracts with S-100 of the *truD* deletion mutant. Medium and low concentrations of TruD S-100s were prepared by 1:10 or 1:50 dilutions of normalized overexpressed S-100s with S-100 from *truD* cells. The 50-mer RNA samples were treated with H_2O_2 at either 0 mM (for normal control RNA) or 20 mM (for oxidized RNA) that were marked on top of the lanes. Purified His-tagged TruD proteins were run along with cell lysates and were labeled as purified TruD.

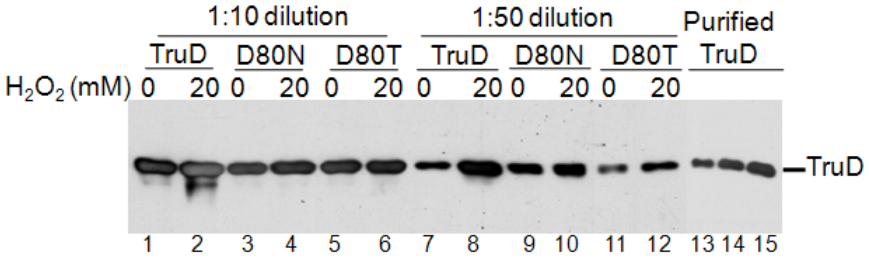

Figure 28. Western blot analysis of pulled out cell lysate with anti-His antibody. Crude cell extracts (S-100 fractions) His-tag versions were incubated with RNA that was cross-linked to agarose beads. After washing, RNA-bound proteins were eluted, separated by 10% SDS–PAGE, and visualized transferred to nitrocellulose membrane abd performed western blot analysis as described in materials and methods.

3.3.5 8-oxo-G and abasic sites levels do not alter in WT and TruD deletion mutants under OS

The binding of wild type TruD to oxidized RNA with high affinity and its role in protecting cells against oxidative stress suggests its potential role in the quality control of oxidized RNA. Previous studies have shown that PNPase having higher affinity to oxidized RNA protects cells from oxidative stress and known to be involved in removing the 8-oxo-G containing RNA (Wu *et al*., 2009). It is imperative to study the role of TruD in controlling the levels of 8-oxo-G containing RNA under oxidative stress conditions. This will provide the relation between wild type TruD higher affinity to oxidized RNA and its biochemical function in protecting cells under oxidative stress.

In order to study this, exponentially grown wild type CA244 and CA244Δ*truD* cultures were treated with 5 mM H_2O_2 and total RNA was isolated at indicated time points and 8-oxo-G levels are measured by HPLC-ECD method as described in materials and methods. Results demonstrated that both in CA244 and CA244Δ*truD* cells, 8-oxo-G

levels are elevated to same level after treatment with H_2O_2 and reached to maximum between 15 to 30 min time points and dropped significantly over the time (Fig. 29). These results clearly demonstrate that there is no significant difference wild type CA244 and CA244Δ*truD* cells. These results suggest that specific binding of TruD to oxidized RNA was not subjected to specific removal of 8-oxo-G containing RNA. If the specific binding of TruD with oxidized RNA leads to removal, 8-oxo-G levels in *TruD* deletion mutant will be remain elevated compared to wild type.

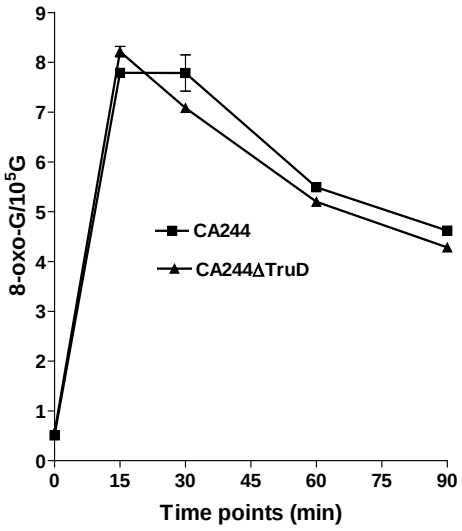

Figure 29. Analysis of 8-oxo-G levels. Expoentially grown wild type CA244 and CA244Δ*truD* cells were treated with 5 mM H_2O_2. Total RNA was isolated at indicated time points and 8-oxo-G levels are determined by HPLC-ECD method . The levels of 8-oxo-G in CA244 and CA244Δ*truD* cells at each time point are represented in a graphical manner. Duplicate samples were used for generating error bars.

We have also analyzed the level of abasic sites in RNA samples that were prepared from wild type and *truD* cells exposed to oxidative stress treatment.

Figure. 30 shows that the difference between wild type and *truD* cells in the levels of RNA abasic sites, if any, is unremarkable in both CA244 and MG1655 strain

backgrounds. It is also important to note that abasic site levels were elevated to peak between 15 to 30 min and dropped significantly over the time (Fig. 30). This pattern is similar to 8-oxo-G levels observed above.

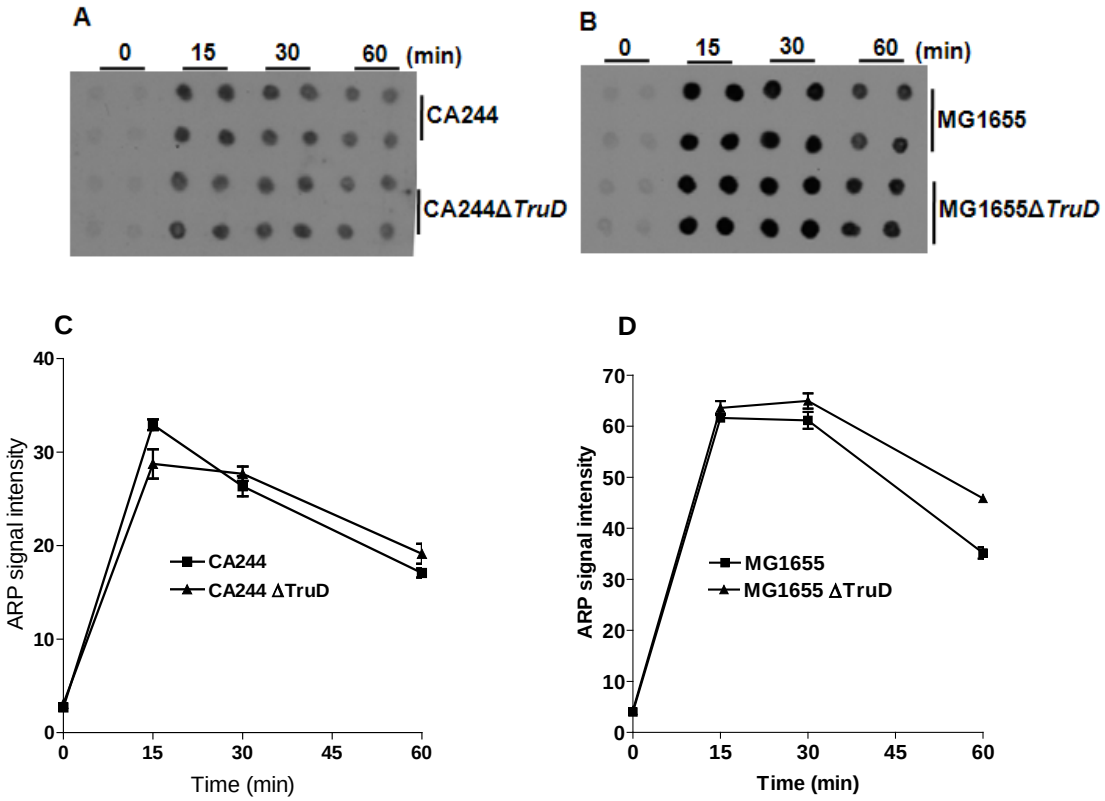

Figure 30. Analysis of *in vivo* Abasic site levels. Expoentially grown wild type CA244 and CA244Δ*truD* cells were treated with 5 mM H_2O_2. Total RNA was isolated at indicated time points and subjected to ARP assay as desribed in materials and methods. (A). dot blot showing abasic site signals in total RNA isolated from CA244 and CA244Δ*truD* cells. (B). dot blot showing abasic site signals in total RNA isolated from MG1655 and MG1655Δ*truD* cells. (C) and (D) are the graphical represenatation of abasic site levels in total RNA at indicated time points for the respective *E. coli* genetic backgrounds as indicated in figure.

These results demonstrate that TruD's protective role is probably not related to the removal of 8-oxo-G containing or abasic RNA. However, the role of TruD protein in repair or degradation of oxidized RNA cannot be ruled for RNA with other types of damages. Because TruD is able to cleave a uracil and to replace a pseudouracil in RNA, it

may be able to repair a damaged residue in RNA in a similar manner. This point was studied in the following section.

3.3.6 TruD has no RNA or DNA glycosylase activity

Our data suggest a specific protective role for TruD under oxidative stress which is yet to be elucidated. Above studies with RNA oxidative damage lesions such as 8-oxo-G and abasic sites levels demonstrated that there is no significant difference between wild type CA244 and CA244Δ*truD* mutant. These results prompted us to study the possible role of TruD in repair of oxidized RNA. According to previous studies oxidized bases in DNA are removed by specific DNA glycosylases and a new base will be added either by the same glycosylase or a new specific enzyme. However, such activity for removal or repair oxidized base in RNA has not been previously reported. As discussed earlier, TruD catalyzes the removal of uracil base from sugar backbone during pseudouridination, an activity similar to that of a DNA glycosylase. Therefore, we have examined if TruD displays any glycosylase activity.

Although we did not find any difference in the *in vivo* abasic site levels of RNA between CA244 and CA244Δ*truD* cells under oxidative stress, we cannot rule out the possible role of TruD in repair of oxidized bases in RNA by removing them by its potential glycosylase activity. If TruD has glycosylase activity on oxidized bases it will remove the damaged base and generate abasic site. In order to find out the TruD glycosylase activity on normal and oxidized RNA, we used purified wild type TruD and its active site mutant proteins D80N and D80T and performed glycosylase reactions as described in materials and methods. Results have shown that abasic site levels were not increased when either normal or oxidized RNA incubated with TruD proteins (Fig. 31A,

B). Both wild type TruD and active site mutant proteins D80N, and D80T showed no significant difference in the levels of abasic site formation (Fig. 31B).

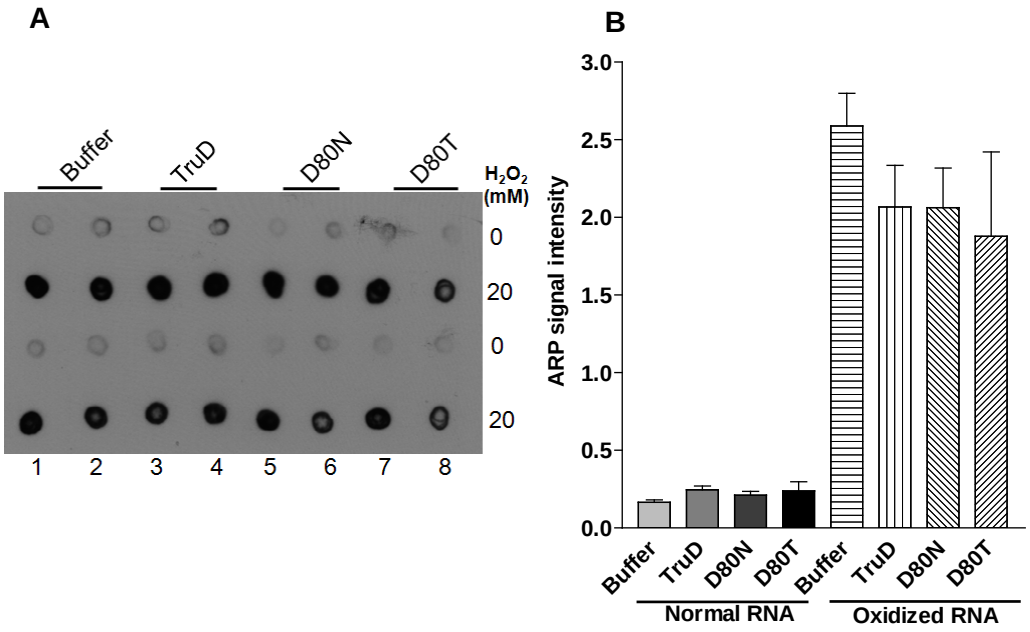

Figure 31. **RNA-TruD glycosylase assay and abasic site determination.** In the figure legend 0 and 20 represents RNA untreated and treated with 20 mmH_2O_2 respectively. RNA was incubated with purified proteins such as wild type TruD, and TruD active site mutant proteins D80N and D80T as described in material and methods. Buffer represents the negative control where RNA was treated with buffer alone. (A). Dot-blot of RNA containing abasic sites. (B). Graphical representation of signal intensities of abasic sites.

These results clearly demonstrated that TruD protein has no glycosylase activity on either normal or oxidized RNA. However it is important to note that if oxidized base is removed and added back by TruD, then there will be no increase in the levels of abasic sites although repair of oxidized base has been accomplished. This requires new methodologies to detect the repaired base in RNA.

It is well known that under oxidative stress conditions, hydroxyl radicals interact with cytosine in DNA and convert it to an unstable cytosine glycol, which further

undergoes deamination and forms uracil glycol (Ug) (Purmal *et al*., 1998). Cytosine glycol upon dehydration can form 5-hydroxycytosine (5-OHC) and additionally upon sequential deamination and dehydration, it can form 5-hydroxyuracil (5-OHU) (Wagner *et al*., 1992). These uracil residues are removed effectively by uracil DNA glycosylases (UDG). Previous studies have shown that even in the absence of all DNA repair enzymes in *E. coli*, uracil was still removed from DNA by some unknown novel mechanisms. It is known that TruD protein converts uridine to pseudouridine by breaking the glycosidic bond between sugar and the base and separating the base from sugar backbone (Chan and Huang, 2009). This mechanism is similar to DNA glycosylases. Because *TruD* deletions mutants are sensitive to oxidative stress and no other biochemical evidence in relation to cell viability was observed at the RNA level except specific binding to oxidized RNA, we assumed that TruD might be involved in the removal of oxidized uracil base from DNA.

In order to study the role of TruD in removal of uracil or oxidized residues from DNA, we chose an *E. coli* strain CJ236 lacking UDG (Uracil DNA glycosylase) and dUTPase genes. In this strain, the external supply of uridine in growth media leads to incorporation of 6000 Uracil/10^6 bases in DNA (Lari *et al*., 2006). DNA isolated from this strain was *in vitro* oxidized as described in materials and methods and incubated with purified UDG and wild type TruD and TruD active site mutant proteins D80N and D80T in independent reactions and analyzed abasic sites as described in materials and methods.

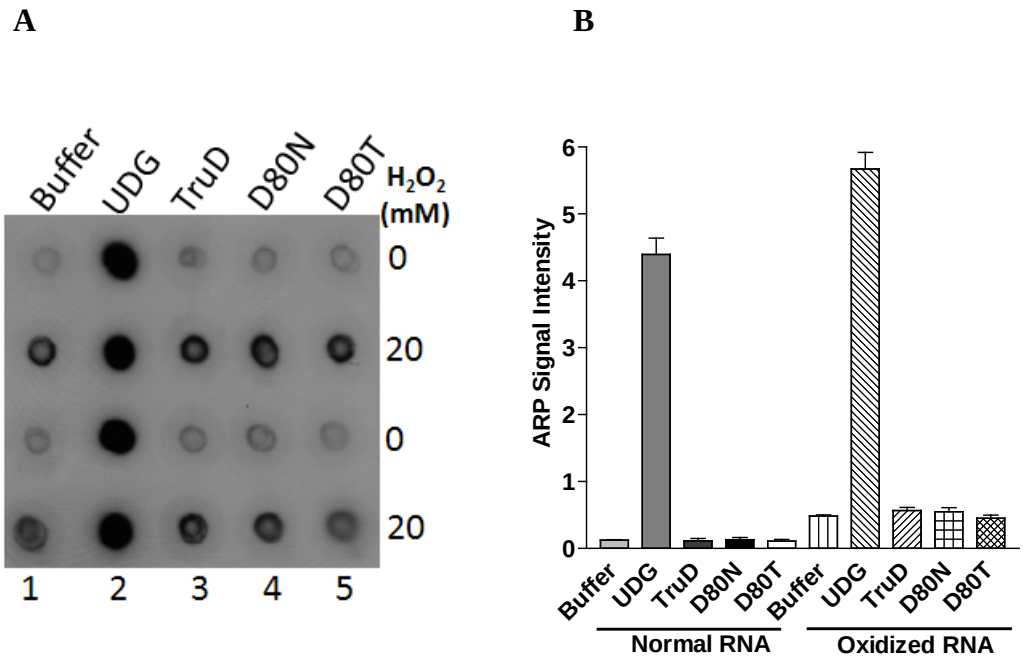

Figure 32. DNA- TruD glycosylase assay and abasic site determination. In the figure legend 0 and 20 represents DNA untreated and treated with 20 mmH_2O_2 respectively. DNA was incubated with purified proteins such as UDG (Uracil DNA glycosylase, a positive control), TruD (Wild type), and TruD active site mutant proteins D80N and D80T as described in material and methods. Buffer represents the negative control where DNA was treated with buffer alone. (A). Dot-blot of DNA containing abasic sites. (B). Graphical representation of signal intensities of abasic sites.

Results demonstrated that UDG as a positive control removed uracil residues from both oxidized and normal DNA at similar levels and signal intensities are elevated (Fig. 32 lane 2; Fig. 32B). Whereas wild type TruD and D80N and D80T proteins did not show increase in abasic site formation when treated with either normal RNA or oxidized RNA. And the abasic site levels are similar to buffer treated control reactions (Fig. 32 lanes 1, 3, 4, 5). These results demonstrated that TruD do not have any uracil glycosylase activity in either normal or oxidized DNA.

All these studies points to the future experiments need to be performed in order to understand the biochemical function of TruD in protecting cells under oxidative stress conditions.

3.3.7 Discussion

In the present study we demonstrated that TruD protein protects *E. coli* cells under oxidative stress condition by unknown mechanism in spite of its high affinity binding to oxidized RNA. According to previous studies, PNPase protein having high affinity to oxidized RNA is involved in degradation of 8-oxo-G containing RNA (Wu *et al*., 2009). However, its direct role in degradation is not evident. In light of this we predict that TruD like PNPase might be involved in the control of oxidized RNA levels either unaided or accompanied with other protein partners. Surprisingly, our results have shown that 8-oxo-G containing RNA was not degraded in the presence of TruD. This prompted us to look for the other biochemical processes to which TruD is related.

TruD protein being a modification enzyme and its specificity to $tRNA^{Glu}$ led us to study the effect of TruD under oxidative stress conditions on aminoacylation and stability of $tRNA^{Glu}$. Experimental results from these studies revealed that $tRNA^{Glu}$ was stable throughout the oxidant treatment and levels of $tRNA^{Glu}$ aminoacylation were not affected in the *truD* deletion mutant (Fig. 24). This suggests that the protective role of TruD under oxidative stress is not due to deficiencies in either aminoacylation or stability of $tRNA^{Glu}$. TruD by its natural mechanistic activity removes uracil base from the sugar backbone and flips and add back as pseudouridine. This principle of TruD led us to study if it can able to remove any damaged bases from oxidized RNA and helps in quality control. If it does so abasic site levels in RNA will be elevated, interestingly abasic site levels were not

increased in RNA both *in vivo* and *in vitro*. However, it is possible that damaged base removed by TruD from the oxidized RNA might have been added back to the sugar backbone by TruD itself or by other unknown proteins. This will not detected by the present ARP assay.

It is also known that more than 100 ribonucleoside modifications were found in both tRNA and rRNA among all organisms (Czerwoniec *et al*., 2009). Recent studies have demonstrated that tRNA modifications are playing a critical role in response to cellular stress (Thomposon and Parker, 2009; Begley *et al*., 2007) and tRNA stability (Motorin and Helm, 2010). When yeast cells are exposed to hydrogen peroxide, tRNA modifications levels such as Cm, m(5)C, and m(2) (2)G are elevated and the cells lacking these enzymes are hypersensitive to hydrogen peroxide. Yeast cells lacking tRNA methytransferases such as *trm9* and *trm5* are hypersensitive to oxidative stress. These demonstrate that some tRNA modifications are highly essential and critical under cellular stress responses. Because *truD* is highly conserved among many eukaryotes such as yeast, it is also likely that the hypersensitivity of *truD* deletion mutants might be due to lack of modification at 13^{th} position under oxidative stress. However, further studies need to be performed in order to explain this possibility.

The most promising of all the experiments performed is RNA binding studies with wild type TruD and its active site mutant proteins D80N and D80T. Results clearly demonstrated that wild type TruD can bale to differentiate normal and oxidized RNA very well with endogenous or low protein concentrations. Whereas D80N and D80T lack such discriminating ability, however they do bind when protein is over expressed. Unpublished reports from Dr. Arun Malhotra's laboratory have shown that, D80N and

D80T proteins bind to synthetic full length $tRNA^{Glu}$ with 4 time lower affinity than wild type TruD (Kaya, 2006). However, with oxidized RNA they completely lack binding and discriminating ability. It is very important to note that D80N protein at over expression level binds more to normal RNA and has significantly less affinity to oxidized RNA. This observation is quite opposite what was observed with wild type TruD. However D80N has similar binding affinity as wild type TruD to normal RNA. These results clearly demonstrate the importance of aspartic acid in catalytic center in discriminating normal and oxidized RNA. This will shed light to understand the behavior of these active site mutants in protecting cells under oxidative stress conditions. This will also provide direct evidence and relation between the oxidized RNA binding and the ability of TruD proteins in protecting cells under oxidative stress. If active site mutant TruD proteins do not protect cells under oxidative stress, then there is a strong and direct relation between oxidized RNA binding and cell protection.

In summary, our studies with this novel TruD protein demonstrates that it binds to oxidized RNA with high affinity and protects cells under oxidative stress, yet the true biochemical mechanism remains to be explored. Despite our attempts to solve the mystery behind the biochemical mechanism of TruD in protecting cells against oxidative stress, further in depth studies need to be performed in future.

4. Concluding Remarks and Future Directions

In summary *M. genitalium* RNase R is able to remove 3' trailers very efficiently and generate mature 3' ends efficiently in a single step reaction. RNase R has the ability to recognize sequence and structural features within tRNA. Our studies have shown that disruptions in the acceptor stem leads to partial or complete degradation of tRNA precursors. Sequence features such as discriminator base A/G and CC residues in CCA terminus are more preferred in stopping RNase R at mature 3' end. Replacement of C residues in CCA terminus to either A/G resulted in removal of two extra residues suggesting its role in quality control of defective tRNAs. tRNAs undergo oxidative damage both *in vivo* and *in vitro* and the levels of 8-oxo-G in tRNA are increased in a dose dependent manner. Additionally rRNAs appears to be more protected than tRNA under normal conditions. Interestingly tRNA with native structural conformation are more prone to oxidative damage than their denatured forms. These studies suggest the importance of RNA secondary structures in promoting oxidative damage.

E. coli TruD protein binds to oxidized RNA with high affinity and protects cells from oxidative stress caused by various oxidizing agents such as TBHP and H_2O_2 in a dose dependent manner. Studies to show biochemical evidence behind the protective role of TruD under oxidative stress revealed no significant correlation.

In *TruD* deletion mutant Aminoacylation of $tRNA^{Glu}$ was not affected under oxidative stress conditions and additionally $tRNA^{Glu}$ was stable throughout the oxidative stress treatment. TruD was also shown to be not involved the specific removal of 8-oxo-G containing RNA and removal of damaged bases either from oxidized RNA or DNA. RNA binding experiments with wild type TruD and active site mutants D80N and D80T proteins revealed that only wild type TruD possess the ability to bind oxidized RNA with high affinity.

Future studies regarding *M. genitalium* RNase R should be directed to explore the *in vivo* role in *E. coli ex vivo* system. Role of RNase R in various mutants lacking tRNA processing enzymes should be studied elaborately on cell viability. Additionally action of RNase R on various tRNA precursors with secondary structures in the trailer sequence, mutations should be studied.

Future studies on tRNA oxidation should be focused on studying how tRNA oxidation influences protein synthesis both *in vivo* and *in vitro*. tRNA fragmentation is a prominent feature of oxidative damage in yeast and other eukaryotes however, no study have shown this in *E. coli*. Our future studies also focused on studying the tRNA fragmentation and repair under oxidative stress in *E. coli* system.

TruD is the most promising protein to study elaborately. TruD has protective role under oxidative stress and its relation to oxidized RNA binding has to be studied further. TruD being specific to Uracil base in RNA, we intended to study to what base exactly TruD has affinity in oxidized RNA. This can be accomplished by using RNA homopolymers as substrates in RNA binding experiments. Only wild type TruD has high affinity to oxidized RNA and protects cells under oxidative stress, however D80N and

D80T do not have high affinity binding to oxidized RNA and their role in cell protection is not known. Here we are further interested to make chromosomal mutants of D80N and D80T by site directed mutagenesis and studying their role in protecting cells under oxidative stress. This will directly demonstrates the correlation between oxidized RNA binding and cell protection under oxidative stress.

Appendices

A.1 Role of *M. genitalium* RNase R in *E. coli ex- vivo* system

Studying the precise role of RNase R in *in vivo* system is not feasible due to unavailability of efficient genetic tools in *M. genitalium*. Hence, we came up with an approach to study the role of RNase R in tRNA 3' end maturation in *ex-vivo* system of *E. coli* strain CA244I⁻Δrph Δrnt lacking RNase T and PH. In this strain, tRNAs with 2 to 4 3' overhang nucleotides accumulate to a greater level. We predict that when *M. genitalium* RNase R (MgR) harbored in a plasmid vector transferred into *E. coli* strain, generates mature tRNAs efficiently and helps in faster cell growth.

A.1.1 *M. genitalium* RNase R protects *E. coli* cells probably by making more mature tRNA

CA244I⁻Δrph Δrnt cells are transduced with lysogenic λDE3 as described in materials and method, which produces T7 RNA polymerase upon IPTG induction. RNase R on pET-15b (pET-mgR) vector was transfected into *E. coli* cells by heat shock method. Growth curve results clearly demonstrated that CA244I⁻ΔrphΔrnt with pET-mgR recovers faster than CA244I⁻Δrph Δrnt with an empty pET-15b plasmid (Fig. 33C and D). Additionally, we did not find any significant difference with and without IPTG induction. Importantly, no difference was observed in the growth rates of wild type strains CA244I⁻

λDE3-pET-mgR and CA244IΔλDE3-pET-15b (Fig. 33A and B) demonstrating that RNase R is helping CA244I-Δrph Δrnt cells in the growth recovery.

In order to test if pET-mgR is expressed irrespective of λDE3 lysogen, we tested the growth curves of strains CA244IΔrph Δrnt with pET-mgR and CA244I-Δrph Δrnt with pET-15b both lacking λDE3 lysogen. Interestingly, we did not find any growth recovery in strain with pET-mgR, demonstrating that RNase R is expressed by T7 RNA polymerase and the effect was clearly due to RNase R (Fig. 34).

We further studied the effect of *M. genitalium* RNase R in *E. coli* strain CA244I-T-PH-BN-D-II^ts (ZL150) lacking all tRNA maturation enzymes with RNase II as temperature sensitive. This strain produces mature tRNA by RNase II at very low efficiency and the cells are very sick. These cells were lysogenized with λDE3 lysogen as described before and transfected with pET-mgR and pET-15b plasmids. Growth curve results demonstrated some stunning observations that both strains were grown to similar level up to 7 hrs and later cells with pET-15b started to grow rapidly (Fig. 35A). However, the growth in cells with pET-mgR reached a peak OD of 0.4 slowly at 11^{th} hr and from there dropped significantly (Fig. 35B).

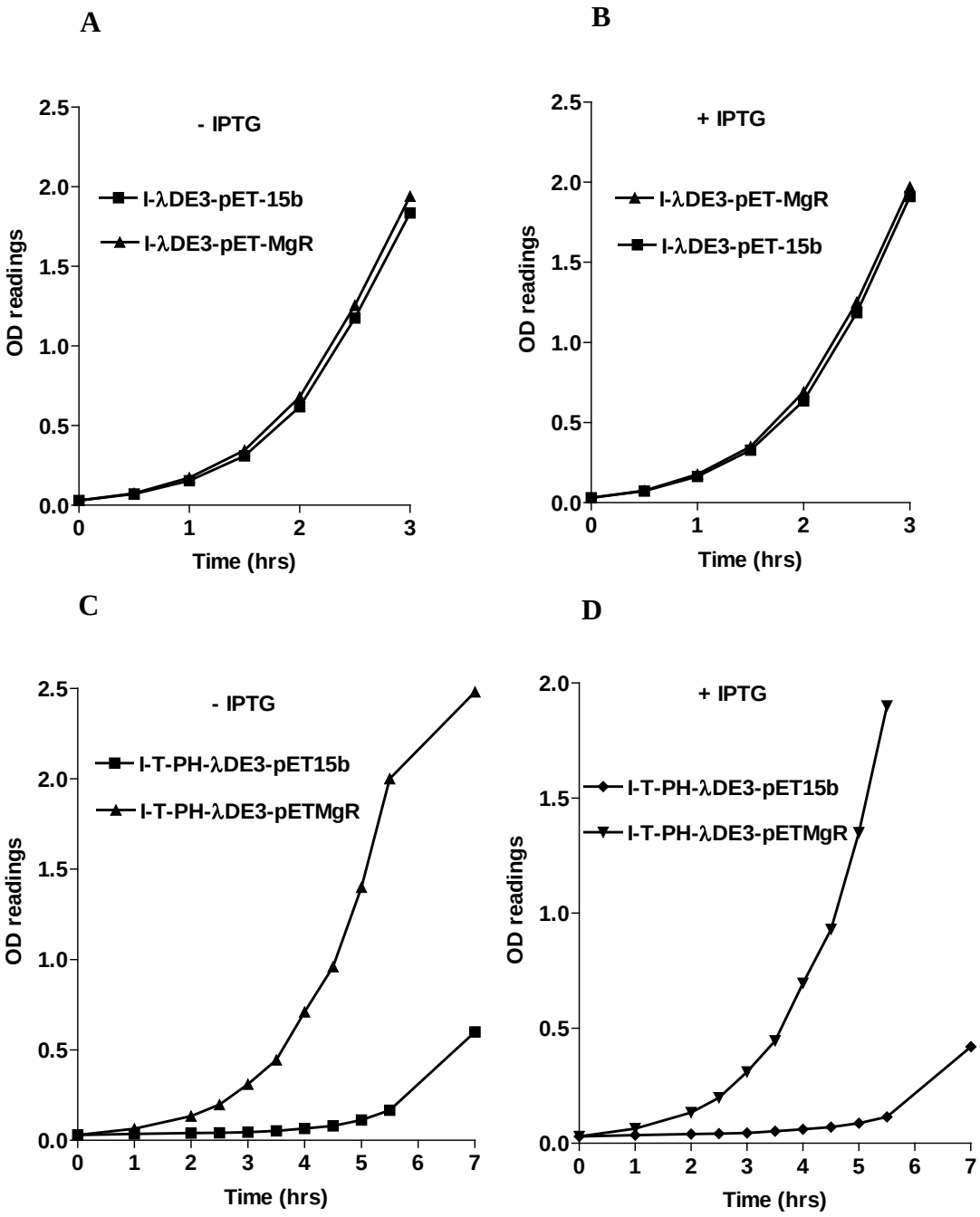

Figure 33. Growth curve of CA244 I⁻T⁻PH⁻λDE3 and CA244 I⁻λDE3 strain backgrounds with empty pET-15b plasmid and pET-15b plasmid harboring mgR. (A) and (B) are growth curves of CA244 I⁻λDE3 pET-15b and CA244 I⁻ λDE3 pET-mgR with and without IPTG induction. (C) and (D) are growth curves of CA244 I⁻T⁻PH⁻λDE3 pET-15b and CA244 I⁻T⁻PH⁻λDE3 pET-mgR with and without IPTG induction.

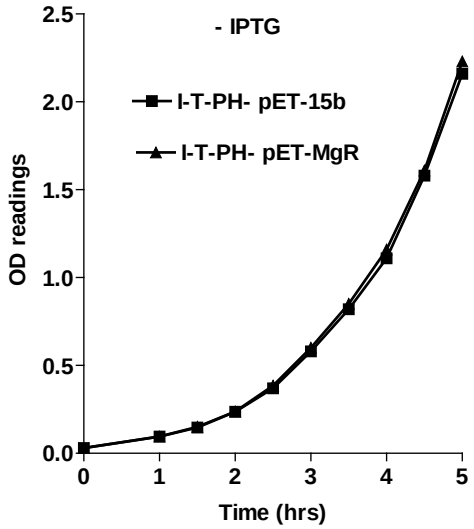

Figure 34. Growth curve of CA244 I-T-PH- strain lacking λDE3 lysogen with pET-15b and pET-mgR.

This is a quite contrasting result when compared to the above strain backgrounds, where only RNase T and PH are missing. From this, it is evident that RNase R of *M. genitalium* in *E. coli* strain lacking RNase T and PH alone helps cells in growth. However, in *E. coli* strain lacking all tRNA maturation enzymes RNase T, PH, BN and D RNase R is lethal to cells. From this data, it is to say that in the absence of RNase BN and D, the presence of *M. genitalium* RNase R may be lethal in *E. coli*.

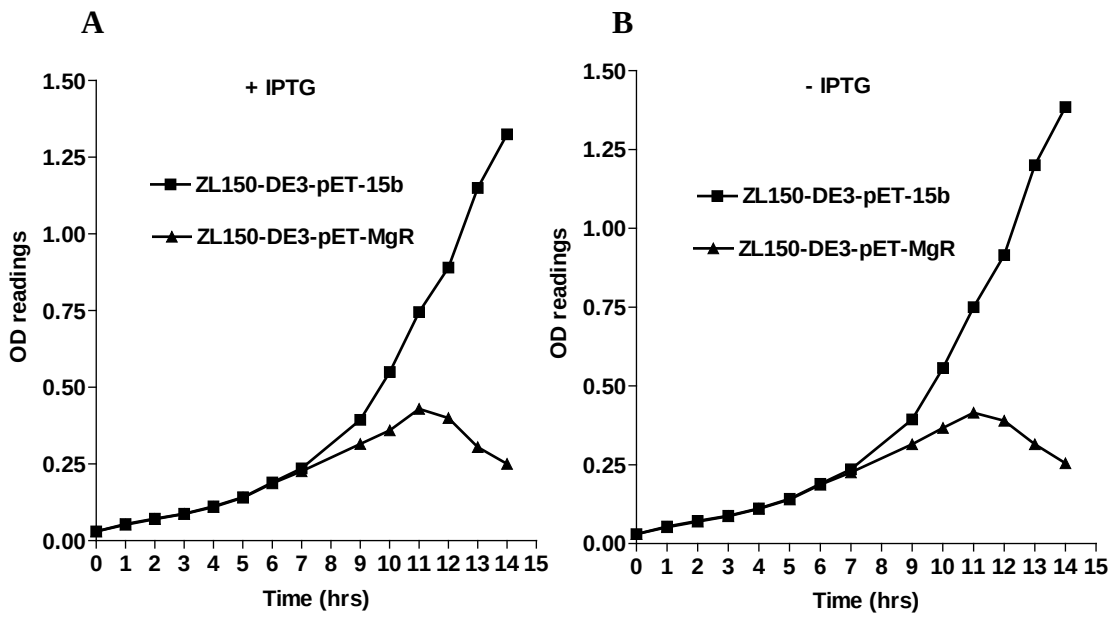

Figure 35. Growth curve of ZL150-λDE3 pET-15b and ZL150-λDE3 pET-mgR strains. (A) With IPTG and, (B) without IPTG induction

A.1.2 *M. genitalium* RNase R make more mature tRNA in *E. coli* cells

Northern blot analysis of total RNA isolated from these strains revealed that in control strains (CA244I- λDE3-pET-mgR and CA244I- λDE3-pET-15b), there is no accumulation of tRNA precursors or no significant difference in the levels of mature tRNA formation (Fig. 36A). However, in strains CA244I-Δrph Δrnt λDE3-pET-mgR and CA244I-Δrph Δrnt λDE3-pET-15b, we observed accumulation of short tRNA precursors as expected (Fig. 36A). Quantitative analysis of ratio of mature to precursor tRNA revealed that cells with MgR has more mature tRNA suggesting that RNase R is helping in maturation of tRNA precursors (Fig. 36B).

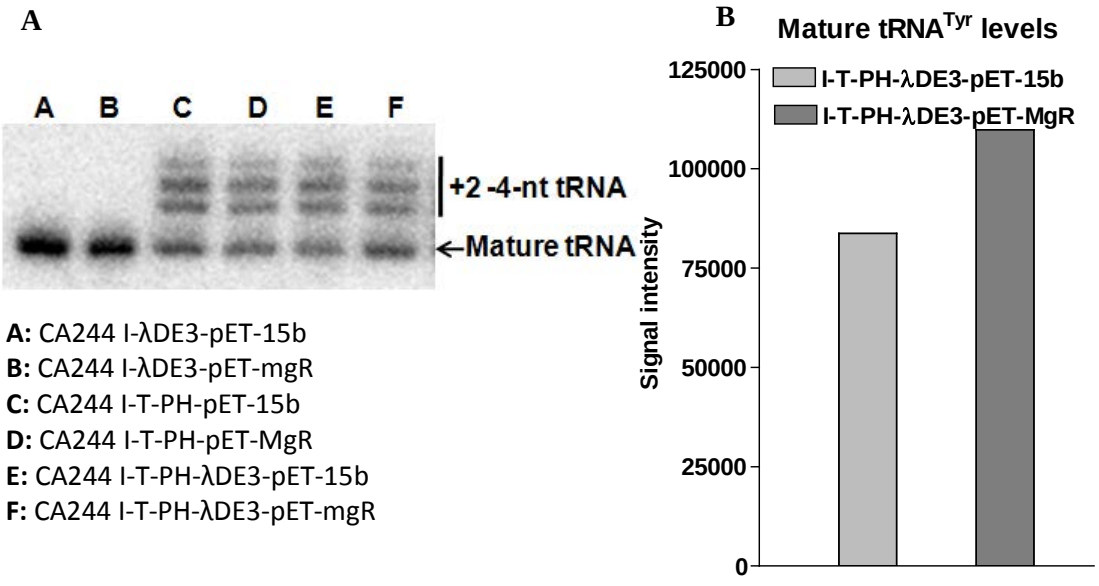

Figure 36. Northern blot analysis of tRNA^{Tyr}. Total RNA was isolated at exponential growth phase without IPTG treatment from CA244 I^{-}T^{-}PH^{-}λDE3 and CA244 I^{-}λDE3 strain backgrounds with pET-15b and pET-mgR. Total RNA was subjected to northern blotting with tRNA^{Tyr} probe and signal are quantified with phosphor imager screen. (A). Northern blot showing the tRNA^{Tyr}. (B). Graphical representation of mature tRNA levels.

List of ratios of mature to total tRNA and precursor to total tRNA are provided in Table. 4. According to the data generated it is very clear that presence of MgR containing *E. coli* strains generated more mature tRNA and less precursor tRNA was accumulated demonstrating the role of *M. genitalium* RNase R in making mature tRNA in *E. coli ex vivo* system.

Table 5. List of ratios of mature and precursor tRNAs formed v/s total tRNA

Ratios	IT⁻PH⁻λDE3-pET-15b	IT⁻PH⁻λDE3-pET-mgR
Precursor/total	0.714	0.656
Mature/total	0.286	0.343
Mature/precursor	0.400	0.523

A.1.3 *M. genitalium* RNase R specifically degrades 5S rRNA *in vitro*

From the above studies it is clear that RNase R did not digest the 74-nt tRNA transcript with CCA end even after 30 min (Fig. 37). It may be due to mature tRNA with 4-nt overhang not being a substrate for *M. genitalium* RNase R. It is well known that *E. coli* RNase R require a minimum of 7-nt overhang in order carry out the processing action. As we have not tested the minimum length of overhang required for the action of *M. genitalium* RNase R, it is speculated that 74-nt tRNA transcript with 4-nt overhang may not be the substrate.

Here we studied the processing activity of *M. genitalium* RNase R on small RNA isolated from *E. coli* cells. Small RNAs isolated from *E. coli* cells contain 95% of tRNA and 5% of 5S rRNA. When small RNAs are incubated with *M. genitalium* RNase R, surprisingly only 5S rRNA was degraded completely after 30 min (Fig. 37), while tRNAs were unaffected.

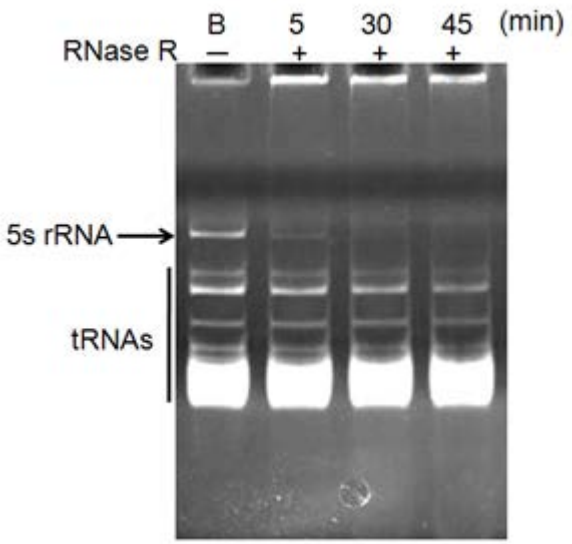

Figure 37. Analysis of 5S rRNA degradation by *M. genitalium* RNase R *in vitro*. Small RNA fraction isolated from *E. coli* cells containing tRNA and 5S rRNA are incubated with RNase R for indicated points of time and reaction was stopped by adding loading buffer as indicated before. In the figure legend B represents the negative control where RNA was treated with buffer alone for 45 min.

A.1.4 Discussion

Here we have shown that *M. genitalium* RNase R is able to help *E. coli* cells lacking RNase T and PH to recover fast by generating more mature tRNA. However it is still unclear how RNase R is working on different tRNA species and its action on other stable RNA species. In support to this northern blot analysis of $tRNA^{Tyr}$ has shown that presence of RNase R in *E. coli* cells lacking RNase T and PH mature tRNA levels increased to 20% and precursor tRNA levels reduced by approximately 10%. These results suggest the strong correlation between the recoveries in cell growth and mature tRNA levels generated by RNase R. Very importantly in *E. coli* cells lacking RNase T, PH, D, BN, and harboring a temperature sensitive RNase II (II^{ts}) (ZL150), presence of RNase R has shown negative effect on cell viability. ZL150 cells with RNase R grown to

OD_{600} 0.4 and dropped significantly over the time (Fig. 35A, B). It is important to note that we did not find any difference between with and without IPTG induction. However further studies needed to be performed in order to decipher the exact mechanism behind this differential role of RNase R in two different strain backgrounds.

In *E. coli* mature 5S rRNA has a single nucleotide 3' overhang. These 5S rRNAs containing a single nucleotide overhang formed the substrate and were degraded completely by RNase R, whereas the tRNAs with 4-nt overhang did not. From this, it is evident that the length of 3' overhangs may not be the factor that differentiated the differential activity of RNase R on 5S rRNA and mature tRNA. The specificity of RNase R either to the structure of tRNA molecule or to some other domains of tRNA tertiary structure might play an important role in this differential activity. It is important to speculate the possible relation between RNase R's ability to degrade 5S rRNA and its negative effect on growth of ZL150 *E. coli* strain. We predict that in *E. coli* cells (ZL150) lacking all tRNA maturation enzymes presence of RNase R resulted in inhibited growth and this might be due to specific degradation of 5S rRNA *in vivo*. However further studies need to performed in order to decipher the exact mechanism of RNase R in these strain backgrounds.

A.2 Oxidized tRNA inhibits protein synthesis

Oxidative damage to mRNA and rRNA has been shown reduce protein synthesis. Effect of oxidized tRNA in translation and protein synthesis has not been reported yet. Here, we made an attempt to study the effect of oxidized tRNA on protein synthesis in *in vitro* pure translation system. *In vitro* translation reactions were carried out as described in materials and methods. Results demonstrated that additional supplement of normal

tRNA to the pure translation system did not cause any effect on total protein synthesized (Fig. 38A). Very interestingly when the same amount of oxidized tRNA was supplemented additionally total protein production was reduced by 30% (Fig. 38B). This result shows that oxidized tRNA has negative effect on protein synthesis during translation, however we did not find any short peptides made when oxidized tRNAs were added.

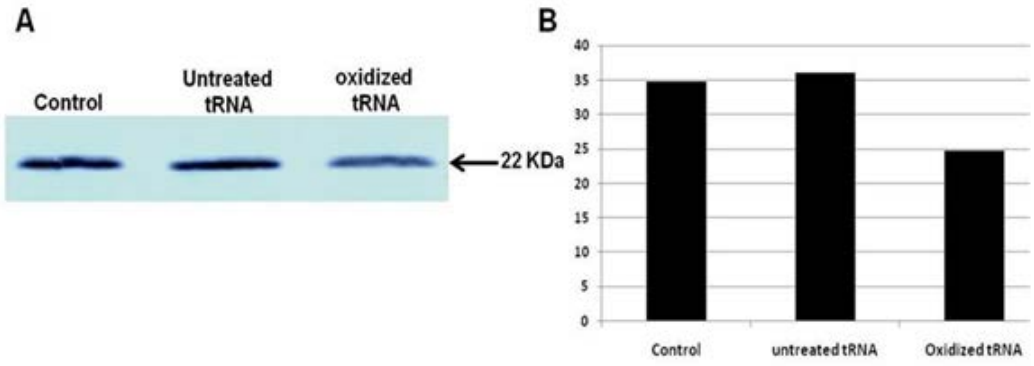

Figure 38. Effect of oxidized RNA on *in vitro* translation. *In vitro* oxidized and normal tRNA added to the NEB pure system as describe in the materials and methods and analyzed by running SDS PAGE gel. A. 10% SDS PAGE gel showing the signal intensities of DHFR protein synthesized *in vitro* translation system with normal and oxidized tRNA added. B. Graphical representation of signal intensities of protein synthesized.

A.2.1 Discussion

From this in vitro translation system experiment it is clear that addition of oxidized tRNA to the NEB pure system resulted in 30% reduction in protein synthesis. Whereas addition of normal tRNA did not cause any effect on protein synthesis compared to control reaction where no additional tRNA was added except the tRNA provided with NEB pure system. These results suggest that oxidized tRNA is affecting translation by a mechanism which yet to be elucidated. Previous studies have shown that

under oxidative stress conditions tRNA undergoes cleavage and only the 5’ end halves of tRNA inhibit protein synthesis (Kato *et al.*, 2012). However how it inhibits is yet to be known. Hence is this a open area of further research to be continued to understand the mechanisms how in cells under oxidative stress global protein synthesis is affected with the role of tRNA oxidation being the important determinant.

References

Alexandrov, A., Chernyakov, I., Gu, W., Hiley, S, L., Hughes, T. R., Grayhack, E. J., Phizicky, E. M. (2006) Rapid tRNA decay can result from lack of nonessential modifications. Mol. Cell. 21:87-96.

Altman, S. (1990) Ribonuclease P. J. Biol. Chem. 265:20053-20056.

Ames, B. N., and Gold, L. S. (1991) Endogenous mutagens and the causes of aging and cancer. Mutat Res. 250:3–16

Atwood, C. S., Moir, R. D., Huang, X., Scarpa, R. C., Bacarra, N. M., Romano, D. M., Hartshorn, M. A., Tanzi, R. E., and Bush, A. I. (1998) Dramatic aggregation of Alzheimer abeta by Cu(II) is induced by conditions representing physiological acidosis. J Biol Chem. 273:12817–12826

Awano, N., Rajagopal, V., Arbing, M., Patel, S., Hunt, J., Inouye, M., and Phadtare, S. (2010) Escherichia coli Rnase R has dual activities, helicase and RNase. J. Bacteriol. 192:1344-1352

Beal, M. F. (2005) Mitochondria take center stage in aging and neurodegeneration. Ann Neurol. 58:495–505

Begley, U., Dyavaiah, M., Patil, A., Rooney, J. P., Direnzo, D. (2007) Trm9-catalyzed tRNA modifications link translation to the DNA damage response. Mol Cell. 28:860–870

Brännvall, M., and Kirsebom, L. A. (1999) Manganese ions induce miscleavage in the *Escherichia coli*RNase P RNA-catalyzed reaction. J. Mol. Biol. 292: 53–63.

Brannvall, M., Fredrik Pettersson, B. M., and Kirsebom, L. A. (2002) The residue immediately upstream of the RNase P cleavage site is a positive determinant. Biochimie. 84: 693–703

Bulmer, M. (1991) The selection-mutation-drift theory of synonymous codon usage. Genetics. 129**:**897-907

Busch, S., Kirsebom, L. A., Notbohm, H., and Hartmann, R. K. (2000) Differential role of the intermolecular base-pairs G292-C(75) and G293-C(74) in the reaction catalyzed by Escherichia coli RNase P RNA. J. Mol. Biol. 299:941–951

Bycroft, M., Hubbard, T. J., Proctor, M., Freund, S. M., Murzin, A. G. (1997) The solution structure of the S1 RNA binding domain: A member of an ancient nucleic acid-binding fold. Cell. 88:235–242.

Caputi, M., Freund, M., Kammler, S., Asang, C., Schaal, H. (2004) A bidirectional SF2/ASF- and SRp40-dependent splicing enhancer regulates human immunodeficiency virus type 1 rev, env, vpu, and nef gene expression. J Virol. 78:6517–6526

Carpousis A. J., Van Houwe, G., Ehretsmann, C., Krisch, H. M. (1994) Copurification of *E. coli* RNAase E and PNPase: evidence for a specific association between two enzymes important in RNA processing and degradation. Cell. 76:889–900

Cate, J. H., Doudna, J. A. (1996) Metal-binding sites in the major groove of a large ribozyme domain. Structure 4: 1221–1229

Chan, C. M, and Huang, R. H. (2009) Enzymatic characterization and mutational studies of TruD--the fifth family of pseudouridine synthases. Arch Biochem Biophys. 489:15-9

Chan, P.P. & Lowe, T.M. (2009) GtRNAdb: A database of transfer RNA genes detected in genomic sequence. Nucl. Acids Res. 37(Database issue):D93-D97

Cheng, Z. F., and Deutscher, M. P. (2002). Purification and characterization of the Escherichia coli exoribonuclease RNase R. Comparison with RNase II. J. Biol. Chem. 277:21624–21629

Cheng, Z. F., and Deutscher, M. P. (2003). Quality control of ribosomal RNA mediated by polynucleotide phosphorylase and RNase R. Proc. Natl. Acad. Sci. USA. 100: 6388–6393

Cheng, Z. F., and Deutscher, M. P. (2005). An important role for RNase R in mRNA decay. Mol. Cell 17: 313–318

Cheng, Z. F., Zuo, Y., Li, Z., Rudd, K. E., Deutscher, M. P. (1998) The *vacB* gene required for virulence in*Shigella flexneri* and *Escherichia coli* encodes the exoribonuclease RNase R. J. Biol. Chem. 273:14077–14080

Coburn, G. A., and Mackie, G. A. (1996) Overexpression, purification, and properties of Escherichia coli ribonuclease II. J. Biol. Chem. 271:1048-1053

Codon, C., Dionysios, L., Squires, C., Schwartz, I., Squires, C. L. (1995) rRNA operon multiplicity in *Escherichia coli* and the physiological implications of *rrn* inactivation. J. Bacteriol.177**:**4152-4156.

Cohen, S. N., McDowall, K. J. (1997) Mol. Microbiol. 23:1099–1106

Comeron, J., Aguade, M. (1998) An evaluation of measures of synonymous codon usage bias. J. Mol. Evol. 47:268–274.

Condon, C. (2003) RNA Processing and Degradation in Bacillus subtilis. Microbiol. Mol. Biol. Rev. 67, 157-174

Condon, C., and Putzer, H. **(**2002**).** The phylogenetic distribution of bacterial ribonucleases. Nucleic Acids Res. 30:5339–5346

Cooke, M. S., Evans, M. D., Dizdaroglu, M., and Lunec, M. (2003) Oxidative DNA damage: Mechanisms, mutation, and disease. FASEB J. 17:1195–1214

Czerwoniec, A., Dunin-Horkawicz, S., Purta, E., Kaminska, K. H., Kasprzak, J. M., Bujnicki, J. M., Grosjean, H., Rother, K. (2009) MODOMICS: a database of RNA modification pathways. 2008 update.Nucleic Acids Res 37: D118–D121

de Souza-Pinto, N. C., Bohr, V. A. (2002) The mitochondrial theory of aging: involvement of mitochondrial DNA damage and repair. Int. Rev. Neurobiol. 53:519–534

de Vries, M. C., Siezen, R. J., Wijman, J. G., Zhao, Y., Kleerebezem, M., de Vos, W. M., Vaughan, E. E. (2006) Comparative and functional analysis of the rRNA-operons and their tRNA gene complement in different lactic acid bacteria. Syst. Appl. Microbiol. 29:358-67.

Deutscher, M. P. Degradation of stable RNA in bacteria. (2003) J. Biol. Chem. 278:45041-4.

Ding, Q., Dimayuga, E., Markesbery, W. R., and Keller, J. N. (2004) Proteasome inhibition increases DNA and RNA oxidation in astrocyte and neuron cultures. J. Neurochem. 91:1211-1218

Ding, Q., Markesbery, W. R., Chen, Q., Li, F., and Keller, J. N. (2005) Ribosome dysfunction is an early event in Alzheimer's disease. *J. Neurosci.* 25:9171-9175

Dittmar, K, A., Mobley, E. M., Radek, A, J., Pan, T. (2004) Exploring the regulation of tRNA distribution on the genomic scale. J. Mol. Biol. 337:31-47.

Ericsson, U. B., Andersson, M. E., Engvall, B., Nordlund, P., and Hall-berg, B. M. 2004. Expression, purification, crystallization and preliminary diffraction studies of the tRNA pseudouridine synthase TruD from *Escherichia coli.* Acta Crystallogr. D 60**:** 775–776

Ermolaeva, M. D. (2001). Synonymous codon usage in bacteria. *Curr. Issues. Mol. Biol.* 3: 91–97

ESCODD (European Standards Committee on Oxidative DNA Damage) Gedik CM, Collins A. (2005) Establishing the background level of base oxidation in human lymphocyte DNA : results of an interlaboratory validation study. FASEB J. 19:82–84

Fiala, E. S., Conaway, C. C., and Mathis, J. E. (1989) Oxidative DNA and RNA damage in the livers of Sprague-Dawley rats treated with the hepatocarcinogen 2-nitropropane. Cancer Res. 49:5518–5522.

Floyd, R. A., West, M. S., Eneff, K. L., and Schneider, J. E. (1989) Methylene blue plus light mediates 8-hydroxyguanine formation in DNA. Arch Biochem Biophys. 273:106-111

Folichon, M., Arluison, V., Pellegrini, O., Huntzinger, E., Regnier, P., Hajnsdorf, E. 2(003) The poly(A) binding protein Hfq protects RNA from RNase E and exoribonucleolytic degradation. Nucleic Acids Res. 31: 7302–7310

Giegé, R., Sissler, M., and Florentz, C. (1998) Universal rules and idiosyncratic features in tRNA identity. Nucleic Acids Res. 26:5017–5035

Gong, X., Tao, R., and Li, Z. (2006) Quantification of RNA damage by reverse transcription polymerase chain reactions. Anal. Biochem. 357:58–67

Guerrier-Takada, C., Gardiner, K., Marsh, T., Pace, N., Altman, S. (1983) The RNA moiety of ribonuclease P is the catalytic subunit of the enzyme. Cell. 35: 849–857

Guerrier-Takada, C., Gardiner, K., Marsh, T., Pace, N., Altman, S. (1983) The RNA moiety of ribonuclease P is the catalytic subunit of the enzyme. Cell. 35:849–857

Halliwell, B. and Gutteridge, J. (1999). Free Radicals in Biology and Medicine. Oxford, New York: Oxford science publications, Oxford University Press

Hansen, A., Pfeiffer, T., Zuleeg, T., Limmer, S., Ciesiolka, J., Feltens, R., Hartmann, R. K. (2001) Exploring the minimal substrate requirements for trans-cleavage by RNase P holoenzymes from*Escherichia coli* and *Bacillus subtilis*. Mol. Microbiol. 41: 131–14

Hayakawa, H., Hofer, A., Thelander, L., Kitajima, S., Cai, Y., Oshiro, S., Yakushiji, H., Nakabeppu, Y., Kuwano, M., and Sekiguchi, M. (1999) Metabolic fate of oxidized guanine ribonucleotides in mammalian cells.Biochemistry. 38:3610–3614.

Hayakawa, H., Kuwano, M., and Sekiguchi, M. (2001) Specific binding of 8-oxoguanine-containing RNA to polynucleotide phosphorylase protein. Biochemistry. 40:9977–9982

Hoang, C., and Ferré-D'Amaré, A. R. (2004) Crystal structure of the highly divergent pseudouridine synthase TruD reveals a circular permutation of a conserved fold. RNA. 10:1026-1033

Hofer, T., Badouard, C., Bajak, E., Ravanat, J. L., Mattsson, A., and Cotgreave, I. A. (2005) Hydrogen peroxide causes greater oxidation in cellular RNA than in DNA. Biol. Chem. 386:333–337

Hofer, T., Seo, A. Y, Prudencio, M., and Leeuwenburgh, C. (2006) A method to determine RNA and DNA oxidation simultaneously by HPLC-ECD: greater RNA than DNA oxidation in rat liver after doxorubicin administration. Biol. Chem. 387:103–111

Honda, K., Smith, M. A., Zhu, X., Baus, D., Merrick, W. C., Tartakoff, A. M., Hattier, T., Harris, P. L., Siedlak, S. L., Fujioka, H., Liu, Q., Moreira, P. I., Miller, F. P., Nunomura, A., Shimohama, S., and Perry, G. (2005) Ribosomal RNA in Alzheimer disease is oxidized by bound redox-active iron, J. Biol. Chem. 280:20978-86

Hori, Y., Sakai, E., Tanaka, T., Kikuchi, Y. (2001) Hyperprocessing reaction of tRNA by *Bacillus subtilis*ribonuclease P ribozyme. FEBS Lett. 505:337–339

Hsiao, Y. Y., Yang, C. C., Lin, C. L., Lin, J. L., Duh, Y., and Yuan, H. S. (2011) Structural basis for RNA trimming by RNase T in stable RNA 3'-end maturation. Nature chemical biology. 7:236-243

Hussain, S. P., Hofseth, L. J., and Harris, C. C. (2003) Radical causes of cancer. Nat. Rev. Cancer. 3: 276–285

Ikemura , T. (1982) Correlation between the abundance of yeast transfer RNAs and the occurrence of the respective codons in its protein genes. J. Mol. Biol. 158: 573–597

Ikemura , T. (1985) Codon usage and tRNA content in unicellular and multi-cellular organisms. Mol. Biol. Evol. 2: 13–34

Ikemura, T. (1981) Correlation between the abundance of Escherichia coli transfer RNAs and the occurrence of the respective codons in its protein genes: a proposal for a synonymous codon choice that is optimal for the E. coli translational system. J. Mol. Biol. 151:389-409.

Ishibashi, T., Hayakawa, H., Ito, R., Miyazawa, M., Yamagata, Y., and Sekiguchi, M. (2005) Mammalian enzymes for preventing transcriptional errors caused by oxidative damage. Nucleic Acids Res. 33:3779–3784

Jenner, P. (2003). Oxidative stress in Parkinson's disease. Ann. Neurol., 53:26–S36

Jones, S., Daley, D. T., Luscombe, N. M., Berman, H. M., and Thornton, J. M. (2001) Protein-RNA interactions: a structural analysis. Nucleic Acids Res. 29:943–954

Kanaya, S., Yamada, Y., Kudo, Y., Ikemura, T. (1999) Studies of codon usage and tRNA genes of 18 unicellular organisms and quantification of Bacillus subtilis tRNAs: gene expression level and species-specific diversity of codon usage based on multivariate analysis. Gene. 238:143–155

Kato, M., and Slack, F. J. (2012) Ageing and the small, non-coding RNA world. Ageing Res. Rev. http://dx.doi.org/10.1016/j.arr.2012.03.012

Kaya, Y., and Ofengand, J. (2003) A novel unanticipated type of pseudouridine synthase with homologs in bacteria, archaea, and eukarya. RNA. 9**:** 711–721

Kaya, Yusuf. (2006) Identification of three Escherichia coli pseudouridine synthases, and characterization of TruD structure and function6). Dissertations from ProQuest. Paper 2466. http://scholarlyrepository.miami.edu/dissertations/2466

Kaya, Y., Del Campo, M., Ofengand, J., and Malhotra, A. (2004) Crystal structure of TruD, a novel pseudouridine synthase with a new protein fold. J Biol Chem. 279:18107–18110

Kikovska, E., Brännvall, M., Kufel, J., and Kirsebom, L. A. (2005) Substrate discrimination in RNase P RNA-mediated cleavage: importance of the structural environment of the RNase P cleavage site. Nucleic Acids Res. 33:2012-2021

Kong, Q., and Lin, C. L. (2010) Oxidative damage to RNA: mechanisms, consequences, and diseases. Cell Mol. Life Sci. 67:1817–1829

Koppele, J., Lucassen, P. J., Sakkee, A. N., van Asten, J. G., Ravid, R., Swaab, D. F., van Bezooijen, C. F. A. (1996) 8-OHdG levels in brain do not indicate oxidative DNA damage in Alzheimer's disease, Neurobiol. Aging. 17:819–826

Lafauci, G., Widom, R. L., Eisner, R. L., Jarvis, E. D. & Rudner, R. (1986) Mapping of rRNA genes with integrable plasmids in *Bacillus subtilis.* J. Bacteriol . 165:204–214

Lalonde, M. S., Zuo, Y., Zhang, J., Gong, X., Wu, S., Malhotra, A., and Li, Z. (2007) Exoribonuclease R in*Mycoplasma genitalium* can carry out both RNA processing and degradative functions and is sensitive to RNA ribose methylation. RNA. 13:1957–1968

Lari, S. U., Chen, C. Y., Vertessy, B. G, Morre, J., and Bennett, S. E. (2006) Quantitative determination of uracil residues in Escherichia coli DNA: contribution of ung, dug, and dut genes to uracil avoidance. DNA Repair. 5: 1407–1420

Laslett, D., Canback, B. (2004) ARAGORN, a program to detect tRNA genes and tmRNA genes in nucleotide sequences. Nucleic. Acids. Res. 32:11-6

Lee, S. R., and Collins, K. (2005) Starvation-induced cleavage of the tRNA anticodon loop in *Tetrahymena thermophila*. J Biol Chem. 280:42744–42749

Levinger, L., Mörl, M., and Florentz, C. (2004) Mitochondrial tRNA 3' end metabolism and human disease. Nucleic Acids Res. 32:5430-5441

Levinger, L., Vasisht, V., Greene, V., Bourne, R., Birk,A., Kolla, and S. (1995) Sequence and structure requirements for *Drosophila* tRNA 5′- and 3′-end processing. J Biol Chem. 270: 18903–18909

Li, Z., and Deutscher, M. P. (2004) Endoribonucleases and exoribonucleases. In Escherichia coli and Salmonella: Cellular and Molecular Biology, the EcoSal Edition, Chapter 4.6.3 http://www.ecosal.org/ecosal/index.jsp). American Society for Microbiology

Li, Z., and Deutscher, M. P. (1994) The role of individual exoribonucleases in processing at the 3' end of Escherichia coli tRNA precursors. J Biol Chem. 269:6064–6071

Li, Z., and Deutscher, M. P. (1995) The tRNA processing enzyme RNase T is essential for maturation of 5S RNA.Proc Natl Acad Sci U S A. 92:6883–6886

Li, Z., and Deutscher, M. P. (1996) Maturation pathways for *E. coli* tRNA precursors: a random multienzyme process in vivo. Cell. 86:503–512

Li, Z., Deutscher, M. P. (2002) RNase E plays an essential role in the maturation of Escherichia coli tRNA precursors. RNA. 8:97-109

Li, Z., Gong, X., Joshi, V. H., Li, M. (2005) Co-evolution of tRNA 3' trailer sequences with 3' processing enzymes in bacteria. RNA. 11(5):567-77

Li, Z., Pandit, S, Deutscher, M. P. (1998) 3' exoribonucleolytic trimming is a common feature of the maturation of small, stable RNAs in Escherichia coli. Proc Natl Acad Sci U S A. 95:2856–2861

Li, Z., Pandit, S., Deutscher, M. P. (1999) RNase G (CafA protein) and RNase E are both required for the 5' maturation of 16S ribosomal RNA. EMBO. J. 18:2878-85

Li, Z., Reimers, S., Pandit, S., Deutscher, M. P. (2002) RNA quality control: degradation of defective transfer RNA. EMBO. J. 21:1132-8

Li, Z., Wu, J., Deleo, C. J. (2006) RNA damage and surveillance under oxidative stress. IUBMB Life. 58:581–588

Liao, D. (2000) Gene conversion drives within genomic sequences: concerted evolution of ribosomal RNA genes in Bacteria and Archaea. J. Mol. Evol. 51:305-317

Liou, G. G., Jane, W. N., Cohen, S. N., Lin, N. S., Lin-Chao, S. (2001) RNA degradosomes exist in vivo in *Escherichia coli* as multicomponent complexes associated with the cytoplasmic membrane via the N-terminal region of ribonuclease E. Proc. Natl. Acad. Sci. 98:63–68.

Liu, M., Gong, X., Alluri, R. K., Wu, J., Sablo, T., and Li, Z. (2012) Characterization of RNA damage under oxidative stress in Escherichia coli. Biol Chem. 393:123-32

Lovell, M. A., Robertson, J. D., Teesdale, W. J., Campbell, J. L., and Markesbery, W. R. (1998) Copper, iron and zinc in Alzheimer's disease senile plaques. J Neurol Sci. 158:47–52

Lowe, T. M., Eddy, S. R. (1997) tRNAscan-SE: a program for improved detection of transfer RNA genes in genomic. Nuc. Acids. Res. 25:955-964

Maes, A., Gracia, C., Hajnsdorf, E., and Régnier, P. (2012) Search for poly(A) polymerase targets in ***E. coli*** reveals its implication in surveillance of Glu tRNA processing and degradation of stable RNAs. Mol. Microbiol. 83:436-451

Mathews, D. H., Sabina, J., Zuker, M., Turner, D. H. (1999) Expanded sequence dependence of thermodynamic parameters improves prediction of RNA secondary structure. J. Mol. Biol. 288:911-40

Mathews, D. H., Turner, D. H., Zuker, M. (2007) RNA secondary structure prediction. Curr. Protoc. Nucleic. Acid. Chem. Chapter 11:Unit 11.2

Maynard, C. J, Cappai, R., Volitakis, I. Cherny, R. A., White, A. R., Beyreuther, K., Masters, C. L., Bush, A. I., and Li, Q. X. (2002) Overexpression of Alzheimer's disease amyloid-beta opposes the age-dependent elevations of brain copper and iron. J Biol Chem. 277:44670-44676

McDowall K. J., Cohen, S. N. (1996) The N-terminal domain of the rne gene product has RNase E activity and is non-overlapping with the arginine-rich RNA-binding site. J. Mol. Biol. 255: 349-355

Melov, S. (2004) Modeling mitochondrial function in aging neurons. Trends Neurosci. 27:601–606

Minagawa, A., Takaku, H., Takagi, M., and Nashimoto, M. 2004. A novel endonucleolytic mechanism to generate the CCA 3′ termini of tRNA molecules in *Thermotoga maritime*. J. Biol. Chem. 279**:** 15688–15697

Mirzaei, H., and Regnier, F. (2006). Protein-RNA cross-linking in the ribosomes of yeast under oxidative stress. J Proteome Res. 5:3249–59

Mohanty, B. K., and Kushner, S. R. (2010) Processing of the Escherichia coli leuX tRNA transcript, encoding tRNA(Leu5), requires either the 3'-->5' exoribonuclease polynucleotide phosphorylase or RNase P to remove the Rho-independent transcription terminator. Nucleic Acids Res. 38:597-607

Mohanty, B. K., Maples, V. F., Kushner, S. R. (2004) The Sm-like protein Hfq regulates polyadenylation dependent mRNA decay in *Escherichia coli*. Mol. Microbiol. 54:905–920

Morita, A., Kimura, M., Itokawa, Y. (1994) The effect of aging on the mineral status of female mice. Biol Trace Elem Res. 42:165–177

Motorin, Y., Helm, M. (2010) tRNA stabilization by modified nucleotides. Biochemistry. 49:4934–4944

Nagan, M. C., Beuning, P., Musier-Forsyth ,K., Cramer, C. J. (2000) Importance of discriminator base stacking interactions: molecular dynamics analysis of A73 microhelix(Ala) variants. Nucleic Acids Res. 28:2527–2534

Netzer, N., Goodenbour, J. M., David, A., Dittmar, K. A., Jones, R. B., Schneider, J. R., Boone, D., Eves, E. M., Rosner, M. R., Gibbs, J. S., Embry, A., Dolan, B., Das, S., Hickman, H. D., Berglund, P., Bennink, J. R., Yewdell, J. W. and Pan, T.

(2009) Innate Immune and Chemically Triggered Oxidative Stress Modifies Translational Fidelity. Nature. 462:522–526

Nunomura, A., G. Perry, G. Aliev, K. Hirai, A. Takeda, E.K. Balraj, P.K. Jones, H. Ghanbari, T.Wataya, S. Shimohama, S. Chiba, C.S. Atwood, R.B. Petersen, M.A. Smith, Oxidative damage is the earliest event in Alzheimer disease, J Neuropathol. Exp. Neurol. 60 (2001) 759–767

Nunomura, A., Perry, G., Pappolla, M. A, Wade, R., Hirai, K., and Smith, M. A. (1999) RNA oxidation is a prominent feature of vulnerable neurons in Alzheimer's disease. JNeurosci. 19:1959–64

Nunomura, A., Perry, G., Pappolla, M. A., Wade, R., Hirai, K., Chiba, S., and Smith, M. A. (1999) RNA oxidation is a prominent feature of vulnerable neurons in Alzheimer's disease. J. Neurosci. 19:1959-1964

Ow, M. C., and Kushner, S. R. (2002) Initiation of tRNA maturation by RNase E is essential for cell viability in ***Escherichia coli.*** Genes and development. 16:1102-1115

Pacher, P., Beckman, J. S, and Liaudet, L. (2007) Nitric oxide and peroxynitrite in health and disease. Physiol Rev. 87:315-24

Park, B. H., Lee, J. H., Kim, M., and Lee, Y. (2000) Effects of C5 protein on *Escherichia coli* RNase P catalysis with a precursor tRNAPhe bearing a single mismatch in the acceptor stem. Biochem. Biophys. Res. Commun. 268:136–140

Park, E. M., Shigenaga, M. K., Degan, P., Korn, T. S., Kitzler, J. W., Wehr, C. M., Kolachana, P., and Ames, B. N. (1992) Assay of excised oxidative DNA

lesions:isolation of 8-oxoguanine and its nucleoside derivatives from biological fluids with a monoclonal antibody column. Proc Natl Acad Sci USA 89:3375-79

Pellegrini, O., Nezzar, J., Marchfelder, A., Putzer, H., and Condon, C. (2003) Endonucleolytic processing of CCA-less tRNA precursors by Rnase Z in Bacillus subtilis. EMBO J. 22:4534-4543

Puglisi, E. V., Puglisi, J. D., Williamson, J. R., RajBhandary , U. L. (1994) NMR analysis of tRNA acceptor stem microhelices: discriminator base change affects tRNA conformation at the 3′ end. Proc. Natl Acad. Sci. USA. 91:11467–11471

Purmal AA, Lampman GW, Bond JP, Hatahet Z, Wallace SS. Enzymatic processing of uracil glycol, a major oxidative product of DNA cytosine. J Biol Chem. 273:10026–10035

Pyle, A. M. (2002) Metal ions in the structure and function of RNA. J. Biol. Inorg. Chem. 7: 679–690

Radak, Z., and Boldogh, I. (2010) 8-Oxo-7,8-dihydroguanine: links to gene expression, aging, and defense against oxidative stress. Free Radic Biol Med. 49:587–596

Randau L, Schroder I, Soll, D. (2008) Life without RNase P. Nature. 453:120–123

Reichert, A. S., Mörl, M. (2000) Repair of tRNAs in metazoan mitochondria. Nucleic Acids Res. 28:2043–2048.

Robinson, M., Lilley, R., Emtage, J. S., Yarranton, G., Stephens, P., Millican, A., Eaton, M., Humphreys, G. (1984) Codon usage can affect efficiency of translation of genes in Escherichia coli. Nucl. Acids. Res.12: 6663–6671

Samarrai, W., Liu, D. X., White, A. M., Studamire, B., Edelstein, J., Srivastava, A., Widom, R. L., Rudner, R. (2011) Differential responses of *Bacillus subtilis* rRNA promoters to nutritional stress. J. Bacteriol. 193:723–733

Sayre, L. M., Smith, M. A., & Perry, G. (2001). Chemistry and biochemistry of oxidative stress in neurodegenerative disease. Curr. Med. Chem., 8, 721–738

Shan, X., Chang, Y., and Lin, C. L. (2007) Messenger RNA oxidation is an early event preceding cell death and causes reduced protein expression. FASEB J. 21:2753–2764

Shan, X., Tashiro, H., and Lin, C. L. (2003) The identification and characterization of oxidized RNAs in Alzheimer's disease, J. Neurosci. 23:4913-21

Sharp, P. M., Li, W. H. (1987) The codon adaptation index-a measure of directional synonymous codon usage bias, and its potential applications. Nucleic. Acids. Res. 15:1281–1295

Shen, Z., Wu, W., and Hazen, S. L. (2000) Activated leukocytes oxidatively damage DNA, RNA, and the nucleotide pool through halide-dependent formation of hydroxyl radical. Biochemistry. 39:5474–5482

Shibutani, S., Takeshita, M., and Grollman, A. P. (1991) Insertion of specific bases during DNA synthesis past the oxidation-damaged base 8-oxodG. Nature. 349:431–434

Sies, H. (1991) Role of reactive oxygen species in biological processes. Klin Wochenschr. 69:965–968

Singh, S., Dwarakanath, B. S, and Mathew, T. L. (2004) DNA ligand Hoechst-33342 enhances UV induced cytotoxicity in human glioma cell lines. J Photochem Photobiol B. 77:45–54

Singh, U., Jialal, I. (2006). Oxidative stress and atherosclerosis. Pathophysiology, 13(3), 129–142

Slagter-Jäger, J. G., Puzis, L., Gutgsell, N. S., Belfort, M., Jain, C. (2007) Functional defects in transfer RNAs lead to the accumulation of ribosomal RNA precursors. RNA. 13:597-605

Smith, M. A., Harris, P. L., Sayre, L. M., and Perry, G. (1997) Iron accumulation in Alzheimer disease is a source of redox-generated free radicals. Proc Natl Acad Sci USA. 94:9866–9868

Sorensen, S. B., Svendsen, I., Breddam, K. (1989) Primary structure of carboxypeptidase III from malted barley. Carlsberg. Res. Commun. 54:193-202

Stams, T., Niranjanakumari, S., Fierke, C., and Christianson, D. W. (1998). Ribonuclease P protein structure: evolutionary origins in the translationalapparatus. Science. 280:752-756

Taddei, F., Hayakawa, H., Bouton, M., Cirinesi, A., Matic, I., Sekiguch, M., and Radman, M. (1997) Counteraction by MutT protein of transcriptional errors caused by oxidative damage. Science. 278: 128–130

Tallsjo, A., Kufel, J., and Kirsebom, L. A. (1996) Interaction between *Escherichia coli* RNase P RNA and the discriminator base results in slow product release. RNA. 2: 299–307

Tanaka, M., Chock, P. B., and Stadtman, E. R. (2007) Oxidized messenger RNA induces translation errors. Proc Natl Acad Sci U S A. 104:66–71

Tanaka, M., Han, S., Kupfer, P. A., Leumann, C. J., Sonntag,W. E. (2011) Quantification of oxidized levels of specific RNA species using an aldehyde reactive probe. Anal. Biochem. 417:142–148

Tanaka, N., and Shuman, S. (2011) RtcB is the RNA ligase component of an *Escherichia coli* RNA repair operon.J Biol Chem. 286:7727–7731

Tanaka, N., Meineke, B., and Shuman, S. (2011) RtcB, a novel RNA ligase, can catalyze tRNA splicing and HAC1 mRNA splicing in vivo. J Biol Chem. 286:30253–30257

Tang, B., Boisvert, P., Higgs, P. G. (2004) Comparison of tRNA and rRNA phylogenies in proteobacteria: implications for the frequency of horizontal gene transfer

Tåquist, H., Cui, Y., Ardell, D. H. (2007) TFAM 1.0: an online tRNA function classifier, Nucleic. Acids. Res. 35:350-353

Thompson, D. M., and Parker, R. (2009) The RNase Rny1p cleaves tRNAs and promotes cell death during oxidative stress in *Saccharomyces cerevisiae*. J Cell Biol. 185:43–50

Vincent, H. A., and Deutscher, M. P. (2009) Insights into how RNase R degrades structured RNA: Analysis of the nuclease domain. J Mol Biol. 387:570–583

Vogiatzi, G., Tousoulis, D., & Stefanadis, C. (2009). The role of oxidative stress in atherosclerosis. Hellenic Journal of Cardiology, 50(5), 402−409

Wagner, J. R., Hu, C. C., and Ames, B. N. (1992) Endogenous oxidative damage of deoxycytidine in DNA, Proc. Natl. Acad. Sci. U.S.A. 89:3380–3384

Wang, X., Jia, H., Jankowsky, E., Anderson, J. T. (2008) Degradation of hypomodified tRNA(iMet) *in vivo* involves RNA-dependent ATPase activity of the DExH helicase Mtr4p. RNA. 14: 107–116

Wardman, P., Candeias, L. P. (1996) Fenton chemistry: an introduction. Radiat. Res. 145:523–531

Wegscheid, B., and Hartmann, R. K. (2006) The precursor tRNA 3′-CCA interaction with *Escherichia coli* RNase P RNA is essential for catalysis by RNase P *in vivo*. RNA. 12:2135–2148

Wegscheid, B., Hartmann, R. K. (2007) *In vivo* and in vitro investigation of bacterial type B RNase P interaction with tRNA 3′-CCA. Nucleic Acids Res. 35: 2060–2073

Wen, T., Oussenko, I. A., Pellegrini, O., Bechhofer, D. H., Condon, C. (2005) Ribonuclease PH plays a major role in the exonucleolytic maturation of CCA-containing tRNA precursors in *Bacillus subtilis*. Nucleic Acids Res. 33: 3636–3643

Willkomm, D. K., Feltens, R., Hartmann, R. K. (2002) tRNA maturation in *Aquifex aeolicus* . Biochimie. 84:713–722.

Wu, J., and Li, Z. (2008) Human polynucleotide phosphorylase reduces oxidative RNA damage and protects HeLa cell against oxidative stress. Biochem Biophys Res Commun. 372:288–292

Wu, J., Jiang, Z., Liu, M., Gong, X., Wu, S., Burns, C. M, and Li, Z. (2009) Polynucleotide phosphorylase protects*Escherichia coli* against oxidative stress. Biochemistry. 48:2012–2020

Wurtmann, E. J., and Wolin, S. L. (2009) RNA under attack: cellular handling of RNA damage. Crit. Rev. Biochem. Mol. Biol. 44:34–49

Yin, B., Whyatt, R. M., Perera, F. P., Randall, M. C., Cooper, T. B., and Santella, R. M. (1995) Determination of 8-hydroxydeoxyguanosine by an immunoaffinity chromatography-monoclonal antibody-based ELISA. Free Radic. Biol. Med. 18:1023-32

Zhang, J. R., Deutscher, M. P. (1988) Transfer RNA is a substrate for RNase D *in vivo*. J Biol Chem. 263: 17909–17912

Ziehler, W. A., Day, J. J, Fierke, C. A, and Engelke, D. R (2000). Effects of 5' Leader and 3' Trailer Structures on pre-tRNA Processing by Nuclear RNase P. Biochemistry. 39:9909-9916

Zuo, Y., and Deutscher, M. P. (2001). Exoribonuclease superfamilies:structural analysis and phylogenetic distribution. Nucleic Acids Res.29:1017–1026

Zuo, Y., Deutscher, M. P. (2002) The physiological role of RNase T can be explained by its unusual substrate specificity. J. Biol. Chem. 277:29654-29661

Zuo, Y., Vincent, H. A, Zhang, J., Wang, Y., Deutscher, M. P., and Malhotra, A. (2006) Structural basis for processivity and single-strand specificity of RNase II. Mol Cell. 24:149–56

Zuo, Y., and Deutscher, M. P. (2002) J. Mechanism of Action of RNase TII. A structural and functional model of the enzyme. J. Biol. Chem. 277:50155–50159